“STUDY OF VISUAL ADAPTATION LUMINANCE IN MESOPIC PHOTOMETRY SYSTEM FOR OUTDOOR LIGHTING”

A THESIS
SUBMITTED IN PERTIAL FULFILLMENT OF
THE REQUIREMENTS FOR DEGREE OF

MASTER OF ENGINEERING

IN

ILLUMINATION ENGINEERING

Submitted by

SOHEL RANA MALITHA

EXAMINATION ROLL NUMBER: M4ILN23008

REGISTRATION NO.: 160193 of 2021-22

Under the guidance of

Mrs. SANGITA SAHANA

ASSISTANT PROFESSOR

DEPARTMENT OF ELECTRICAL ENGINEERING

FACULTY OF ENGINEERING AND TECHNOLOGY

JADAVPUR UNIVERSITY

KOLKATA – 700032

INDIA

2023

JADAVPUR UNIVERSITY

FACULTY OF ENGINEERING AND TECHNOLOGY

ELECTRICAL ENGINEERING DEPARTMENT

CERTIFICATE OF RECOMMENDATION

This is to certify that the thesis entitled **"STUDY OF VISUAL ADAPTATION LUMINANCE IN MESOPIC PHOTOMETRY SYSTEM FOR OUTDOOR LIGHTING"** is a bonafide work carried out by **SOHEL RANA MALITHA** (Exam. Roll No. **M4ILN23008** Registration No.**160193 of 2021-22**) under my supervision and guidance for partial fulfilment of the requirement of Master of Engineering in Illumination Engineering**,** during the academic session 2022 - 2023.

_____

(Thesis supervisor)
Mrs. SANGITA SAHANA
Assistant Professor,
Electrical Engineering Department,
Jadavpur University,
Kolkata - 700032.

Countersigned:

_____

Prof. (Dr.) BISWANATH ROY
Head of the Department
Electrical Engineering Department,
Jadavpur University,
Kolkata- 700032

_____

Prof.(Dr.) SASWATI MAZUMDAR
Dean of the Faculty of Engg. & Tech
Jadavpur University,
Kolkata-700032

CERTIFICATE OF APPROVAL

This foregoing thesis is hereby approved as a credible study of an engineering subject carried out and presented in a manner satisfactorily to warranty its acceptance as a prerequisite to the degree for which it has been submitted. It is understood that by this approval the undersigned do not endorse or approve any statement made or opinion expressed or conclusion drawn therein but approve the thesis only for purpose for which it has been submitted.

Committee of final examination for evaluation of Thesis

_____

_____

DECLARATION OF ORIGINALITY AND OF ACADEMIC ETHICS

It is hereby declared that this thesis contains literature survey and original research work by the undersigned candidate, as part of his Master of Engineering in Illumination Engineering, studies during academic session 2022-2023.

All information in this document has been obtained and presented in accordance with academic rules and ethical conduct.

I also declare that, as required by this rules and conduct, I have fully cited and referred all material and results that are not original to this work.

NAME	**SOHEL RANA MALITHA**
ROLL NUMBER	**M4ILN23008**
REGISTRATION NUMBER	**160193 of 2021-22**
THESIS TITTLE	**STUDY OF VISUAL ADAPTATION LUMINANCE IN MESOPIC PHOTOMETRY SYSTEM FOR OUTDOOR LIGHTING**
SIGNATURE	**DATE**

ACKNOWLEDGEMENT

I take this opportunity to express my deep sense of gratitude and indebtedness to Mrs. Sangita Sahana, Assistant Professor, Electrical Engineering Department, Jadavpur University, Kolkata, without his mission and vision, this project would not have been possible.

I would like to acknowledge my sincere thanks to Prof. (Dr.) Saswati Mazumdar, Electrical Engineering Department, Jadavpur University, and Prof (Dr.) Suddhasatwa Chakraborty, Electrical Engineering Department, Jadavpur University for their constant guidance and supervision. I would also like to thank them for providing me their valuable time and helpful suggestions.

Again, I would like to acknowledge my sincere thanks to Prof. (Dr.) Biswanath Roy, HOD of Electrical Engineering Department, Jadavpur University for providing me the opportunity to carry out my project work in Illumination Engineering Laboratory, Jadavpur University.

I am also thankful to Mr. Samir Mandi and Mr. Pradip Pal of the illumination Engineering Laboratory for their Co-operation during my project work.

Last but not least, I wish convey my gratitude to my parents, whose love, teachings and support have brought me this far.

Date:

Place: Jadavpur University
Kolkata – 700032

SOHEL RANA MALITHA

Table of Contents

Abstract:

The mesopic photometry region, characterized by luminance levels between 0.005 cd/m² and 5 cd/m², plays a critical role in outdoor lighting, encompassing a spectrum between the scotopic and photopic regions. While significant research has been conducted in the context of road lighting applications, the realm of outdoor lighting remains relatively unexplored in the mesopic domain.

Adaptation luminance is a fundamental parameter in mesopic photometry used to derive mesopic luminances for a given measurement field. This adaptation luminance is determined by the average luminance of the visual adaptation field. This research project aims to fill the gap in understanding the performance of different lamps within the mesopic zone for outdoor lighting installations, with a particular focus on calculating the adaptation luminance of various lamps using MATLAB simulation considering the factors such as lamp type and surrounding ambient lighting effect.

The findings of this research are expected to have profound implications for the optimization of outdoor lighting systems. By gaining a deeper understanding of how different lamps perform in the mesopic range and how adaptation luminance is influenced by various factors, can make more informed decisions in the design and implementation of outdoor lighting installations.

CHAPTER: 1 INTRODUCTION

Mesopic photometry is a branch of photometry that deals with the measurement and characterization of visual perception under lighting conditions where both the cones (responsible for colour vision and operating in brighter light) and the rods (responsible for low-light vision and operating in dimmer light) in the human eye are simultaneously active. Mesopic vision occurs during twilight or under street lighting at night, when the average scene luminance is between approximately 0.005 cd/m^2 to 5 cd/m^2 (Commission Internationale de l'Eclairage Recommended). [1]

Traditional photometry systems are based on either photopic or scotopic vision alone, but they might not accurately reflect human visual perception in mesopic lighting conditions. The CIE (Commission Internationale de l'Eclairage) developed a mesopic photometry system to address this issue. The CIE's mesopic system takes into account the spectral sensitivities of both the cones and rods to provide a more accurate representation of how humans perceive light in these intermediate lighting conditions.

Human eyes respond to certain light levels differently. This is because under high light levels typical during daylight or under bright artificial lighting (photopic vision), the eye uses cones to process light. Under very low light levels, corresponding to moonless nights without artificial lighting (scotopic vision), the eye uses rods to process light. Cone cells are photoreceptors responsible for colour vision and visual acuity. Rod cells are photoreceptors that are highly sensitive to light but do not distinguish colour. They are primarily responsible for detecting motion and providing peripheral vision. In most night time environments, enough ambient light prevents true scotopic vision. [2]

Mesopic vision is particularly relevant when designing lighting systems for outdoor areas, as it requires a balance between providing sufficient illumination for visibility and considering the comfort and visual experience of individuals. The distinction between photopic, scotopic, and mesopic vision is crucial in various fields such as lighting design, where understanding how different light levels impact human perception helps in creating lighting systems that enhance visibility, safety, and overall user experience.

The primary aim of this thesis is to assess the performance of various lamps within an outdoor lighting context while operating under mesopic luminance levels. Additionally, the thesis aims to measure and contrast the adaptation luminance for lamps that possess varying Scotopic/Photopic (S/P) ratios. To achieve this, the study involves the measurement of photopic luminance and vertical illuminance across different lamp and adaptation settings. Following this, S/P ratios, Correlated Colour Temperature (CCT), and Spectral Power Distribution (SPD) of the lamps are determined. MATLAB software is utilized to simulate photopic luminance and adaptation luminance. Subsequently, the obtained outcomes are utilized to compare the L_p (photopic luminance) and La (adaptation luminance) of distinct lamps across diverse ambient luminance conditions.

1.1 Literature Survey

- **Irena Fryc ,Dariusz Czy˙zewski , Jiajie Fan and Catalin D. Gala¸tanu , "**The Drive towards Optimization of Road Lighting Energy Consumption Based on Mesopic Vision—A Suburban Street Case Study" **.** Energies 2021, 14, 1175.

This research paper is focused on optimizing road lighting energy consumption based on human mesopic vision and the spectral composition of lamps. The research was conducted in access road leading to a town located in Warsaw (The capital of Poland and a large metropolitan city) illuminated by smart LED road luminaires with a luminous flux control system with which different luminance levels can be achieved on the road. During peak hours, when traffic is heavy and visibility is crucial for safe driving, the lighting might need to be set at higher levels to ensure drivers can see clearly and react to changing road conditions. During off-peak hours, when traffic is light, the lighting can potentially be adjusted to lower levels to conserve energy while still maintaining minimal visibility for safety. For the peak hours of the traffic, the road luminance should follow the M4 class requirements. After peak hours, it is possible to reduce the level of road illumination to M5 and for some night hours even to M6 class. This Research paper has shown that a 15% annual saving in electricity consumption for road lighting by utilizing such scenarios in mesopic conditions is a notable accomplishment. The research results also show a high potential for saving energy when the mesopic vision is taken into account at the design process of road lighting.

- **Eduardo G. Vicente1 & Isabel Arranz1 & Luis Issolio & Beatriz M. Matesanz1 & Alejandro H. Gloriani & José A. Menéndez4 & Miguel Rodríguez-Rosa1 & Bárbara Silva & Elisa Colombo2 & Santiago Mar1 & Juan A. Aparicio , "**Influence of age and spectral power distribution on mesopic visual sensitivity". The Psychonomic Society, Inc. 2018.

In this research paper results of two experiments focused on the effect of spectral power distribution and age on contrast threshold in a typical mesopic illumination environment. Two typical light sources are used, a high-pressure sodium lamp (HPS), with a higher content of long wavelengths, and a metal halide lamp (MH), with a higher content of short wavelengths. Two experiments were performed, in Experiment 1, three age groups (young, middle-aged and old, n = 2 each), two retinal locations (on-axis and off-axis vision), four background luminances (0.01, 0.07, 0.45, and 3.2 cd/m^2), and two photometry systems (photopic and the MES2 systems) were considered. In Experiment 2, contrast threshold measurement was performed with two age groups (young and old, n = 11 each), one retinal location (off-axis vision), one background luminance (0.01 cd/m^2), and two photometry systems (photopic and the MES2 systems). In on-axis vision, regardless of a person's age or the specific light spectrum being used, their ability to detect contrasts remains relatively consistent. Whereas there is a significant relationship between a person's age and the spectral power distribution of light sources in terms of how it affects vision in off-axis conditions. When adaptation luminance changes from photopic to mesopic values, the visual spectral sensitivity curve gradually shifts as a consequence of the transition from a cone response to a rod–cone response (i.e., the Purkinje effect). This change gives rise to an increase in sensitivity to short wavelengths in relation to long wavelengths. This is why, in the mesopic illumination range, one might expect that street lamps with a greater content of short wavelengths (MH lamps) in its spectral power distribution

(SPD) should be more efficient than those with a greater content of long wavelengths (HPS lamps).

- **Yukio Akashi PhD, MS Rea PhD and JD Bullough PhD,** "Driver decision making in response to peripheral moving targets under mesopic light levels". Lighting Research Center, Rensselaer Polytechnic Institute, Troy, NY, USA, accepted 27 June 2006

  This paper describes research conducted to measure people's ability to perform a high-order decision-making task during driving a vehicle and respond to peripheral targets at mesopic and low photopic light levels. The subjects in the study were tasked with identifying the direction of an off-axis target (toward or away from the street) and responding by either braking or accelerating their movement. Two types of light sources were compared: ceramic metal halide and high-pressure sodium lights. The study was conducted both during the day and at night. The outcomes revealed a consistent reduction in both braking and acceleration response times as the unified luminance increased. This indicates that unified luminance serves as a suitable standardizing factor for evaluating light levels across different light sources in relation to intricate visual tasks. This study showed that off-axis response times under a 'white' metal halide light source are shorter than they are under HPS at the same photopic light levels. When both rods and cones play a role in visibility, lighting designs that rely on unified photometry are likely to enhance peripheral visibility and potentially enhance road safety without raising energy demands. While the metal halide system employed in this research yielded superior peripheral visibility compared to the HPS system under equivalent photopic lighting conditions.

- **S Fotios PhD and T Goodman BSc,** "Proposed UK guidance for lighting in residential roads". Lighting Res. Technol. 2012; 44: 69–83

  This paper introduces a novel system designed to define optimal illuminances and lamp selections for achieving equivalent visual effects at mesopic illuminance levels in the UK. The research focuses on its practical application in residential streets, primarily considering visual tasks relevant to pedestrians. This article engages into a discourse about the impacts of lamp spectrum while excluding considerations of other factors like the spatial dispersion of light. The study suggests that the recommended standard lamp for UK residential streets is the low-pressure sodium lamp. However, if other lamp types are used and possess a CIE General Colour Rendering Index (CRI) of $Ra \geq 60$, then the average illuminance requirement can be decreased. The extent of reduction is determined using the new CIE system for mesopic photometry and is influenced by the S/P ratio of the lamp in use. Lamps of higher S/P ratio enable a lower (photopic) illuminance to be used, but this reduction is only applied when using lamps of high colour rendering index ($Ra \geq 60$). These criteria were established subsequent to an evaluation of the visual tasks deemed pertinent for pedestrians.

- **E Colombo PhD, J Barraza PhD and L Issolio MSc,** "Effect of brief exposure to glare on brightness perception in the scotopic-mesopic range". Lighting Res. Technol.32(2) 65-69 (2000)

  This paper presents a study investigating the impact of disability glare within the scotopic-mesopic range, simulating the brief exposure to glare experienced during night-time driving. An essential aspect of glare while driving at night is the exceedingly low ambient illuminance, which causes the visual system to operate within the scotopic-

mesopic range. Many existing studies on glare focus solely on photopic levels of illumination and involve constant sources of glare. These studies often overlook the light adaptation effect stemming from the glare source. The research involves subjects comparing the brightness of two sequentially displayed uniform luminance fields, with one of them presented under glare conditions. The study employs a forced-choice paradigm utilizing the method of constant stimuli to establish the luminance that corresponds to the perceptual matching luminance. The results reveal a non-linear relationship between glare illuminance and the matching luminance, with minimal dependence on the luminance reference. These initial findings indicate that glare diminishes the apparent brightness of the central foveal test patch in a manner that follows a non-linear pattern. This behaviour can be effectively characterized using an empirical model that accurately captures the intricate non-linear tendencies of the visual system. The collected data in this experiment closely align with an equation drawn from prior research concerning the effect of peripheral glare sources on the apparent brightness of an object. The correlation between matching luminance and reference luminance offers a straightforward approach for quantifying the impact of glare.

1.2 Problem Definition

Outdoor lighting installations incorporate different types of lamps such as High Pressure Sodium Vapour (HPSV or SON), Metal halide (MH) and CWLEDs. The luminance level generally lies in Mesopic zone for outdoor lighting. Adaptation luminance is also a factor for outdoor lighting. The performance for different lamps in outdoor lighting scenario under Mesopic luminance range and adaptation luminance of each lamp are studied and compared here.

1.3 Objective

The objectives of the thesis are:

- To study the behaviour of different lamps under mesopic conditions.
- Simulation of Photopic luminance and Adaptation Luminance.
- To compare Photopic luminance & adaptation luminance for different lamps.

1.4 Methodology

- Measurement of photopic luminance and vertical illuminance under different lamp and adaptation conditions.
- Determination of S/P ratios, CCT & SPD of the lamps.
- Simulation of photopic luminance and adaptation luminance using MATLAB software.
- Comparison of the obtained results by graphical and analytical comparative studies.

1.5 Outline of Dissertation

- Chapter 1 gives the introduction to the project. It also states the objective and methodology of the project.

- Chapter 2 discusses the topic of area lighting and introduces the concepts of mesopic photometry.

- Chapter 3 discusses the constructional aspects working principle of different lamps used in outdoor lighting system.

- Chapter 4 primarily focuses on the concept of adaptation luminance and the factors influencing it in real-world outdoor scenes. It also presents a comprehensive approach to simulating Adaptation luminance based on various factors.

- Chapter 5 provides a thorough overview of experimental procedures and calculation methods for determining photopic, mesopic, and adaptation luminance. The chapter also provides the layout of the measurement grid and detailed technical specifications for each light source used in the experiment, including power, luminous flux, CCT, CRI and luminous efficacy etc.

- Chapter 6 discusses MATLAB-based simulation for calculating Photopic Luminance (Lp) across all grid points, analyzing three different main light source scenarios.

- Chapter 7 discusses MATLAB-based simulation for calculating Adaptation Luminance (La) across all grid points, analyzing three different main light source scenarios.

- Chapter 8 shows comparisons and analysis of the results.

- Chapter 9 draws the conclusion to the experiment and discusses the future scopes of the field of study.

CHAPTER: 2 AREA LIGHTING & MESOPIC PHOTOMETRY

Area lighting and mesopic photometry are concepts related to lighting design and the measurement of human vision in conditions where both the rods (responsible for low-light vision) and cones (responsible for colour and high-detail vision) in the human eye are active.

2.1 Area Lighting

Area lighting refers to the design and implementation of lighting systems in indoor or outdoor spaces, taking into consideration factors such as illuminance, Luminance, uniformity, glare, and energy efficiency. The goal of area lighting is to provide sufficient and appropriate illumination for a given space, allowing tasks to be performed comfortably and efficiently while also considering visual comfort and aesthetics.

Key considerations in area lighting design include:

- **Illuminance Levels:** Illuminance serves as the central lighting measurement for various non-roadway purposes such as crosswalks, walkways, and bike paths. It quantifies the light received by a surface and is represented in footcandles (fc) or lux when employing the International System of Units (SI units). Notably, one lux is approximately 10 times greater than one footcandles, equating to approximately 10.7639 times when converting between the two units.

    - **Horizontal illuminance** refers to the amount of light falling on a horizontal surface, such as pavement. Proper horizontal illuminance ensures that activities can be carried out effectively, colours are perceived accurately, and the overall visual comfort of the space is maintained. It is measured in lux (lx).

    - **Vertical illuminance** is to the amount of light falling on a vertical surface, such as a person, which is critical for drivers to be able to see objects in the roadway. It is also measured in lux (lx) and is crucial for creating a balanced and visually appealing environment.

- **Luminance Levels:**

    Luminance refers to the amount of light that is reflected from a surface or object and contributes to the perceived brightness of that surface or object within an individual's field of vision. It is measured in units of candela per square meter (cd/m^2).Luminance levels in the mesopic region are a bit more complex to determine compared to purely photopic (daytime) or scotopic (night-time) conditions. As mentioned earlier, the mesopic region involves a transition between cone-based (photopic) and rod-based (scotopic) vision, and the human eye's sensitivity to light is influenced by both systems. Recommended luminance levels for mesopic conditions can vary depending on the specific application, the

surrounding environment, and the age of the observers. Here are some general guidelines for outdoor mesopic lighting:

- **Roadway Lighting:** In roadway lighting, pavement luminance pertains to the perceived brightness of the pavement as observed by drivers. In instances where the pavement lacks sufficient lighting, discerning pavement markings and smaller objects on the road becomes more challenging for drivers. Increased pavement luminance provides the driver with visual information on the roadway boundaries, conflict areas such as crosswalks and intersections. Surfaces with higher reflectivity, such as lighter-coloured and more reflective materials like concrete, exhibit greater light reflection compared to less reflective, darker surfaces like asphalt. Less light is required for more reflective or concrete surfaces to provide the same luminance level.
  - Luminance levels on road surfaces typically range from 0.1 to 1.0 cd/m^2.[3]
  - Pedestrian crosswalks might have slightly higher luminance levels (1.0 to 2.0 cd/m^2) for improved safety.[4]

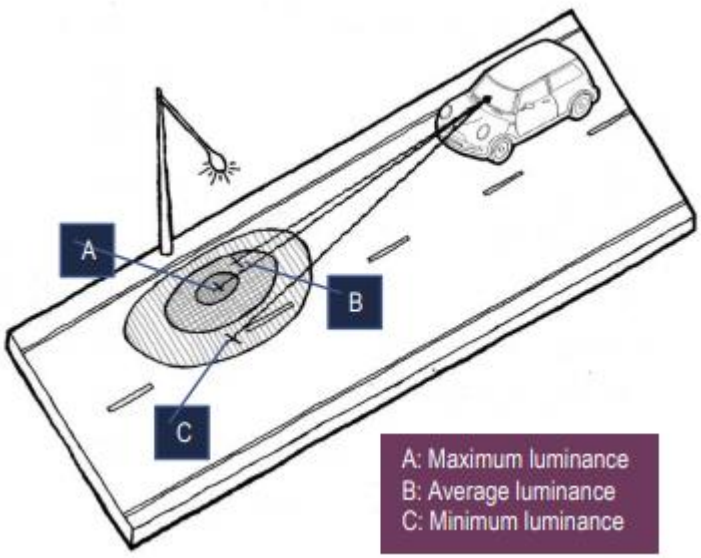

- **Outdoor Public Spaces:**
  - Walkways, plazas, and parks could have luminance levels in the range of 0.1 to 2.0 cd/m^2.

- **Uniformity:**

Lighting uniformity refers to the consistent distribution of light. Our eyes are continually adapting to the brightest object in our field of view. Even an object illuminated

to just a 1/10 the brightest level of the adjacent surroundings appears significantly darker. Achieving uniform illumination across the entire space helps reduce areas of glare and shadow. However, too uniform surfaces (less than 2:1 average to minimum) may minimize surface contrast of an object, which can cause some objects to blend into the background, making them harder to detect. A balance is required between uniformity and contrast. [5]

- **Contrast:**

Contrast represents the distinction in luminance between two adjacent surfaces. Adequate contrast is crucial for ensuring clear visibility. However, when contrast reaches excessive levels, the brighter surface can become a source of glare. The contrast was calculated by the equation: $C = (L_b - L_t)/L_b$ [where C is the contrast, L_b is the background luminance and L_t is the target luminance]. In Figure 2.1.2 and Figure 2.1.1 respectively, you can see examples of good and poor surface contrast.

Figure 2.1.1 Example of Poor Surface Contrast

Figure 2.1.2 Example of good Surface Contrast

- **Glare:**

In area lighting, glare refers to the excessive brightness or contrast that causes visual discomfort or difficulty in perceiving objects or details. It occurs when there is a significant difference in luminance between a light source and its surrounding environment or when there's a direct line of sight to a bright light source. Glare can have various negative effects, such as reduced visibility, eye strain, and even temporary impairment of vision. There are two primary types of glare in area lighting:

- **Disability Glare:** This occurs when excessive brightness causes a decrease in visibility, making it challenging to see clearly (shown in figure 2.1.3). Disability glare can lead to discomfort and difficulties in performing visual tasks. For instance, if a light source is positioned in a way that it directly shines into a person's eyes, it can obscure their vision and create an uncomfortable experience.

- **Discomfort Glare:** Discomfort glare doesn't necessarily impair visibility, but it causes discomfort or annoyance due to the contrast between the bright light source and its surroundings (shown in figure 2.1.4). This type of glare can affect the overall ambiance of a space and might discourage people from spending time in that area.

Figure 2.1.3 Example of Disability Glare

Figure 2.1.4 Example of Discomfort Glare

To mitigate glare in area lighting, several strategies can be employed:

- **Proper Fixture Placement:** Positioning light fixtures in a way that prevents direct line of sight to the light source can minimize glare.
- **Shielding:** Using proper shielding techniques, such as louvers or diffusers, can help direct light downward and reduce its spread in unintended directions, reducing the potential for glare (shown in figure 2.1.5).
- **Light Control:** Implementing controls like dimmers or motion sensors can adjust lighting levels according to the time of day or user presence, preventing over-illumination and glare.
- **Light Distribution:** Choosing fixtures with appropriate light distribution patterns ensures that light is evenly spread without creating overly bright spots.
- **Colour Temperature:** Opting for light sources with warmer colour temperatures can reduce the perception of glare compared to cooler, bluish light.
- **Surface Finishes:** Selecting appropriate surface finishes for walls, ceilings, and floors can help minimize reflections that contribute to glare.

Figure 2.1.5 Reduce Glare with Appropriate Luminaires

- **Adaptation:** Adaptation refers to the eye's ability to quickly adjust between changes in luminance and intensity. Our eye will automatically adjust to the brightest object in our field of view. But it takes time to adapt from photopic to scotopic vision and vice versa. A sudden transition from well-lit to dimly lit areas can affect visibility. Time required for adaptation increases with age due to normal structural and chemical changes in the eye. Glare from headlights can affect one's ability to adapt to a lower intensity of light. Additionally, adaptation occurs when driving from a lighted area to a non-lighted section of roadway (shown in figure 2.1.6). For example, transitions into tunnels are critical during the day as well as at night.

Figure 2.1.6 Daytime Adaptation

- **Energy Efficiency:** Using efficient light sources and controls like dimmers or motion sensors can help conserve energy.

- **Aesthetics:** Lighting can enhance the visual appeal of a space by highlighting architectural features and creating mood.

- **Environmental Considerations:** Balancing the lighting needs of the area with sustainability by minimizing light pollution, respecting natural ecosystems, and adhering to lighting regulations.

Areas that benefit from thoughtful area lighting design include public spaces like plazas, parks, and streetscapes, as well as commercial interiors such as offices, retail stores, educational institutions, and more. Effective area lighting enhances the overall experience within these spaces, supports their intended functions, and contributes to the well-being and satisfaction of occupants and users.

2.2 Mesopic Photometry

2.2.1 Introduction

The basis of all lighting technology and practice lies in photometry, the measurement of visible light. Photometry provides a method with which to assess light in terms of human visual spectral sensitivity. The mesopic luminance region lies between the photopic and scotopic regions where both cones and rods contribute to vision. Mesopic lighting applications include road and street lighting, outdoor area lighting and other night-time traffic environments. In the mesopic region the spectral sensitivity of the human visual system is not constant and changes with light level. This is due to the changing contribution of the rods and cones on the retina. Unlike the photopic and scotopic spectral luminous efficiency functions, it is not possible to describe mesopic spectral luminous efficiency with a single function since the interaction between cones and rods differs with light levels. A recommended system for mesopic photometry based on visual performance was introduced by CIE in 2010. **[1]** In this system, the upper limit for mesopic luminance is 5 cd/m^2 and the lower limit is 0.005 cd/m^2. In night-time driving conditions, the luminances in the visual scene are in the mesopic range; thus, mesopic photometry should be adopted when assessing lighting in outdoor areas and other night-time traffic environments.

2.2.2 Spectral Eye Sensitivity Curve

Spectral eye sensitivity, also known as the spectral sensitivity curve or the photopic spectral sensitivity curve, refers to the sensitivity of the human eye to different wavelengths of light under well-lit conditions, typically in daytime or bright lighting(larger than some 5 cd/m^2). This curve describes how the human eye responds to light at various wavelengths across the visible spectrum when its cone cells are predominantly active.

The spectral sensitivity curve for the human eye can be approximated by the standard photopic curve, which is based on experimental measurements. The spectral sensitivity curve of the average human eye under daylight conditions (photopic vision) is defined by the CIE spectral luminous efficiency function $V(\lambda)$. The curve shows that the human eye is most sensitive to light in the green-yellow part of the spectrum, peaking at around 555 nanometres. This is why many outdoor signs and traffic lights use green and yellow colours because they are more easily detectable by the human eye under normal lighting conditions.

The spectral sensitivity curve (Shown Figure 2.2.2) also shows that the eye is less sensitive to light at the extremes of the visible spectrum, towards the blue (shorter wavelengths)

and red (longer wavelengths) ends. This means that, for example, it takes more blue or red light to appear as bright to the human eye compared to green or yellow light of the same intensity.

The scotopic curve, also known as the scotopic spectral sensitivity curve, represents the sensitivity of the human eye under low-light or night-time conditions (lower than some 0.005 cd/m^2), when the eye relies primarily on rod cells for vision. Rod cells are more sensitive to shorter wavelengths of light. The spectral sensitivity with scotopic vision is characterized by the V′(λ) curve[6]. The scotopic curve peaks at a shorter wavelength, typically around 507 nanometres, which corresponds to a bluish-green colour.

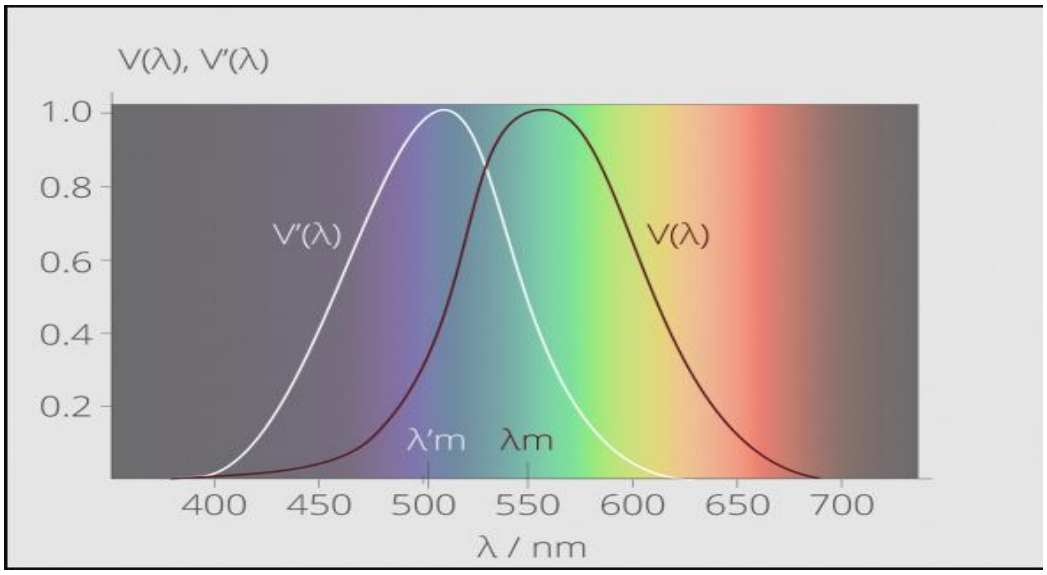

Figure 2.2.2 Spectral eye sensitivity curves for photopic vision (CIE 1926) and scotopic vision (CIE 1951)

2.2.3 The retina's structural and compositional characteristics: Exploring the Eye's Light-Capturing Mechanism

The retina is a layer of tissue lining the back of the eye that contains photoreceptor cells (rods and cones) responsible for detecting light and initiating the process of vision. Photons, which are particles of light, enter the eye through the cornea and pass through the pupil. The lens of the eye helps to focus the incoming light onto the retina. The lens adjusts its shape to ensure that the light rays converge onto the retina's surface. When photons from the incoming light strike the photoreceptor cells (rods and cones) in the retina, a chemical reaction occurs. In the case of rods and cones, a pigment molecule called rhodopsin is involved. When rhodopsin absorbs photons, it undergoes a structural change. The absorption of photons by rhodopsin triggers a series of biochemical events within the photoreceptor cells. This process, known as phototransduction, involves the conversion of light energy into electrical signals in

the form of electrochemical impulses. The optic nerve carries the visual information in the form of electrical signals from the retina to the brain. Specifically, the optic nerve fibers project to the lateral geniculate nucleus (LGN) of the thalamus and then to the primary visual cortex in the occipital lobe of the brain. This sets off a cascade of events that ultimately leads to the transmission of visual information to the brain, where it is processed and interpreted, allowing us to perceive the world around us.

2.2.4 Roles of Rods and Cones in Human Vision

There are two primary types of photoreceptor cells in the human retina: rod cells and cone cells. The central part of the retina, known as the macula, contains a high density of cone cells, which are responsible for detailed vision and colour perception. In contrast, the peripheral retina has a higher density of rod cells, which are highly sensitive to light but do not provide detailed or colour vision. This difference in photoreceptor distribution creates a functional division in our visual system:

- **Central Vision:** The macula and the fovea, a small depression at the center of the macula, are responsible for central vision. Cone cells in this area provide high acuity and colour perception, making it ideal for tasks that require fine detail and distinguishing colours. This area is essential for activities like reading, recognizing faces, and appreciating the finer details of objects. There are three types of cone cells, each containing a different photopigment. Here are the three primary cone cell pigments [38]:
  - L-cones (Long-wavelength cones): These cone cells contain a photopigment called "erythrolabe" or "long-wavelength-sensitive opsin." The photopigment in L-cones is most sensitive to longer wavelengths of light, which are perceived as red or reddish colours.
  - M-cones (Medium-wavelength cones): M-cones contain a photopigment called "chlorolabe" or "middle-wavelength-sensitive opsin." The photopigment in M-cones is most sensitive to medium wavelengths of light, which correspond to green or greenish-yellow colours.
  - S-cones (Short-wavelength cones): S-cones contain a photopigment known as "cyanolabe" or "short-wavelength-sensitive opsin." The photopigment in S-cones is most sensitive to shorter wavelengths of light, which are associated with blue and blue-violet colours.

- **Peripheral Vision:** The peripheral region of the retina rod cells are predominate. Rod cells contain a light-sensitive pigment called rhodopsin which are composed of a protein called opsin and a molecule called retinal. It is better suited for detecting motion and for vision in low-light conditions. While peripheral vision lacks the sharpness and colour discrimination of central vision, it plays a crucial role in our ability to detect movement and changes in our surroundings, particularly in dimly lit environments.

- **Intrinsically photosensitive retinal ganglion cells (ipRGCs**): These cells are a more recent discovery and are sometimes referred to as the "third type" of photoreceptor. Retinal Ganglion Cells (RGCs) contain a photopigment called

melanopsin. [39] Unlike rods and cones, which are primarily involved in image formation, ipRGCs are involved in non-image-forming functions of vision. [40] They are sensitive to a specific range of wavelengths, primarily in the blue spectrum, and play a critical role in regulating circadian rhythms, pupil constriction, and other light-mediated processes that are not directly related to conscious vision. Schematic view of the eye with the retina containing cones, rods and the intrinsically photosensitive retinal ganglion cells are shown in figure 2.2.4(a) and Spectral sensitivities of the photoreceptors in the human eye are shown in figure 2.2.4(b).

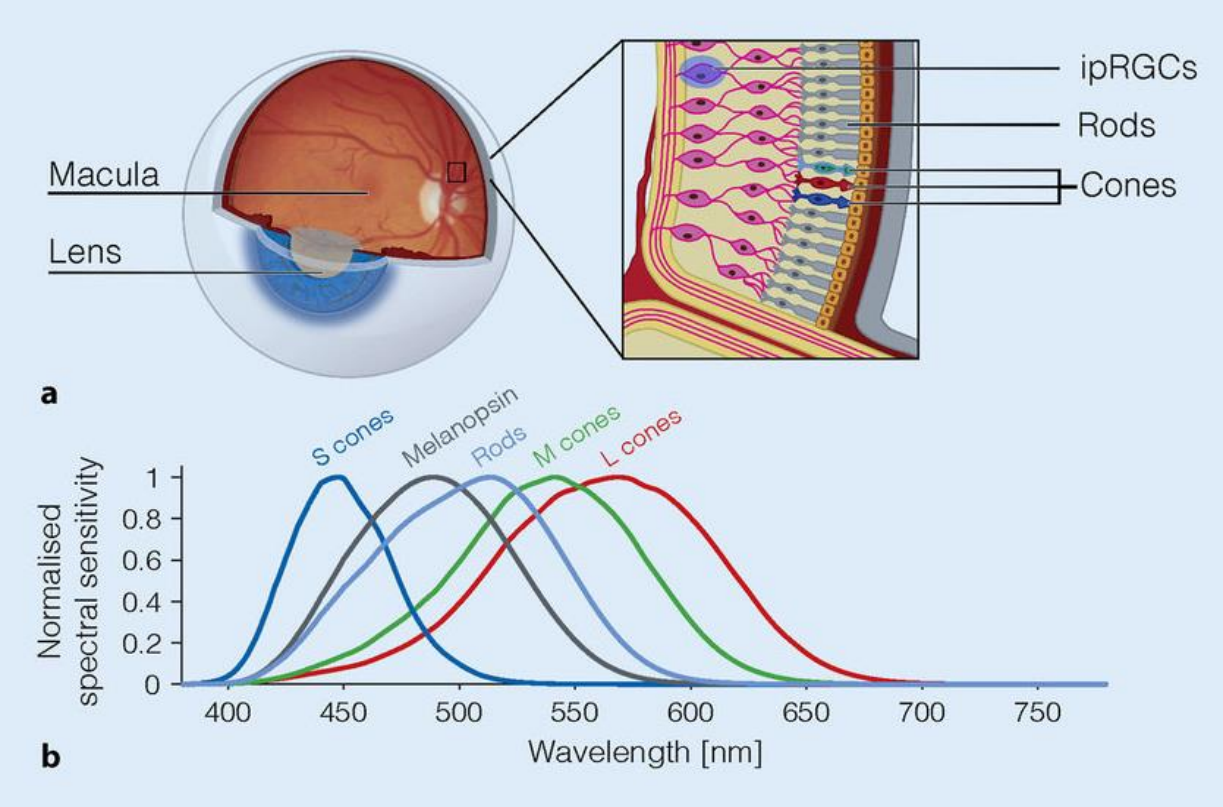

Figure 2.2.4 a) Schematic view of the eye with the retina containing cones, rods and the intrinsically photosensitive retinal ganglion cells b) Spectral sensitivities of the photoreceptors in the human eye

2.2.5 Visual performance-based mesopic photometry

To describe mesopic visual performance, a linear combination of the photopic and scotopic spectral luminous efficiency functions is used. These functions are typically represented as V(λ) and V'(λ), respectively, and they describe how the human eye's sensitivity to different wavelengths of light varies under photopic and scotopic conditions.

The spectral luminous efficiency function V(λ) represents the eye's sensitivity to light under photopic (daylight) conditions. It is based on cone cells in the retina and is used to quantify brightness perception during well-lit situations.

The spectral luminous efficiency function V'(λ), on the other hand, represents the eye's sensitivity to light under scotopic (low-light) conditions. It is based on rod cells in the retina and is used to quantify brightness perception in very dim lighting conditions.

When dealing with mesopic vision, which is a combination of both photopic and scotopic vision, it's common to use a linear combination of these two spectral luminous efficiency functions. The resulting mesopic spectral luminous efficiency function, $V_{mes}(\lambda)$, is calculated as follows[1]:

$$V_{mes}(\lambda) = \frac{1}{M(m)}[mV(\lambda) + (1 - m)V'(\lambda)] \qquad (1) \qquad \text{for } 0 \leq m \leq 1$$

And

$$L_{mes} = \frac{K_{cd}}{V_{mes}(\lambda_o)} \int V_{mes}(\lambda) L_e(\lambda) d\lambda \qquad (2)$$

Where,

- m is a coefficient, the value of which depends on the visual adaptation conditions;
- M(m) is a normalizing function so that $V_{mes}(\lambda)$ attains a maximum value of 1;
- K_{cd}=683 lm/W is the luminous efficacy of monochromatic radiation at λ_o; [7]
- $V_{mes}(\lambda_o)$is the value of $V_{mes}(\lambda)$ at 555 nm;
- L_{mes} is the mesopic luminance; and
- $L_e(\lambda)$ is spectral radiance [$W \cdot m^{-2} \cdot sr^{-1} \cdot nm^{-1}$].

Combining equations (1) and (2), the mesopic luminance L_{mes} can be expressed as a weighted sum of the photopic luminance L_p and the scotopic luminance L_s

$$L_{mes} = \frac{mL_p + (1-m)L_s V'(\lambda_o)}{m + (1-m)V'(\lambda_o)} \qquad (3)$$

Where, $V'(\lambda_o) = 0.40175$ is the value of the scotopic luminous efficiency functions at λ_o. [8]

In mesopic photometry, the adaptation level "m" is a key parameter that characterizes the level of visual adaptation within the mesopic visual adaptation field. This parameter is used to determine the appropriate combination of photopic and scotopic vision in mesopic conditions. The value of the adaptation level m is calculated from the mesopic luminance L_{mes} in the visual adaptation field and both values are solved using an iterative algorithm. The iteration is carried out as

$$m_o = 0.5$$

$$L_{mes,n} = \frac{m_{n-1}L_p + (1-m_{n-1})L_s V'(\lambda_o)}{m_{n-1} + (1-m_{n-1})V'(\lambda_o)} \qquad (4)$$

$$m_n = a + b \log_{10}(L_{mes,n}) \qquad (5) \qquad \text{for } 0 \leq m_n \leq 1$$

Where,

- L_p is photopic luminance in cd/m^2 ;
- L_s is scotopic luminance in cd/m^2;
- V'(λ_o) is scotopic spectral luminous efficiency function at λ_o=555 nm;
- a=0.7670;
- b=0.3334 and
- n is iteration step.

The iteration with equations (4) and (5) continues until the values of L_{mes} and m have converged to an acceptable precision level. It is also stated in the recommendation that the adaptation level gets a value of m=1 for mesopic luminance values $L_{mes} \geq 5.0$ cd.m^{-2} and a value of m=0 for mesopic luminance values $L_{mes} \leq 0.005$ cd.m^{-2}.

2.2.6 Scotopic / photopic Ratio

In order to implement CIE mesopic photometry (i.e. calculate mesopic luminance values), the background photopic luminance (i.e. the adaptation luminance) is required as an input value. Also, the ratio of scotopic to photopic luminous output (the S/P ratio) – this is the ratio of the luminous output of a light source evaluated according to the CIE scotopic spectral luminous efficiency function, V´(λ) to the luminous output evaluated according to the CIE photopic spectral luminous efficiency function, V(λ) – is needed, accounting for the spectral power distribution (SPD) of the light source. A light source will produce different luminance values, depending on whether it is evaluated with a photopic or a scotopic spectral weighting. The ratio of the scotopic luminance to the photopic luminance obtained for the same radiance spectrum is called the scotopic/photopic ratio (S/P-ratio, R_{sp}). [9]

$$\textbf{S/P Ratio} = \frac{K'_m \int S_\lambda(\lambda) V'(\lambda) d\lambda}{K_m \int S_\lambda(\lambda) V(\lambda) d\lambda}$$

Where,

- Km = 1700 lm.W^{-1} is the maximum value of the spectral luminous efficacy for scotopic vision.
- Km= 683 lm.W^{-1} is the maximum value of the spectral luminous efficacy for photopic vision, K(λ).
- $S_\lambda(\lambda)$ = the spectral power distribution of the light source.
- λ = the wavelength.

Photopic luminous efficiency function is defined in the 360–830nm range, and scotopic luminous efficiency function in a slightly narrower 380–780nm range. All defined values for both functions in their respective ranges are positive. [10] Using values in the overlapping range, theoretical limits for the S/P-ratio can be obtained. Figure 2.2.6 presents photopic and scotopic luminous efficacy functions at the 380–780nm range, and S/P-ratios for monochromatic light, where the range of possible S/P-ratios is approximately $0.01 \leq R_{sp} \leq 73$. The limiting values can only be achieved with monochromatic light.

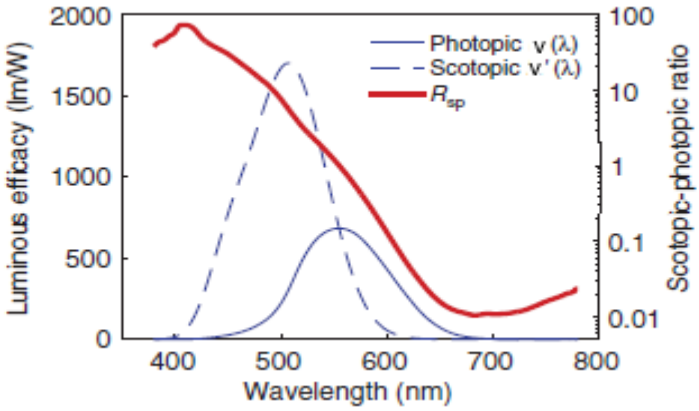

Figure 2.2.6 Photopic V(λ), (thin solid blue line) and scotopic V´(λ) ,(thin dashed blue line) spectral luminous efficacies and the S/P-ratio R_{sp} (thick red line) produced by monochromatic light

2.2.7 Common Light Sources and Their Corresponding S/P Ratio

The S/P ratio (Scotopic/Photopic ratio) values for different light sources can vary significantly based on the spectral distribution of light emitted by the source. S/P Ratios for Various Conventional Light Sources in Lighting, Along with Notable Quasi-Monochromatic Sources Exhibiting Extreme S/P Ratios are shown here in table.

Light source	R_{sp}
Low pressure sodium	0.23
High pressure sodium	0.4
Mercury vapour lamp	0.8
Incandescent	1.41
Quartz halogen	1.5
Fluorescent	1.5–2.4
Cool white LED	2.3
LED – red (635 nm)	0.06
LED – blue (470 nm)	14.3
LED – royal blue (450 nm)	28
Diode laser – red (650 nm)	0.016
Diode laser – blue (445 nm)	32

Figure 2.2.7Typical light sources and their S/P-ratio values

A high S/P ratio suggests that a light source emits more short-wavelength (blue and green) light, which is more effective for scotopic vision, making it suitable for low-light applications. Conversely, a low S/P ratio indicates that the light source emits more long-wavelength (red and yellow) light, which is better for photopic vision and well-lit conditions. For example, Red LED flashlights are employed for their advantageous low S/P-ratio, helping to preserve scotopic adaptation and enhance night vision. In contrast, blue LEDs are frequently found in decorative lighting, advertising signs, and automobile interiors.

2.2.8 Visualisation of the Mesopic Region

The entirety of the mesopic range can be represented by a three-dimensional graph, wherein mesopic luminance is depicted as a function of both photopic and scotopic luminances, denoted as $L_{mes}(L_p, L_s)$. Likewise, the mesopic range can be illustrated as the adaptation value $m(L_p, L_s)$ as shown in Figure 2.2.8(a). Since light sources emitting between 380nm and 780nm ($0.01 \leq Rsp \leq 73$) can only produce specific ratios of Lp and Ls, it could prove advantageous to represent the mesopic space as a function of photopic luminance and the S/P-ratio, denoted as m(Lp, Rsp). This choice preserves the rectangular shape of the permissible value space and aids in parameterization. In Figure 2.2.8(b), you can observe the specific Lp and Rsp values that delimit the boundaries of the mesopic range. In both graphs presented in Figure 2.2.8, the shaded regions fall within the permissible S/P-ratio range. Here, m = 0 represents the scotopic extreme of the range, while m = 1 signifies the photopic extreme**.** [11]

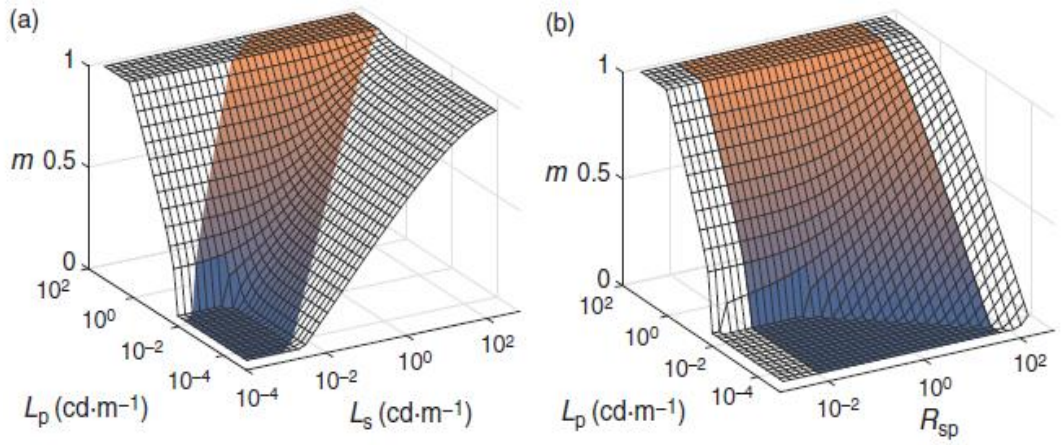

Figure 2.2.8Adaptation level m as a function of (a) L_p and L_s and (b) L_p and R_{sp}. The non-shaded areas represent S/P-ratios that are outside the mathematically possible range for light sources emitting between 380nm and 780nm.

2.2.9 Visual adaptation field for mesopic photometry:

In order to implement the CIE 191 mesopic photometric system, the coefficient 'm' needs to be known. It is determined by adaptation luminance. The field of view which contributes to adaptation luminance is called the 'visual adaptation field'. Once it is defined in terms of its size and shape, determining $V_{mes}(\lambda)$ for any scene is possible. It is also expected that the visual adaptation field is dependent on the behaviour of the person (driving/walking) and also on environmental and illumination conditions.

The adaptation field refers to how the surrounding luminance distribution affects the adaptation state for a peripheral point in an observer's visual field. It essentially defines the region within the visual field where the observer's visual system adapts to changes in lighting conditions. Two Factors Affecting Surrounding Luminance Effects:

- **Surrounding Luminance Distribution:** The first factor influencing the adaptation state within the adaptation field is the luminance distribution in the surroundings. This factor takes into account how the brightness levels in the environment surrounding the observer impact the adaptation process. Potential mechanisms for this factor include stray light within the eye and lateral neural interactions, which can affect the way the visual system adapts to changes in luminance.

- **Movement of Line of Sight:** The second factor affecting the adaptation state is the movement of the observer's line of sight. This factor depends on the specific lighting application or the direction in which the observer is looking. It effectively broadens the adaptation field determined by the first factor, as

the observer's gaze may shift within the visual field depending on the task or environment.

Foveal adaptation has been studied in the context of how the surrounding luminance affects the adaptation state when the observer's line of sight remains fixed. This relationship has been explored using the veiling luminance formula in studies conducted by Narisada [12][13]. Narisada's research focuses on understanding how glare sources influence foveal adaptation, with an emphasis on the veiling luminance concept, rather than delving into the aspects related to glare's effect on reducing luminance contrast. In these studies, the adaptation luminance L_a can be predicted by the equation:

$$\mathbf{L_a = L_{local} + L_{veil}}$$

Where,

- $\mathbf{L_{local}}$ = the local luminance at which the fovea looks;
- $\mathbf{L_{veil}}$ = the veiling luminance caused by the surrounding luminance distribution;
- $\mathbf{L_a}$ = The adaptation luminance which includes the surrounding luminance effect;

L_{veil} can be calculated by using models for foveal veiling luminance, such as the Stiles Holladay disability glare formula or the CIE general disability glare equation. [14] Based on the Stiles–Holladay formula, L_{veil} is obtained by

$$\mathbf{L_{veil}} = \frac{10}{\theta^2} E$$

Where,
E is the vertical illuminance at the observer's eye due to a glare source and θ is the visual angle (in degrees) between the glare source and the line of sight.

According to studies taking into account age, eye pigment and the data for ranges of angle near fovea, CIE has developed and recommended a general disability glare equation[14] as

$$\mathbf{L_{veil}} = \left[\frac{10}{\theta^3} + \left\{\frac{5}{\theta^2} + \frac{0.1p}{\theta}\right\} \cdot \left\{1 + \left(\frac{A}{62.5}\right)^4\right\} + 0.0025p\right] \mathbf{E}$$

Where,
A is the age of the observer in years, p is the eye pigment factor, which ranges from 0 for black eyes to 1.2 for very light-blue eyes. The experimental data for these models are also for foveal vision.

On the other hand, Stiles and Crawford proposed a model [15] for the veiling luminance on the peripheral task, based on a number of vision experiments, as

$$L_{veil} = \frac{16}{\theta^2} E_n$$

Where,

E_n is the normal illuminance (on a plane perpendicular to the direction from the source) at the observer's eye due to a glare source and θ is visual angle (in degrees) between the glare source and a task point where the veiling luminance is caused. A value of veiling luminance predicted by the model is more than 1.6 times the value predicted by the Stiles–Holladay equation.

Uchida &Ohno model for the veiling luminance [16] as,

$$L_{veil} = \frac{260}{\theta^3} E_v$$

Where,

E_v is the vertical illuminance at the observer's eye due to a glare source and θ is the visual angle (in degrees) between the glare source and the line of sight. We use this equation to calculate the adaptation luminance in this paper.

The adaptation state for a peripheral detection task in the mesopic range is primarily influenced by the local luminance of the task point. However, it is also slightly influenced by the surrounding luminance. These experiments have indicated that the impact of surrounding luminance might be greater than what is predicted by foveal veiling luminance models. The veiling luminance levels used in the experiments were insufficient for accurately assessing the extent of the surrounding luminance effect. Moreover, the experimental outcomes do not provide any insights into the correlation between the surrounding luminance effect and factors such as the position (angle) or intensity of the surrounding source, as the experiments exclusively examined the impact of an area light source with a fixed luminance level.

While the surrounding luminance can often be neglected for situations with uniform surrounding luminance distributions, it remains crucial to investigate the impact of surrounding luminance when dealing with high-luminance point-like sources (glare sources) in relation to their positions. This is particularly important because outdoor lighting environments frequently feature high-luminance stimuli, such as direct light from luminaires and the headlights of oncoming vehicles, which can have a significant influence on the adaptation state.

Chapter: 3 LAMPS; CLASSIFICATION, CONSTRUCTION & WORKING

Outdoor lighting serves both functional and aesthetic purposes, and the choice of lamps or light sources for outdoor fixtures depends on the specific requirements of the space, the desired ambiance, and energy efficiency considerations. Here are some common types of lamps used in outdoor lighting:

- **Incandescent Lamps:** These are traditional light bulbs that emit a warm and inviting light. While they are less energy-efficient compared to other options, they are still used in outdoor fixtures like decorative lanterns and string lights.

- **Halogen Lamps**: Halogen bulbs are a type of incandescent lamp that produces a bright, white light. They are often used in floodlights, spotlights, and landscape lighting due to their ability to provide intense illumination.

- **Compact Fluorescent Lamps (CFLs):** CFLs are more energy-efficient than incandescent bulbs and are suitable for outdoor fixtures such as wall-mounted sconces and post lights. They come in various colour temperatures, allowing you to choose between warm and cool white light.

- **LED Lamps:** LED (Light Emitting Diode) lamps are the most energy-efficient and durable option for outdoor lighting. They have a long lifespan and are available in various colour temperatures, making them suitable for various outdoor applications, including pathway lighting, garden lighting, and security lighting.

- **Sodium Vapour Lamps:** High-pressure sodium (HPS) and low-pressure sodium (LPS) lamps are known for their high efficiency and long life. They emit a distinct orange or yellow light, often used in street lighting and parking lots.

- **Metal Halide Lamps:** These lamps provide a bright, white light and are commonly used in commercial and industrial outdoor lighting applications, such as sports stadiums, parking lots, and large outdoor spaces.

- **Solar-Powered Lamps:** Solar-powered outdoor lighting fixtures use photovoltaic cells to charge batteries during the day and illuminate the surroundings at night. They are energy-efficient and require no wiring, making them suitable for remote or off-grid locations.

- **Fluorescent Tube Lights:** These are used in some outdoor applications, such as under awnings or covered outdoor areas. They provide a good amount of light and can be energy-efficient if used with T8 or T5 fluorescent tubes. But utilizing fluorescent T5 tube lamps can lead to reduced electricity consumption when they replace the widely used fluorescent T8 tube lamps in current applications.[17]

- **Gas Lamps:** While less common today, gas lamps add a classic and decorative touch to outdoor lighting. They use natural gas or propane and are often found in historic or upscale residential areas.

When choosing a lamp for outdoor lighting, consider factors like the desired brightness, colour temperature (warm or cool white), energy efficiency, durability, and the specific requirements of your outdoor space. LED lamps, in particular, have become the preferred choice for many outdoor lighting applications due to their versatility and energy-saving benefits.

3.1 Correlated Colour Temperature (CCT):

The CCT indicates the colour temperature of the light emitted by a particular luminaire (figure 3.1). CCT is expressed in Kelvin (K) and helps to describe the relative warmth or cool of the emitted light. This does not refer to the actual temperature of the luminaire: the CCT numerical value describes the temperature to which a particular black body would need to be heated to glow in the same colour as the luminaire.

For example, if a fluorescent lamp has a CCT of 4500K, it means that if you were to heat a black body to 4500K, it would emit light with the same colour as the fluorescent lamp. In essence, CCT is a way to quantify and describe the warmth or coolness of light, helping consumers select lighting that matches their preferences and intended use of a space. It's like a scale that helps you understand whether the light will appear warm, neutral, or cool.

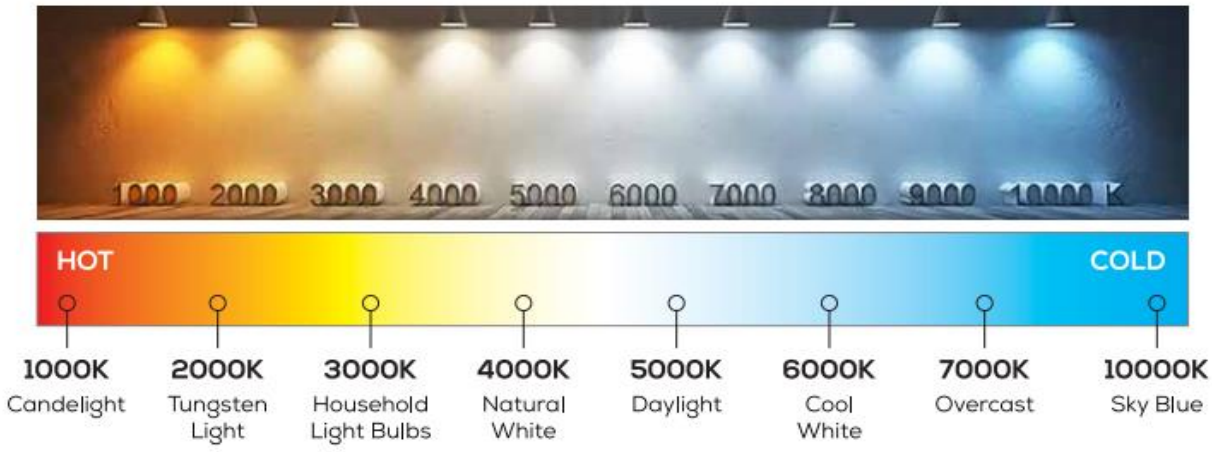

Figure 3.1 Kelvin colour temperature chart

3.2 Warm, Neutral & Cool white Lamps

Warm, Neutral & Cool white Lamps refer to three different colour temperatures of light produced by lighting fixtures shown in figure 3.2. Here's a more detailed explanation of Warm , Neutral & Cool white Lamps:

3.2.1 Warm White Lamps:

- **Colour Temperature:** Typically less than 3000K.
- **Appearance:** Warm white light appears more yellow or orange, resembling the warm glow of traditional incandescent bulbs or candlelight.
- **Characteristics:** Warm white light creates a cozy and inviting atmosphere.
- **Common Uses:** It is often used in residential spaces, such as living rooms, bedrooms, and dining areas, to create a relaxed and comfortable ambiance.

3.2.2 Neutral White Lamps:

- **Colour Temperature:** Typically ranges from 3000K to 4000K.
- **Appearance:** Neutral light is neither too warm nor too cool, appearing as a natural white nor off-white light.
- **Characteristics:** It provides a balanced and versatile illumination, suitable for various settings.
- **Common Uses:** Neutral light is used for general or task lighting in homes, offices, and commercial spaces where a neutral and clear lighting environment is desired.

3.2.2 Cool White Lamps:

- **Colour Temperature:** Generally more than 4000K.
- **Appearance:** Cool white light appears whiter and has a slightly bluish or cool-toned hue compared to warm white light.
- **Characteristics:** Cool white light is often associated with a more vibrant and energetic atmosphere.
- **Common Uses:** It is commonly used in commercial and industrial settings, as well as task-oriented spaces like kitchens, bathrooms, and offices, where clarity and visibility are important.

The choice between warm white and cool white lamps depends on various factors, including your personal preference, the intended use of the lighting, and the ambiance you want to create. Warm white is favoured for its cozy and relaxing feel, while cool white is preferred for its crisp and vibrant appearance.

In regions with warm climate, people may prefer white light, which is often associated with daylight. White light can create a bright and refreshing atmosphere, which may complement the outdoor environment and the desire for well-lit spaces even when the sun is not shining. In colder or cooler regions, people may prefer warmer light tones, such as those resembling candlelight or incandescent bulbs.

Figure 3.2 Objects under lamps with different CCT

For practical applications, here are some considerations:

- **Residential Spaces:** Warm white is generally chosen for most residential areas, as it provides a comfortable and inviting atmosphere.
- **Task Lighting:** Cool white is often used in areas where tasks like reading or cooking are performed because it enhances visibility and concentration.
- **Commercial and Office Spaces:** Cool white is commonly used in offices, retail stores, and other commercial settings where a more alert and focused environment is desired.
- **Art and Display Lighting:** The choice of colour temperature can impact how artwork and displays appear. Cool white may be preferred for art galleries and jewellery stores to make colours and details pop.
- **Outdoor Lighting:** The choice of colour temperature for outdoor lighting depends on the specific purpose. Warm white is often chosen for landscape and garden lighting to create a welcoming outdoor atmosphere, while cool white may be used for security lighting and pathways for better visibility.

Ultimately, the selection of warm white or cool white lamps should align with your lighting goals, the function of the space, and your aesthetic preferences.

3.3 Colour Rendering Index (CRI):

Colour rendering defines how accurately a light source renders the colours of objects it illuminates compared to a natural or ideal light source, such as daylight. The CRI is measured

from 0 to 100 where the maximum value indicates that colours under artificial light are displayed in the same way as in natural sunlight.

The higher the CRI, the better the colour rendering ability of the light and the colours are displayed accurately which is shown in figure (3.3). While CRI is a valuable measurement for evaluating the colour quality of light sources in various indoor applications and also extremely important in the lighting industry. Its significance in outdoor lighting can be different due to specific environmental and functional considerations:

- **Outdoor Environment:** In outdoor settings, the colour of objects is influenced not only by the lighting source but also by natural daylight, weather conditions, and the colours of surrounding surfaces. As a result, the importance of high CRI may be somewhat diminished because the natural environment has a significant impact on colour perception

- **Functional Lighting:** Many outdoor lighting applications, such as street lighting, parking lot lighting, and security lighting, prioritize functionality and safety over colour accuracy. In these cases, the focus is on providing adequate illumination and visibility rather than perfect colour rendering.

while CRI is an essential consideration in indoor lighting design, but outdoor lighting focuses on functionality, energy efficiency, and cost-effectiveness, with colour rendering taking a secondary role in the overall design considerations.

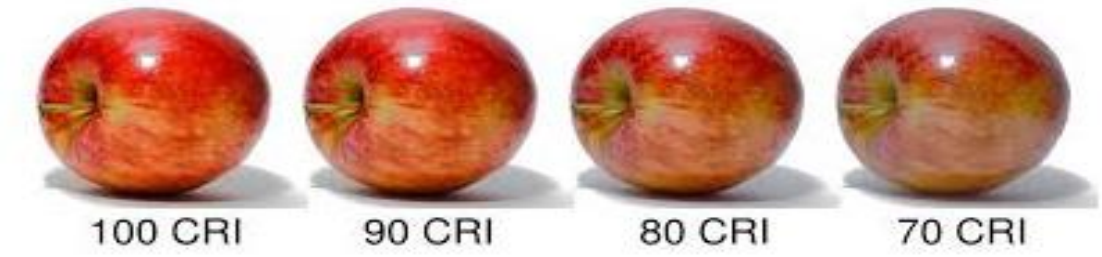

Figure 3.3 Objects with different CRI

3.4 Different types of Lamp Construction & operation

Outdoor lighting luminaires use various types of lamps to provide illumination in different settings and applications. Here are four common types of lamps used in outdoor lighting:

- **Metal Halide Lamps (MH)**
- **Fluorescent Tube Lights (FTL)**
- **High pressure sodium lamp (HPSV)**
- **White Light Emitting Diodes (WLED)**

3.4.1 Metal Halide Lamps (MH)

A metal halide lamp, often referred to as a metal halide light or MH lamp(figure 3.4.1), is a type of high-intensity discharge (HID) lamp commonly used for lighting in various applications, including outdoor lighting, sports arenas, industrial facilities, and indoor horticulture. A metal-halide lamp is an electrical lamp that produces light by an electric arc through a gaseous mixture of vaporized mercury and metal halides (compounds of metals with bromine or iodine).

Charles P. Steinmetz is the first to use halide salts in a mercury vapour lamp in 1912. He used the halides to correct colour and was successful, but he could not get a consistent arc. Robert Reiling used recent developments in the high pressure mercury vapour lamp to create the first reliable MH lamp in 1962.

Figure 3.4.1 Metal Halide Lamps

3.4.1.1 Components of a Metal Halide Lamp:

The main components of a metal halide lamp (Figure 3.4.1.1) include:

- **Glass bulb:** The outer envelope or bulb is typically made of a specialized type of glass that can withstand high temperatures and contains the other components of the lamp.

- **Base:** At the bottom of the lamp, there is a base that allows for electrical connection to a socket or fixture. This base typically contains the lamp's electrodes and electrical contacts.

- **Arc tube:** This is the heart of the metal halide lamp. The arc tube is made of a high-temperature quartz or ceramic material, and it contains the gases and metal halide salts necessary for producing light when an electric arc is established inside it.

- **Electrodes:** Metal halide lamps have two electrodes, usually made of tungsten, which are placed at either end of the arc tube. These electrodes are responsible for initiating and maintaining the electric arc within the tube.

- **Auxiliary electrode with high resistance**: Some metal halide lamps may have an auxiliary electrode with high resistance. This electrode helps initiate the arc when the lamp is started.

- **Glass stem:** This is a glass tube that connects the arc tube to the base of the lamp. It also holds the molybdenum wires that carry the current to the electrodes.

- **Molybdenum wire:** Molybdenum wires are used to support and position the arc tube inside the lamp. They possess non-magnetic properties and exhibit an exceptional resistance to high temperatures. Their primary function is to conduct electrical current to the electrodes while also effectively sealing the arc tube from exposure to air and moisture.

- **Argon gas:** Argon gas is typically used as a starting gas in metal halide lamps. It helps facilitate the initial breakdown of the gas and the formation of the electric arc.

- **Mercury vapour:** Metal halide lamps contain a small amount of mercury vapour, which plays a role in the lamp's overall light output and colour temperature.

- **Indium, thallium, and sodium iodides:** These are the metal halide salts that are added to the arc tube. These salts vaporize during lamp operation and produce specific wavelengths of light, contributing to the lamp's colour rendering and spectral output.

These components work together to create the high-intensity, efficient light output characteristic of metal halide lamps.

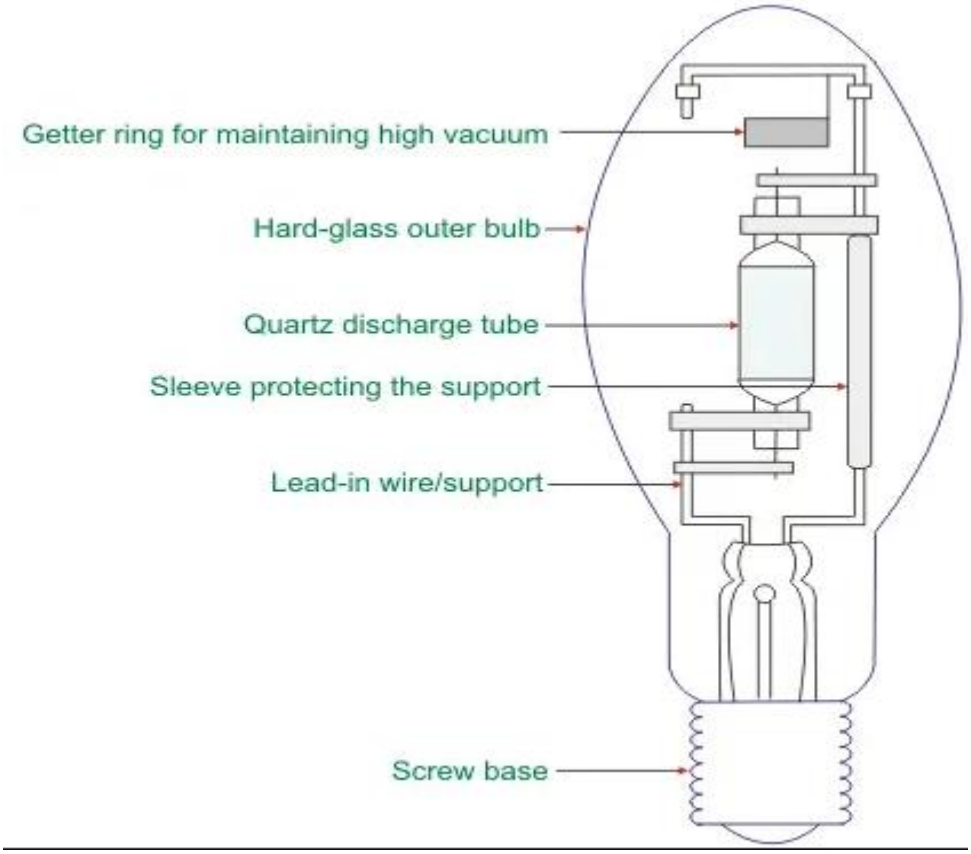

Figure 3.4.1.1 Constructional Feature of a Metal Halide Lamp

3.4.1.2 Working of Metal Halide Lamp:

Like other gas-discharge lamps such as the very-similar mercury-vapour lamps, metal-halide lamps produce light by ionizing a mixture of gases in an electric arc. In a metal-halide lamp, the compact arc tube contains a mixture of argon or xenon, mercury, and a variety of metal halides, such as sodium iodide and scandium iodide. [18]

- When the lamp is turned on, an electrical voltage is applied across the lamp's electrodes, creating an electric field within the arc tube. Initially, no arc is formed between the electrodes.

- The lamp includes an auxiliary electrode or starter electrode located near the main electrodes, typically attached to the glass stem. The purpose of this starter electrode is to create an initial discharge between itself and the main electrodes.

- A bimetal switch is integrated into the lamp's design. This switch is responsible for short-circuiting the starter electrode to the main electrode at the precise moment of lamp ignition.

- The initial discharge generated between the starter electrode and the main electrodes serves as a catalyst for igniting the lamp. This discharge heats up the metal halide salts present within the lamp.

- The starter electrode is designed with high resistance to limit the current during the initial arc formation. This controlled current is essential for safe and reliable lamp ignition.

- When started, the argon gas in the lamp is ionized first, which helps to maintain the arc across the two electrodes with the applied starting voltage.

- The heat generated by the arc and electrodes then ionizes the mercury and metal halides into a plasma, which produces an increasingly brighter white light as the temperature and pressure increases to operating conditions.

- The arc-tube operates at anywhere from 5–50 atm or more[19] (70–700 psi or 500–5000 kPa) and 1000–3000 °C.[20]

- Like all other gas-discharge lamps, metal-halide lamps have negative resistance (with the rare exception of self-ballasted lamps with a filament), and Metal halide lamp requires electrical or electronic ballast to stabilize and regulate the arc current flow and to deliver the proper voltage to the arc.

- To reach the full light output, metal halide lamps require around 3 to 5 minutes.

Metal halide lamps offer high-quality lighting with good colour rendering and efficiency. However, they have drawbacks such as slow start-up, colour instability, and environmental considerations. They are widely used for general lighting purposes both indoors and outdoors. They require special fixtures and ballasts to operate safely and efficiently. They also require proper maintenance to ensure their optimal performance and longevity.

3.4.2 Fluorescent Tube Lights (FTL)

A fluorescent lamp, also known as a fluorescent tube (figure 3.4.2), operates as a low-pressure mercury-vapour gas-discharge lamp that operates on the principle of fluorescence to generate visible light. When an electric current passes through the gas, it stimulates mercury vapour, leading to the emission of short-wave ultraviolet light. This ultraviolet light subsequently stimulate a phosphor coating located on the inner surface of the lamp, causing it to emit visible light. Here's a detailed explanation of the construction and working of fluorescent tube lights:

3.4.2.1 Construction of FTL:

- **Tube:** The most visible part of a fluorescent light fixture is the long, cylindrical glass tube. This tube is typically made of high-quality glass or, in some cases, plastic. It is sealed and contains the components necessary for the lamp to function. A fluorescent lamp tube is filled with a mix of argon, xenon, neon, or krypton, and mercury vapour. The pressure inside the lamp is around 0.3% of atmospheric pressure.[21]

- **Electrodes:** Inside the tube, at each end, there are electrodes. These are usually made of tungsten and are coated with an emissive material. The electrodes play a crucial role in initiating and maintaining the electrical discharge within the tube.

- **Phosphor Coating:** The interior surface of the glass tube is coated with a phosphor layer. This phosphor coating is responsible for emitting visible light when stimulated by ultraviolet (UV) radiation generated within the tube.

- **Mercury Vapour:** A small amount of mercury vapour is present within the tube. Mercury vapour is essential for the lamp's operation as it produces the UV radiation required to excite the phosphors.

- **Ballast:** Fluorescent tube lights require a ballast to regulate the electrical current flowing through them. Ballasts are typically magnetic (core and coil) or electronic. The ballast provides the necessary voltage and current to start and maintain the lamp's operation.

- **End Caps:** At each end of the tube, there are end caps that hold the electrodes in place and provide electrical connections to the ballast. They also contain a mechanism that allows the tube to be securely mounted in a fixture.

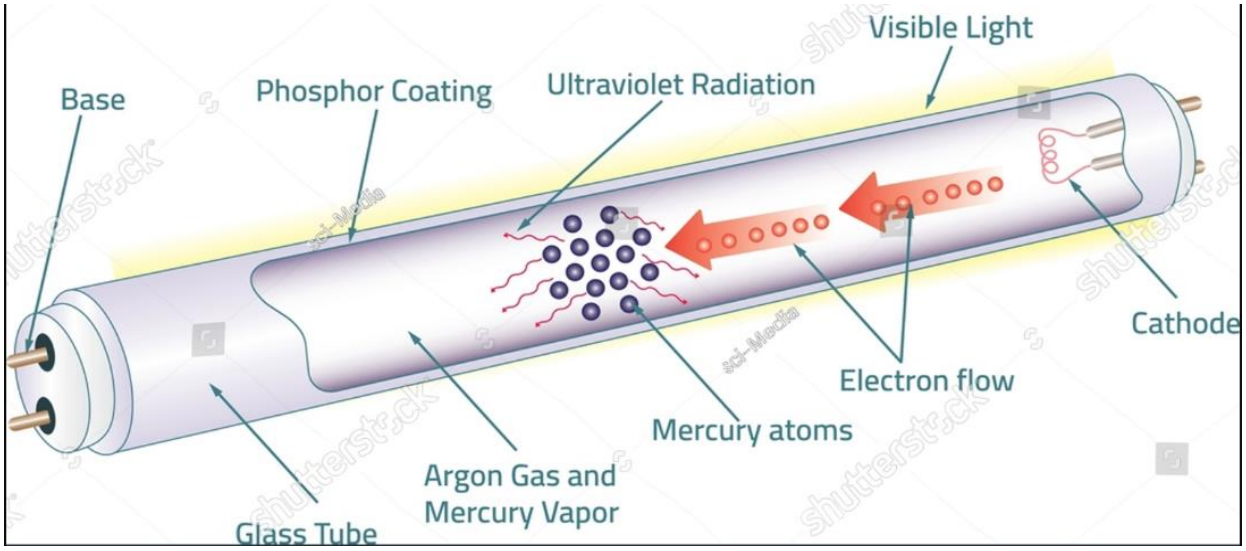

Figure 3.4.2 Fluorescent Tube Light

3.4.2.2 Working principle:

The operation of a fluorescent tube light (figure 3.4.2.2) can be broken down into several steps:

- **Starting:** When you turn on the fluorescent light, electrical voltage is applied across the electrodes at each end of the tube and the starter. But at that instant, no discharge happens, i.e., no lumen output from the lamp.

- **Bi metallic contact:** Bi-metallic contact is typically part of the starter mechanism. The starter is a small, replaceable component in the lighting fixture. The bi-metallic contact inside the starter plays a crucial role in the starting process (also shown in figure 3.4.2.3).

    - It consists of two strips of different metals (hence "bi-metallic") that are bonded together. These metals have different coefficients of thermal expansion, which means they expand at different rates when exposed to heat.

    - When you switch on the power supply to a fluorescent lighting fixture, full voltage is applied across both the lamp (fluorescent tube) and the starter through the ballast.

    - The first step in the starting process is to establish a glow discharge within the starter. This occurs because the gap between the bi-metallic contacts inside the starter is significantly smaller than the gap within the fluorescent lamp.

- The presence of full voltage across bi-metallic contact inside the starter leads to ionization of the gas inside the starter. This ionization process generates heat and results in the bending of the bimetallic strip within the starter.

- This bent configuration of the bimetallic strip causes it to come into contact with the fixed contact point. This creates a momentary short circuit. This short circuit allows a surge of current to flow through the lamp for a brief moment.

- The surge of current helps ionize the gas within the fluorescent tube. Ionization of the gas is necessary to create the initial discharge within the lamp.

- Once the fluorescent tube starts emitting light, the bi-metallic contact begins to cool down. As it cools, the two metal strips contract at different rates, causing the contact to return to its original position.

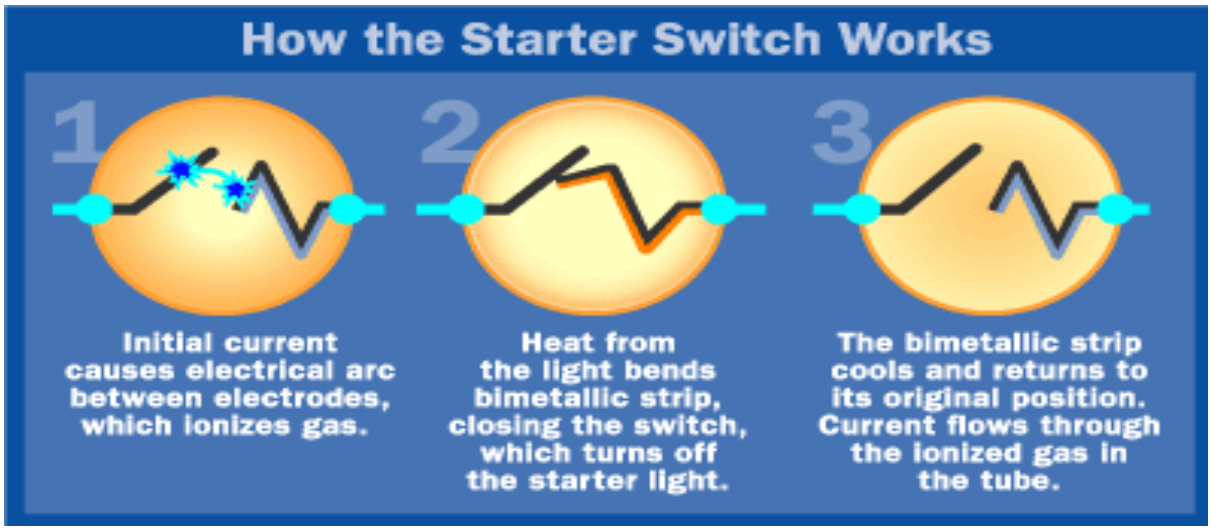

Figure 3.4.2.3 working of starter switch

- **Ballast:** When you turn on the power to a fluorescent lamp, a high initial voltage is required to establish the electrical discharge within the lamp. This high voltage is necessary to ionize the gas inside the fluorescent tube and create a conductive path for the current.

- The inductor (ballast) initially allows a higher voltage to pass through the lamp's electrodes (the filaments at each end of the tube) and the starter.

- When the voltage across the starter decreases or becomes negligible, the gas discharge within bi-metallic contacts stop. As a result, the bimetallic strip within the starter cools down and separates from the fixed contact.

- With the bi-metallic contacts disconnected, a brief high-voltage pulse is generated across the electrodes inside the fluorescent tube. This high-voltage pulse ionizes the gas inside the tube, allowing it to conduct electricity and create the initial discharge.

- **Ionization:** The electrical discharge generates a flow of electrons within the tube. These electrons collide with mercury atoms, causing them to become excited and ionized.

- **Ultraviolet Emission:** The ionized mercury atoms release energy in the form of ultraviolet (UV) radiation. UV radiation is invisible to the human eye but is crucial for the next step in the process.

- **Phosphorescence:** The UV radiation excites the phosphor coating on the interior surface of the tube. The phosphors absorb the UV radiation and then re-emit it as visible light. This is the light that we see and use for illumination.

- **Steady Operation:** Once the lamp is started, the ballast regulates the current flowing through the tube to maintain a stable and continuous discharge. The light output remains constant as long as the lamp is operational.

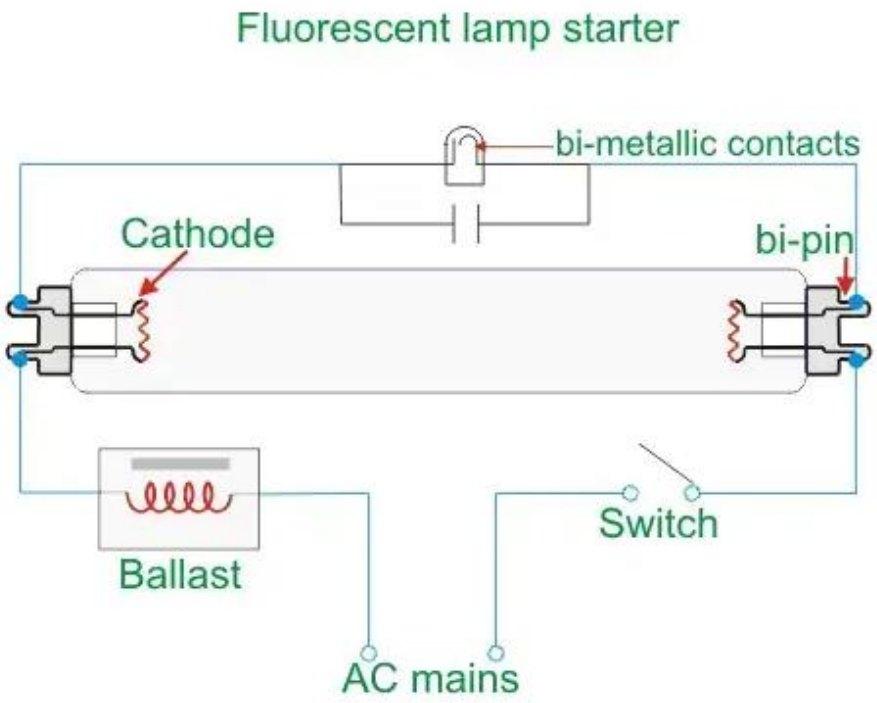

Figure 3.4.2.2 Diagram of FTL

Fluorescent tube lights are known for their energy efficiency because they produce more visible light per unit of electrical power compared to incandescent bulbs. A typical 100 watt tungsten filament incandescent lamp may convert only 5% of its power input to visible white light (400–700 nm wavelength), whereas typical fluorescent lamps convert about 22% of the power input to visible white light.[22] They are commonly used in various indoor and commercial lighting applications, offering a cost-effective and long-lasting lighting solution.

3.4.3 High Pressure Sodium Lamps or HPS Lamps

A sodium-vapour lamp is a type of gas-discharge lamp that harnesses the excited state of sodium to produce light primarily at a well-defined wavelength, typically around 589 nanometres (nm). This characteristic emission results in a distinct yellow-orange light output, making sodium-vapour lamps easily recognizable.

There are two main types of sodium-vapour lamps: low-pressure and high-pressure varieties. Low-pressure sodium lamps are exceptionally efficient but their yellow light restricts applications to outdoor lighting, such as street lamps, where they are widely used. [23]

High-pressure sodium lamps produce a broader spectrum of light compared to their low-pressure counterparts. Despite this broader spectrum, they still exhibit lower colour rendering capabilities compared to other types of lamps.[24] It's worth noting that low-pressure sodium lamps emit monochromatic yellow light, which can hinder colour perception, especially during night-time activities.

High-Pressure Sodium (HPS) lamps are a type of high-intensity discharge (HID) lighting commonly used for street lighting, security lighting, and industrial applications due to their high energy efficiency and long lifespan. They produce light by passing an electric current through a mixture of gases and vaporized sodium metal. Here's an overview of the construction and working principle of High-Pressure Sodium lamps:

3.4.3.1 Construction of High-Pressure Sodium:

The main components of a High-Pressure Sodium (Figure 3.4.3.1) include:

- **Outer Bulb:** HPS lamps typically consist of a borosilicate glass outer bulb that protects the inner components and contains the high-pressure gases. The outer bulb is designed to withstand the high operating temperatures of the lamp.

- **Inner Arc Tube:** Inside the outer bulb, there is a smaller, sealed inner arc tube made of a translucent ceramic material (usually alumina) that can withstand high temperatures. The arc tube contains the key components for generating light.

- **Electrodes:** At each end of the arc tube, there are tungsten electrodes. These electrodes are responsible for initiating and maintaining the electrical discharge within the lamp.

- **Sodium (Na) and Mercury (Hg):** The arc tube contains a small amount of metallic sodium and mercury, along with a mixture of inert gases such as xenon or argon. The sodium is in solid form when the lamp is off.

- **Phosphor Coating:** Some HPS lamps have a phosphor coating on the inside of the arc tube. This coating helps convert some of the ultraviolet (UV) light emitted by the lamp into visible light, improving the lamp's colour rendering properties.

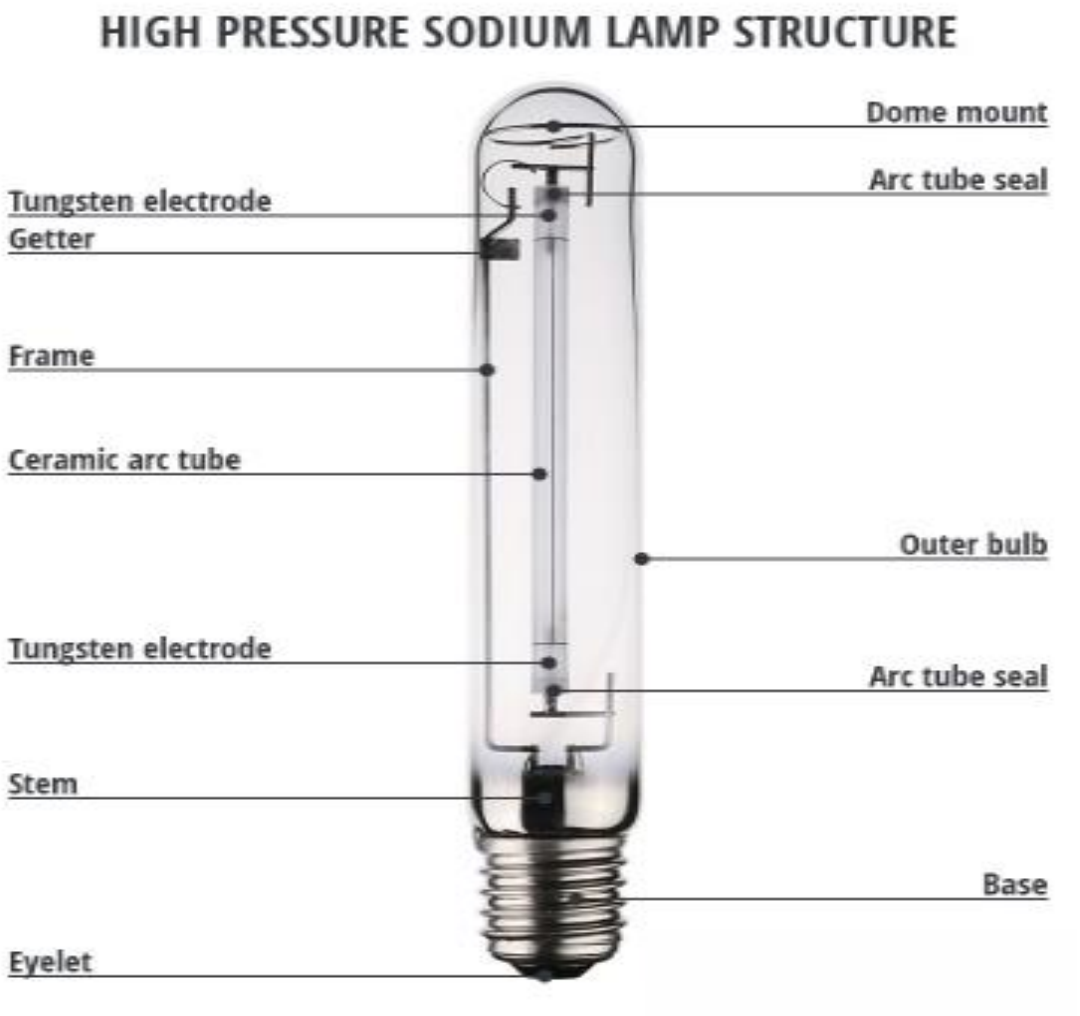

Figure 3.4.3.1 Construction of High-Pressure Sodium

3.4.3.2 Working Principle High-Pressure Sodium:

The operation of an HPS lamp can be broken down into several key steps and Diagram of a high-pressure sodium lamp is shown in figure 3.4.3.2.

- **Ignition:** When the lamp is first turned on, an electrical voltage is applied across the electrodes. This voltage initiates an electrical discharge between the electrodes, creating an arc of high-intensity light**.**

- **Sodium Vaporization:** As the electrical discharge continues, it heats up the sodium metal within the arc tube. The heat causes the sodium to vaporize and become ionized, creating a bright yellow light. This yellow light is the characteristic colour of HPS lamps.

- **Mercury Vaporization:** The mercury in the arc tube also vaporizes due to the high temperatures. The mercury vapour plays a crucial role in producing additional UV light.

- **Phosphor Conversion**: In HPS lamps with a phosphor coating, some of the UV radiation produced is converted into visible light by the phosphor material. This process helps improve the colour quality of the light emitted by the lamp.

- **Steady State:** Once the lamp is fully operational, it reaches a steady state where the sodium and mercury vaporized gases maintain the electrical discharge. The lamp continues to emit a consistent, high-intensity yellow light.

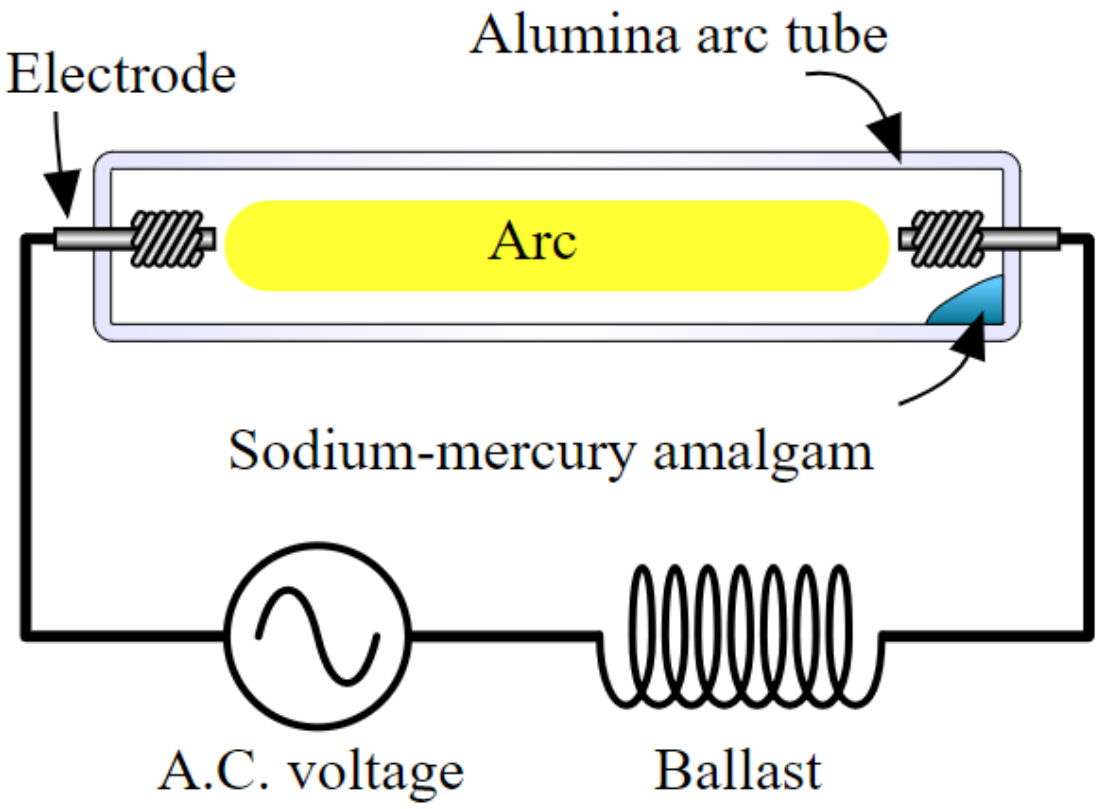

Figure 3.4.3.2 Diagram of a high-pressure sodium lamp

High-Pressure Sodium lamps are known for their high luminous efficacy, which means they produce a significant amount of light for the energy consumed. However, their colour rendering index (CRI) is relatively low, making them less suitable for applications where

accurate colour representation is essential. Additionally, HPS lamps have a warm-up time and may take a few minutes to reach their full brightness after ignition.

3.4.4 Light Emitting Diodes (LED)

LEDs (Light Emitting Diodes) are semiconductor devices that emit light when an electric current flows through them. Different types of LEDs are shown in figure 3.4.4.They are constructed using semiconductor materials and operate based on the principles of electroluminescence.

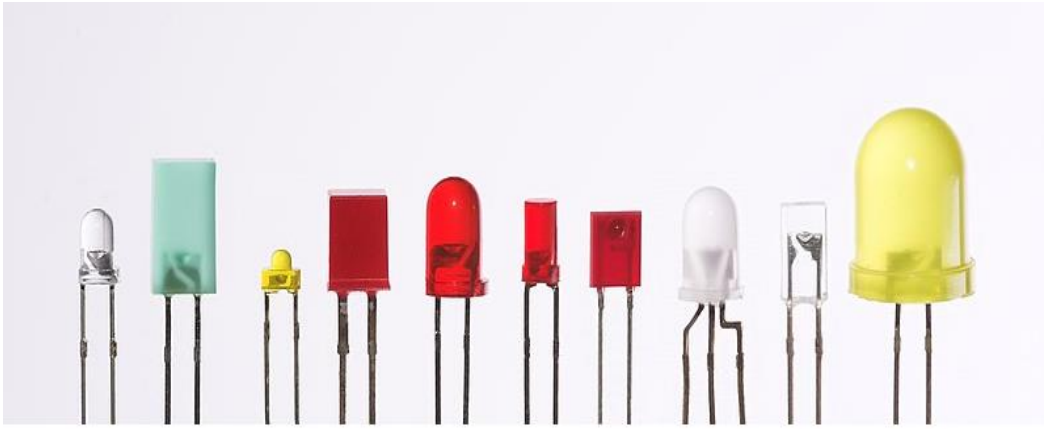

Figure 3.4.4 LEDs are produced in a variety of shapes and sizes.

3.4.4.1 Construction of LED:

The physical structure of an LED is designed to facilitate this light emission. Here's a simplified explanation of the key components and structure of a typical LED and also shown in figure 3.4.4.1:

- **Semiconductor Material:** LEDs are typically made from semiconductor materials. The choice of semiconductor material determines the colour of the emitted light. Common materials include gallium arsenide (GaAs), gallium phosphide (GaP), indium gallium nitride (InGaN), and aluminium indium gallium phosphide (AlInGaP). P-N

Junction: The heart of an LED is a p-n junction. This is a boundary where two types of semiconductor material meet: the p-type and n-type regions.

- **P-Type Region:** In this region, the semiconductor material is doped with elements that create an excess of "holes," which are positive charge carriers.

- **N-Type Region:** In this region, the semiconductor material is doped with elements that introduce an excess of free electrons, which are negative charge carriers.

- **Electrodes:** Each end of the LED is connected to an electrode. The anode (positive electrode) is attached to the p-type material, and the cathode (negative electrode) is connected to the n-type material.

- **Epoxy lenses:** Epoxy lenses are used to control the direction and dispersion of light emitted by LEDs. They can focus, diffuse, or shape the light pattern according to the desired application. Epoxy lenses are typically made from a transparent epoxy resin material that is molded or cast into a specific shape to achieve various optical effects.

- **Reflective cavity:** A reflective cavity, also known as a reflective cup or reflector, is a component commonly used in high-power and high-intensity Light Emitting Diodes (LEDs) to control and enhance the directionality of emitted light. The reflective cavity is typically located behind the LED chip, and its primary purpose is to reflect and redirect light in a specific direction.

- **Lead frame:** It serves as the structural and electrical foundation for the LED package, providing a framework for connecting the LED chip or die to external circuitry.

- **Package:** LEDs are typically encapsulated in a protective package made of epoxy or other materials. The package helps protect the delicate semiconductor material from environmental factors and physical damage.

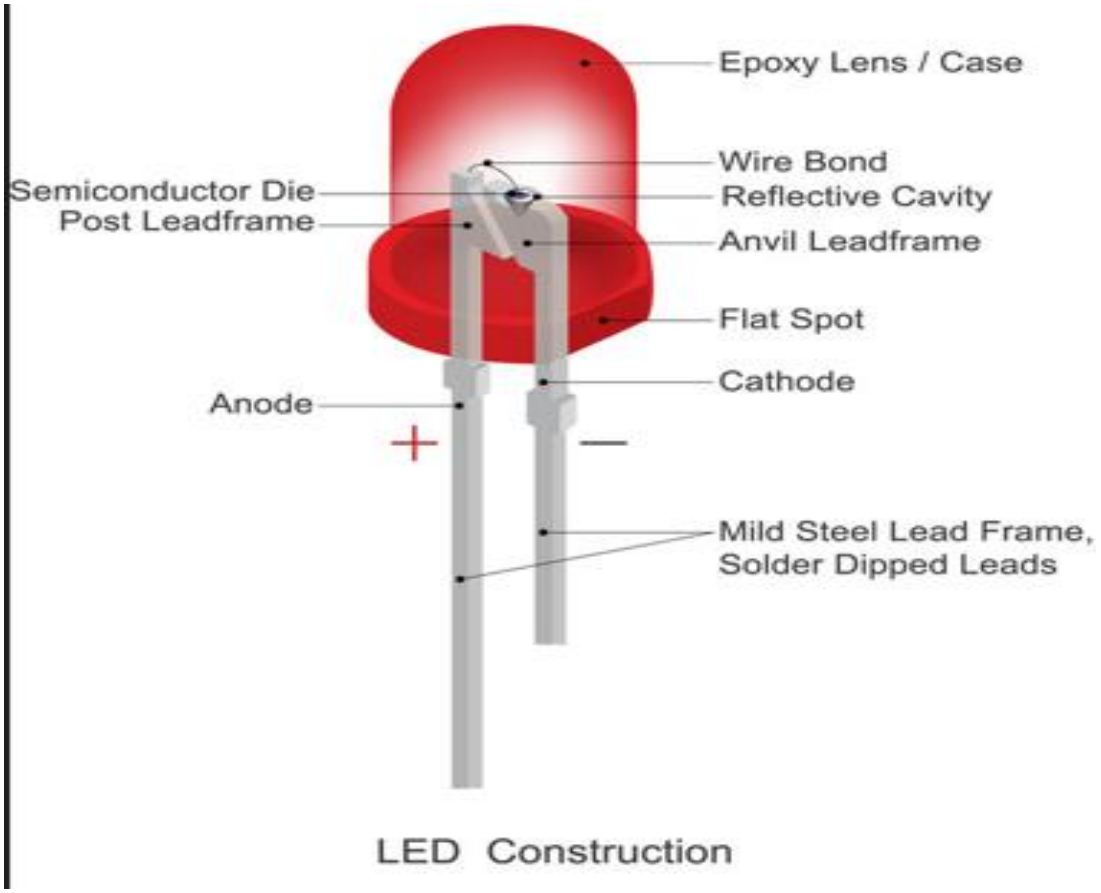

Figure 3.4.4.1 LED Construction

3.4.4.2 Working Principle:

The working principle of an LED is based on the process of electroluminescence, which occurs at the p-n junction within the semiconductor material (shown in figure 3.4.4.2):

- **Electron-Hole Recombination:** When a forward-biased voltage (positive voltage on the anode, negative voltage on the cathode) is applied across the LED, electrons from the n-type region move towards the p-type region, and holes from the p-type region move towards the n-type region. As they cross the p-n junction, electrons and holes recombine.

- **Photon Emission:** When electrons recombine with holes at the p-n junction, they release energy in the form of photons (light). The energy of these photons is determined by the energy band gap of the semiconductor material. The energy of a photon is indeed directly related to the band gap size of the semiconductor material used in an LED. The relationship: $E = h\nu = hc/\lambda$, explains how the energy (E) of a photon is determined by

its frequency (ν) or wavelength (λ).The colour of the emitted light corresponds to the energy of these photons.[25]

- **Light Emission:** The emitted photons are emitted in a specific direction, typically perpendicular to the surface of the p-n junction. This directional emission makes LEDs suitable for various lighting and display applications.

- **Continuous Operation:** As long as a forward-biased voltage is applied, the electron-hole recombination process continues, resulting in a continuous emission of light. The intensity (brightness) of the light is directly proportional to the current passing through the LED.

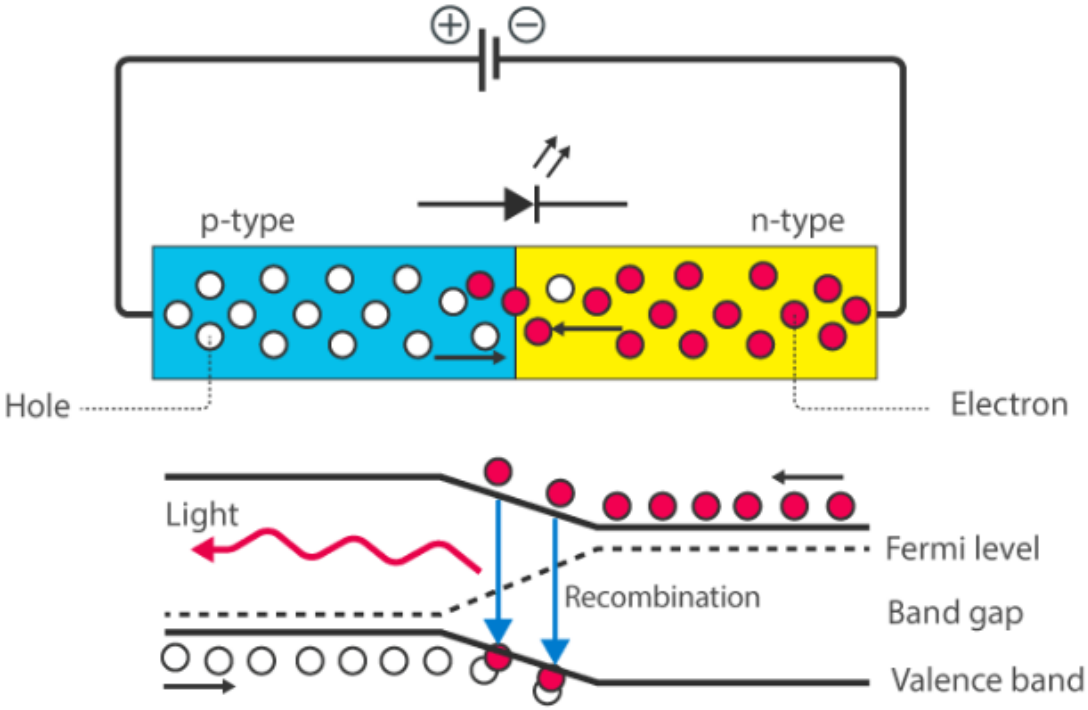

Figure 3.4.4.2 Working Diagram of LED

3.4.4.3 Key Points for LEDs:

- LEDs are highly efficient at converting electrical energy into light, and they emit minimal heat.
- The colour of the light depends on the semiconductor material used in the LED.
- LEDs have a fast response time and can be quickly turned on and off, making them suitable for various applications, including displays, indicators, and general lighting.
- Different semiconductor materials and engineering techniques are used to produce LEDs with specific colours and characteristics for different applications.
- The relationship between light colour (energy) and band gap of an LED is demonstrated in Table 3.4.4.3 below.

Color of Light	Wavelength (nm)	Energy (eV & kJ/mol)
Violet	410	3.0 (290)
Blue	480	2.6 (250)
Green	530	2.3 (225)
Yellow	580	2.1 (205)
Orange	610	2.0 (195)
Red	680	1.8 (175)

Table 3.4.4.3 Relationship between LED Colour, Wavelength and Energy of Light.

3.4.4.4 White Light LEDs or White LED Lamps

LED lamps have gained immense popularity due to the exceptional efficiency of LEDs in converting input power into light output. LEDs emit more lumens per watt than incandescent light bulbs. [26] As a result, white light has become the preferred choice for general-purpose lighting. To generate white light using LEDs, two distinct methods are commonly employed:

- **RGB Mixing:**

- **Principle:** RGB mixing involves using three separate LED chips emitting red (R), green (G), and blue (B) light. By adjusting the intensity of each of these three colours, it's possible to create a wide range of colours, including white, by blending them in various proportions.

- **Advantages:**
  - **High quantum efficiency:** This method allows for precise control over colour and intensity.

  - **Colour tunability:** RGB LEDs can produce a wide range of colours, which can be dynamically adjusted as needed.

  - **Accurate colour rendering:** RGB LEDs can achieve high colour rendering index (CRI) values, which is important for applications where accurate colour representation is crucial, such as in stage lighting and displays.

- **Phosphor Coating:**

  - **Principle:** Phosphor-based LEDs method involves coating LEDs of one colour (mostly blue LEDs made of InGaN) with phosphors of different colours to form white light.[27]

  - **Advantages:**
    - **Simplicity and cost-effectiveness:** Phosphor-converted LEDs (PC-LEDs) are often more straightforward to manufacture and are cost-effective for general lighting applications.

    - **Energy-efficient:** PC-LEDs can be highly energy-efficient, making them suitable for general-purpose lighting, including residential, commercial, and street lighting.

    - **High luminous efficacy:** PC-LEDs can achieve high luminous efficacy (lumens per watt), making them energy-efficient.

Each method has its place in the LED lighting industry, and the choice depends on the specific application and requirements:

- RGB mixing is often used in applications where precise control over colour and dynamic colour changes are important, such as in stage lighting, displays, and some architectural lighting designs.

- Phosphor coating is widely used in general lighting applications, where cost-effectiveness and energy efficiency are paramount. Many LED bulbs and

fixtures available for everyday use employ phosphor-converted LEDs to produce white light.

Certain blue LEDs and cool-white LEDs can exceed safe limits of the so-called blue-light hazard as defined in eye safety specifications such as "ANSI/IESNA RP-27.1–05: Recommended Practice for Photo biological Safety for Lamp and Lamp Systems".[28]

Chapter: 4 ADAPTATION LUMINANCE

4.1 Introduction

Mesopic photometry is an advancement in lighting measurement with significant relevance to road lighting applications. The commission Internationale de l'Eclairage (CIE) 191:2010 system, designed for mesopic photometry, relies on knowledge of adaptation luminance (La) within the visual environment. Adaptation luminance represents the average Luminance level within the unspecified visual adaptation field in the scene. However, the visual adaptation field lacks precise definitions regarding its size, shape, or location within the visual field. The concept of adaptation state in vision refers to the condition or state of the visual system's sensitivity to light, particularly regarding how it perceives different levels of luminance and spectral information. In this study the adaptation state is defined as the sum of two components: the average photopic luminance of the visual adaptation field (L_p) and the veiling luminance (L_{veil}). The veiling luminance, L_{veil} is an increment to the adaptation state caused by high-luminance sources due to intra-ocular scatter. [29]

4.2 Light Adaptation:

Light adaptation is a fundamental process in vision that allows the human eye to adjust its sensitivity to varying levels of illumination. It involves changes in the sensitivity of the photoreceptor cells in the retina. Light adaptation ensures that your visual system remains responsive and functional across a wide range of lighting conditions, from dimly lit to bright light or vice versa. This adaptive process helps maintain visual comfort and allows you to perceive objects and details effectively in different environments. With light adaptation, the eye has to quickly adapt to the background illumination to be able to distinguish objects in this background. The photochemical reaction is:

$$\text{Rhodopsin} \rightleftharpoons \text{retinal} + \text{opsin}$$

- **Increment threshold**

  Using increment threshold experiments, light adaptation can be measured clinically. [30] In an increment threshold experiment, a test stimulus is presented on a background of a certain luminance, the stimulus is increased until the detection threshold is reached against the background. This method yields monophasic or biphasic threshold-versus-intensity (T vs I) curves for both cones and rods, providing valuable insights into the process.

  When the threshold curve for a single system (i.e., just cones or just rods) is taken in isolation it can be seen to possess four sections (also shown in figure 4.2): [31]

  - **Dark light:** The threshold in this portion of the T vs I curve is determined by the dark/light level. Sensitivity is limited by

neural noise. The background field is relatively low and does not significantly affect threshold.

- **Square root law:** This part of the curve is limited by quantal fluctuation in the background. The visual system is usually compared with a theoretical construct called the ideal light detector. To detect the stimulus, the stimulus must sufficiently exceed the fluctuations of the background (noise).

- **Weber's law:** Threshold increases with background luminance proportional to the square root of the background.[32]

- **Saturation:** At saturation, the rod system becomes unable to detect the stimulus. This section of the curve occurs for the cone mechanism under high background levels.[33]

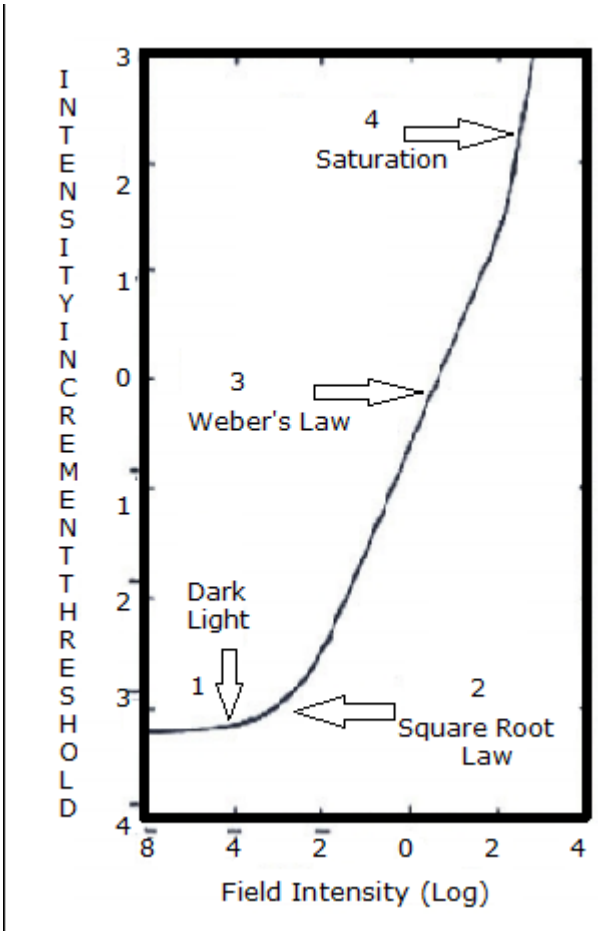

Figure 4.2 Schematic of the increment threshold curve of the rod system

4.3 Variables Influencing Adaptation Luminance

It is difficult to determine an adaptation luminance for a real outdoor lit scene because scenes usually have complex luminance distributions (LDs), while laboratory experiments underpinning the mesopic photometry system were basically conducted with uniform luminance distributions (LDs). The LDs for real lit scenes contain not only non-uniform lit road surfaces but also the dark sky or high-luminance sources such as luminaires. Their luminance ranges are extremely wide and to what luminance the observers' eyes adapt has been a big question.

Several studies have explored the factors influencing peripheral luminance adaptation within the mesopic range, including factors such as eye movements (EMs),surrounding luminance effect (SLE) on the visual system of observers, luminance distributions (LDs) and 'area of measurement' (AOM).[34][35]

To model the four factors and their derivatives as distribution functions in the field of view, two coordinate systems are introduced. One co-ordinate system is a spherical coordinate system (θ,φ), where θ is the horizontal angle and φ is the vertical angle, to basically present the position on the retina. This will be referred to as the 'retinal coordinate system'. Another coordinate system is also a spherical coordinate system that has the same structure with different symbols (θ', φ'), but fixed to the world outside the observer, not to the observer's visual system. This will be referred as the 'object coordinate system'. Both coordinate systems share the origin at the observer's eye position as shown in Figure 4.3

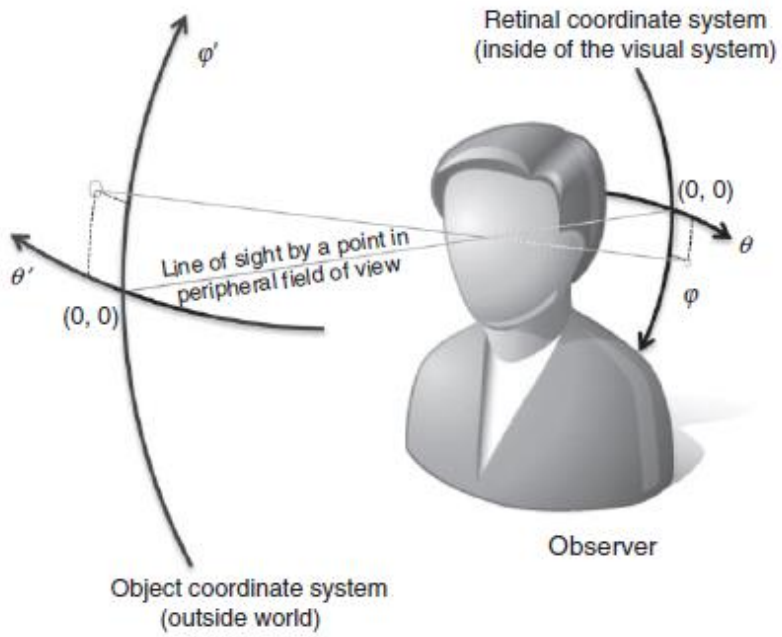

Figure 4.3 Object coordinate system and retinal coordinate system. Both coordinate systems share a pivot at the observer's eye position.

When discussing the adaptation state of an arbitrary peripheral point in the field of view, the point (θ, φ) = (0,0) in the retinal coordinate system corresponds to a peripheral point, not the fovea. The point (θ′,φ′) = (0,0) in the object coordinate system is a point corresponding to the point (θ,φ)=(0,0) in the retinal coordinate system when the observer looks at an 'original point' in the object coordinate system. Since the position of the original point does not matter for the simulation process, it is not given specifically. When the observer moves his/her line of sight, the retinal coordinate system follows the movement while the object coordinate system does not.

4.3.1 Luminance distributions (LDs)

The luminance distribution (LD) within an illuminated environment is a crucial factor influencing adaptation luminance. Typically, the range of luminance in outdoor night-time lighting is considerably broader than that in indoor settings. According to outdoor lighting guidelines, such as CIE 115:2010, an average luminance of 0.3 to 2.0 cd/m² is recommended. [4]These recommendations also permit some degree of non-uniformity, allowing for a minimum luminance, often situated at the extremities of illuminated areas, to be as low as 0.1 cd/m². Conversely, within the same illuminated scene, there can various bright light sources, such as luminaires, headlamps of oncoming cars or luminous signs. For instance, certain luminaires can exhibit luminances exceeding 10,000 cd/m². In this study, the luminance distribution is represented as a function L(θ', φ') relative to the object coordinate system (θ', φ'). Luminance

distribution affects the contrast within a scene. For example, a black text on a white background represents high contrast, while shades of gray on a gray background represent low contrast.

4.3.2 Eye movements (EMs)

Our eyes are not stationary, and they constantly move to gather information from our surroundings. These eye movements can affect adaptation, as different parts of the scene may have different luminance levels. Our eyes continuously adapt to the changing luminance as we shift our gaze. The Eye Movements are modelled as a two-dimensional (2D) Gaussian probability density distribution $f_{EM}(\theta',\varphi')$ with no co-relation expressed as[36]

$$\mathbf{f_{EM}(\theta',\varphi')} = \frac{\mathbf{1}}{\mathbf{2\pi\sigma_{\theta'}\sigma_{\varphi'}}} \times \boldsymbol{e}^{\left[-\frac{\mathbf{1}}{\mathbf{2}}\left\{\left(\frac{\boldsymbol{\theta'}}{\boldsymbol{\sigma_{\theta'}}}\right)^{\mathbf{2}}+\left(\frac{\boldsymbol{\theta'}}{\boldsymbol{\sigma_{\varphi'}}}\right)^{\mathbf{2}}\right\}\right]} \boldsymbol{d\theta' d\varphi'}$$

Where, $\sigma_{\theta'}$, $\sigma_{\varphi'}$ are standard deviations (SD) for the horizontal and vertical directions. This function is defined with respect to the object coordinate system. It should be noted that the EM function is centered at the origin of the object coordinate system so that it just expresses relative movement of the line of sight.

4.3.3 Surrounding luminance effect (SLE)

The SLE is an increment of the adaptation luminance at a point in the field of view caused by the surrounding luminance. It is due to stray light within the human eye and/or lateral neural interactions. For foveal vision, this factor is called as 'veiling luminance' and has been investigated for many years. The angular characteristic, which is the luminance increment as a function of the visual angle between a source causing the veiling luminance and the task point (fovea), is modelled as some equations. Three veiling luminance models are: Fry (equation 1) [37]; CIE general disability glare equation (equation 2) [14]; and Uchida and Ohno (equation 3) [16].Since the mesopic photometry system is based on peripheral task performances, SLE for peripheral vision should be characterized and be taken into account.

$$\mathbf{L_{veil}} = \mathbf{9.2}\sum\frac{\boldsymbol{E}}{\boldsymbol{\theta(\theta+1.5)}} \qquad (1)$$

$$\mathbf{L_{veil}} = \left[\frac{10}{\theta^3} + \left\{\frac{5}{\theta^2} + \frac{0.1p}{\theta}\right\}.\left\{1 + \left(\frac{A}{62.5}\right)^4\right\} + 0.0025p\right] E \quad (2)$$

$$\mathbf{L_{veil}} = \frac{260}{\theta^3} E_v \quad (3)$$

Where, L_{veil} is the veiling luminance caused by a high-luminance light source; θ is the angle (in degrees) between the line of fixation and the high-luminance source; A is the age in years; and p is the eye pigmentation factor. E_v is the illuminance on a plane perpendicular to a straight line between the observer's eye and the light source. E is the illuminance on a vertical plane at the observer's eye. Consequently, E is E_v multiplied by the cosine of θ.

4.3.4 Area of measurement (AOM)

The study [36] adopts a method to calculate the average adaptation luminance within a designated area of measurement (AOM). An AOM represents an illuminated area covered by a lighting installation and is assessed through photometric measurements to validate the effectiveness of the installation. For example, consider a roadway surface targeted for illumination in the lighting design process; this roadway surface serves as the specific AOM. Typically, when viewed from the perspective of drivers, this surface takes on the shape of a trapezoidal area. For the adaptation luminance simulation, AOM is modelled as a 2D function $f_{AOM}(\theta', \varphi')$ with respect to the object coordinate system (θ', φ') .This function takes a value of one for inside the AOM and zero for outside the AOM.

4.4 Simulation Method for Adaptation Luminance

A Simulation Method for calculation of adaptation luminance based on analysis of luminance distribution of light scene consists of four step:

4.4.1. Effective LD calculation
4.4.2. Adaptation LD calculation
4.4.3. AOM hit probability distribution calculation
4.4.4. Adaptation luminance calculation

4.4.1 Effective LD calculation

Effective luminance is the luminance after taking the SLE into account. It is the adaptation LD when the observer's line of sight is fixed. In this case, if there were no SLE, then each point of the retina would adapt to a nominal luminance from each direction. However, light from each direction slightly scatters to an area surrounding the corresponding point in the retinal coordinate system, as characterized as SLE. As a result, SLEs due to the light from each direction overlap each other and slightly diffuse the projected LD.

Since the observer's line of sight is assumed to be fixed at the original point for the effective LD, the LD projected to the retinal coordinate system, $L(\theta,\varphi)$ is determined from LD $L(\theta',\varphi')$ by substituting as $(\theta,\varphi) = (\theta',\varphi')$. Then the effective LD $L_{effective}(\theta,\varphi)$ can be calculated by convolution of the projected LD and the SLE as

$$\mathbf{L_{effective}(\theta , \varphi) = (L * f_{SLE}) (\theta , \varphi)}$$

4.4.2 Adaptation LD calculation

Although the effective LD is the adaptation LD when the line of sight is fixed, actually the observers' line of sight moves as expressed by EM. If a point in the retinal coordinate system looks at two points with 50–50 probability due to the EM, the adaptation luminance can be considered the average of the effective luminances for the two points. Generalizing this concept, each point of the retinal coordinate system adapts to an average effective luminance weighted by the EM. This process can be expressed as

$$\mathbf{L_a(\theta , \varphi) = (L_{effective} * f_{EM}) (\theta , \varphi)}$$

Where, $L_a(\theta,\varphi)$ is the adaptation LD. The $f_{EM}(\theta,\varphi)$ is derived from $f_{EM}(\theta',\varphi')$ just by substituting as $(\theta,\varphi) = (\theta',\varphi')$.

4.4.3. AOM hit probability distribution calculation

Each point on the retinal coordinate system has different probability to look inside the AOM, depending on the EM. For instance, a pedestrian's lower parts of the retinal coordinate system more probably look at a street surface (AOM) than the upper parts of the retinal coordinate system. The probability for each point on the retinal coordinate system to look inside AOM. $P_{AOM}(\theta,\varphi)$ can be calculated as

$$\mathbf{P_{AOM}(\theta,\varphi) = (f_{AOM} * f_{EM}) (\theta , \varphi)}$$

4.4.4. Adaptation luminance calculation

Finally, the adaptation luminance of the AOM, which is the average adaptation luminance weighted with the AOM hit probability distribution, is derived as

$$\mathbf{L_{a,AOM}} = \frac{\iint \mathbf{L_a(\theta,\varphi).P_{AOM}(\theta,\varphi)d\theta d\varphi}}{\iint \mathbf{P_{AOM}(\theta,\varphi)d\theta d\varphi}}$$

Where, $L_{a,AOM}$ is the adaptation luminance of AOM.

Chapter: 5 EXPERIMENTAL PROCEDURE

As discussed in Chapter 4, Adaptation luminance depends on four factors:

a) Luminance Distribution
b) Eye Movement
c) Surrounding Luminance Effect
d) Area of Measurement.

In this project Luminance Distribution, Surrounding Luminance Effect and Area of Measurement have been considered. To calculate Surrounding Luminance Effect model proposed by Uchida &Ohno is taken into account.
According to, Uchida & Ohno model, Veiling Luminance is calculated by the equation,

$$\mathbf{L_{veil} = \frac{260}{\theta^3} E_v}$$

Where,

E_v is the vertical illuminance due to the SLE source and θ is the visual angle between the source and a task point in degrees.

5.1 Calculation Method

5.1.1 Determination of Photopic Luminance (Theoritical)

- STEP 1. The luminous intensity values, often represented in an I-Table, for various luminaires are generated from an IES file.
- STEP 2. C, γ angle of all grid points are calculated for given Layout.[**Figure 5.2**]
- STEP 3. Luminous Intensity values are interpolated from the known I-Table values for all grid point.
- STEP 4. Calculation of illuminance (E) by using Inverse square law, using MATLAB.

$$\mathbf{E = \frac{I(C,\gamma)(\cos\theta)^3}{h_m^2}}$$

- STEP 5. Reflectance (q) values of all grid points are measured by using Lux meter and Luminance meter.

- STEP 6. We multiplied the illuminance (E) values by reflectance (q) values to get the theoretical photopic luminance.

$$\mathbf{L_p = qE}$$

5.1.2 Determination of Mesopic Luminance

To design lighting in the mesopic region, the initial step involves converting the photopic luminance into its corresponding mesopic luminance. We don't calculate mesopic luminance in this paper. But this transformation is achieved through a series of distinct steps.

- **STEP 1**. S/P ratio values of the lamps is determined by Scotopic/Photopic meter.

- **STEP 2**.Mesopic luminance values are interpolated from the known photopic luminance values and s/p ratios using CIE191-2010 table (Table 5.1).The table is shown below.

		Photopic luminance / cd·m^{-2}						
	S/P	0,01	0,03	0,1	0,3	1	3	4,5
LPS ~	0,25	0,002 5	0,014 5	0,070 5	0,246 7	0,913 0	2,926 5	4,478 2
	0,35	0,003 5	0,017 4	0,075 0	0,254 5	0,925 3	2,936 7	4,481 2
	0,45	0,004 5	0,019 8	0,079 3	0,262 0	0,937 3	2,946 8	4,484 2
HPS ~	0,55	0,005 7	0,022 0	0,083 4	0,269 3	0,949 2	2,956 8	4,487 2
	0,65	0,006 9	0,023 9	0,087 3	0,276 4	0,960 8	2,966 6	4,490 1
	0,75	0,007 9	0,025 8	0,091 1	0,283 3	0,972 2	2,976 3	4,492 9
	0,85	0,008 8	0,027 5	0,094 7	0,290 1	0,983 5	2,985 9	4,495 8
	0,95	0,009 6	0,029 2	0,098 3	0,296 7	0,994 5	2,995 3	4,498 6
	1,05	0,010 4	0,030 8	0,101 7	0,303 2	1,005 4	3,004 6	4,501 4
MH warm white ~	1,15	0,011 1	0,032 3	0,105 1	0,309 6	1,016 1	3,013 9	4,504 1
	1,25	0,011 8	0,033 8	0,108 3	0,315 8	1,026 7	3,023 0	4,506 8
	1,35	0,012 5	0,035 3	0,111 5	0,322 0	1,037 1	3,031 9	4,509 5
	1,45	0,013 2	0,036 7	0,114 7	0,328 0	1,047 3	3,040 8	4,512 2
	1,55	0,013 8	0,038 1	0,117 8	0,333 9	1,057 5	3,049 6	4,514 8
	1,65	0,014 5	0,039 5	0,120 8	0,339 8	1,067 4	3,058 2	4,517 4
	1,75	0,015 1	0,040 8	0,123 8	0,345 5	1,077 3	3,066 8	4,520 0
	1,85	0,015 7	0,042 1	0,126 7	0,351 2	1,087 0	3,075 3	4,522 5
	1,95	0,016 3	0,043 4	0,129 5	0,356 8	1,096 6	3,083 6	4,525 0
	2,05	0,016 9	0,044 6	0,132 4	0,362 3	1,106 0	3,091 9	4,527 5
	2,15	0,017 4	0,045 9	0,135 2	0,367 7	1,115 4	3,100 1	4,529 9
	2,25	0,018 0	0,047 1	0,137 9	0,373 1	1,124 6	3,108 2	4,532 3
MH day-light ~	2,35	0,018 5	0,048 3	0,140 6	0,378 4	1,133 8	3,116 2	4,534 7
	2,45	0,019 1	0,049 5	0,143 3	0,383 6	1,142 8	3,124 1	4,537 1
	2,55	0,019 6	0,050 6	0,145 9	0,388 8	1,151 7	3,131 9	4,539 5
	2,65	0,020 1	0,051 8	0,148 5	0,393 9	1,160 5	3,139 6	4,541 8
	2,75	0,020 7	0,052 9	0,151 1	0,398 9	1,169 3	3,147 3	4,544 1

Table 5.1 Values of L_{mes} of the recommended Mesopic system as a function of photopic luminance and s/p ratio

5.1.3 Determination of Adaptation Luminance

- Step1. The visual angles between the source and task points (here grid points) in degrees are calculated using MATLAB for given Layout. **[Figure 5.2]**.

- Step2. Vertical Illuminance values on all grid points for surrounding sources are also calculated using MATLAB.

- Step3.Veiling Luminance is calculated using three veiling luminance models. They are: Fry (equation 1) [37]; CIE general disability glare equation (equation 2) [14]; and Uchida and Ohno (equation 3) [16].Since the mesopic photometry system is based on peripheral task performances, SLE for peripheral vision should be characterized and be taken into account.

$$\mathbf{L_{veil}} = \mathbf{9.2}\sum\frac{\boldsymbol{E}}{\boldsymbol{\theta(\theta+1.5)}} \quad (1)$$

$$\mathbf{L_{veil}} = \left[\frac{\mathbf{10}}{\boldsymbol{\theta^3}} + \left\{\frac{\mathbf{5}}{\boldsymbol{\theta^2}} + \frac{\mathbf{0.1p}}{\boldsymbol{\theta}}\right\}.\left\{\mathbf{1} + \left(\frac{\mathbf{A}}{\mathbf{62.5}}\right)^{\mathbf{4}}\right\} + \mathbf{0.0025p}\right]\mathbf{E} \quad (2)$$

$$\mathbf{L_{veil}} = \frac{\mathbf{260}}{\boldsymbol{\theta^3}}\boldsymbol{E_v} \quad (3)$$

Where, L_{veil} is the veiling luminance caused by a high-luminance light source; θ is the angle (in degrees) between the line of fixation and the high-luminance source; A is the age in years; and p is the eye pigmentation factor. E_v is the illuminance on a plane perpendicular to a straight line between the observer's eye and the light source. E is the illuminance on a vertical plane at the observer's eye. Consequently, E is E_v multiplied by the cosine of θ. We use equation no (3) to calculate Veiling Luminance in this paper.

- STEP 4. Local luminance (L_{local}) values (here photopic luminance values on the grid points for all individual sources) are calculated using MATLAB.
- STEP 5. The values of Local Luminance and Veiling Luminance of each grid points are added to get Adaptation Luminance (La).

$$\mathbf{L_a = L_p + L_v}$$

5.2 Layout of Grid

- Total area of measurement is divided into 66 grid (0.5m x 0.5m) points as shown in Fig. 5.2.
- Two same luminaires (MH/HPSV/CWLED) are used as main light source shown in Fig. 5.2.
- Three surrounding sources (FTL) are used, which are shown in Fig. 5.2.

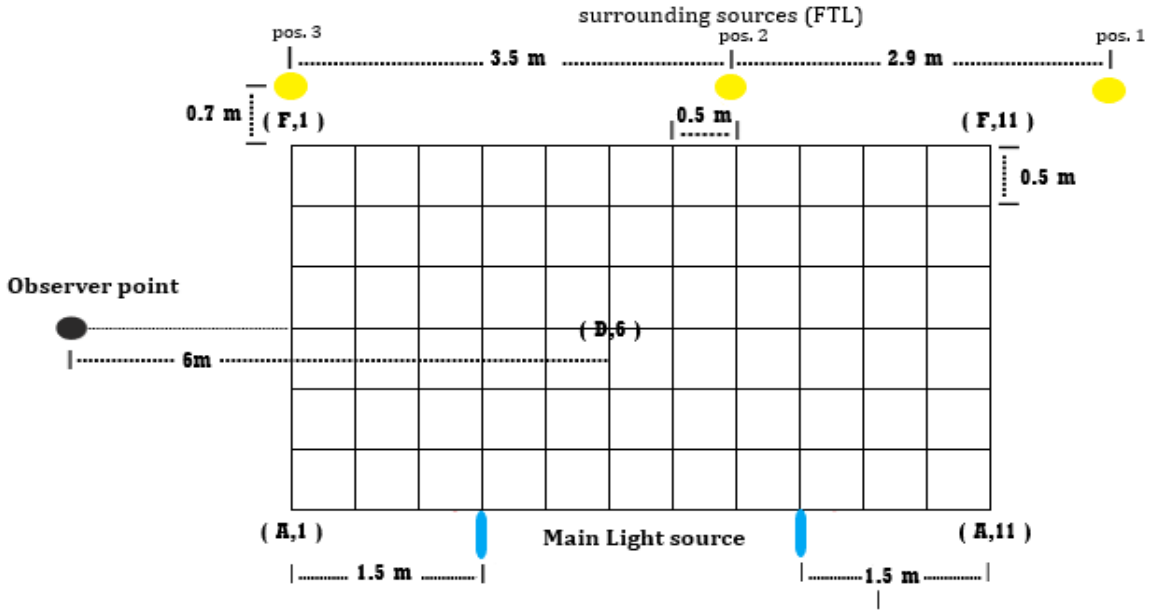

Figure 5.2 Layout of Grid

- The measurement grid was of 11x6 points with both length and breadth wise separation of 0.5m.Length wise the grids were marked as 1, 2 ……11. Breadth wise the grids were marked as A, B …F. The points are shown in figure. The luminance meter was fixed at height of 1.4m at a distance of 6m from the point (D, 6). In this figure the surrounding light source (FTL) positions are shown as pos1, pos2 and pos3. Pos3 is 0.7m away from grid point (F,1). Pos2 is 0.7m away from grid point (F,8). Pos1 is 2.9m away from pos2. Mounting height of the surrounding light sources is 2.5m. Mounting height of the main light sources is 2.5m which are placed at (A,3) and at (A,8) respectively.

5.3 Lamp Details

Different Light source that are used in this experiment are:

5.3.1 Metal Halide Lamps (MH)

5.3.2 High pressure sodium lamp (HPSV)

5.3.3 White Light Emitting Diodes (WLED)

5.3.4 Fluorescent Tube Lights (FTL)

5.3.1 Metal Halide Lamps (MH)

Details of the MH lamp are shown below:

- **Luminaire:** PHILIPS MPF 922 [SYMMETRIC] CLOSED
- **Operating Voltage:** 230V ac
- **Power:** 150W.
- **Frequency:**50Hz
- **Current**- 0.98A
- **Luminous Flux**: Rated- 12100lm
- **CCT:** 4000K
- **Luminous Efficacy:** Rated-80lm/W
- **CRI:** 60
- **S/P RATIO: 1.32**

5.3.2 High pressure sodium lamp (HPSV)

Details of the HPSV lamp that is used in this experiment are shown below:

- **Luminaire:** Philips
- **Operating Voltage**: 230V ac
- **Power**: Rated- 150 W.
- **Frequency**-50Hz
- **Current**- 0.98A
- **Luminous Flux**: Rated- 13500 lm
- **CCT**-2000K
- **Luminous Efficacy**- Rated- 90 lm/W
- **CRI**-35
- **S/P RATIO**-0.48

5.3.3 White Light Emitting Diodes (WLED)

Details of the WLED lamp that is used in this experiment are shown below:

- **Luminaire:** Philips
- **Operating Voltage:** 230V AC
- **Current:**0.32A
- **Power:**101 W
- **Luminous flux:** 15497 lm
- **Frequency:**50Hz
- **Power Factor:**0.98
- **CCT:**4385K
- **Luminous Efficacy**- Rated- 150 lm/W
- **CRI**=87.9
- **S/P Ratio:**1.82

5.3.2 Fluorescent Tube Lights (FTL)

Details of Fluorescent Tube lights (FTL) lamps which are used in this experiment as surrounding light source are shown below:

- **Luminaire:** Philips
- **Operating Voltage:** 220V ac
- **Power:** Rated- 36W.
- **Frequency**-50Hz
- **Current**- 0.44A
- **Luminous Flux:** Rated- 2500lm
- **CCT**-6200K
- **Luminous Efficacy**- Rated-70lm/W
- **CRI**-72

5.4 Calculation of C, γ angle of each grid points

The C, γ angle of each grid points are calculated and the measured angles are shown in table 5.4.1 and table 5.4.2 respectively.

	1	2	3	4	5	6	7	8	9	10	11
A	0	0	90	180	180	180	180	180	180	180	180
B	26.56	45	90	135	153.43	161.56	165.96	168.69	170.54	171.87	172.875
C	45	63.43	90	116.56	135	146.31	153.43	158.19	161.56	164.05	165.964
D	56.31	71.56	90	108.43	123.69	135	143.13	149.04	153.43	156.8	159.444
E	63.43	75.96	90	104.04	116.56	126.87	135	141.34	146.31	150.25	153.435
F	68.198	78.69	90	101.31	111.8	120.964	128.66	135	140.19	144.46	147.995

Table 5.4.1 C angle (in degree) of the grid points

	1	2	3	4	5	6	7	8	9	10	11
A	15.52	7.91	0	7.91	15.52	22.62	29.05	34.77	39.81	44.19	48.013
B	17.25	11.11	7.91	11.11	17.25	23.71	29.79	35.31	40.19	44.48	48.234
C	21.45	17.25	15.52	17.25	21.45	26.6	31.84	36.79	41.29	45.32	48.875
D	26.6	23.71	22.62	23.71	26.6	30.51	34.77	39	42.97	46.61	49.879
E	31.85	29.79	29.05	29.79	31.85	34.77	38.15	41.65	45.04	48.23	51.166
F	36.794	35.31	34.77	35.31	36.794	39	41.65	44.48	47.33	50.07	52.65

Table 5.4.2 γ angle (in degree) of the grid points

5.5 Interpolated intensity value (I-Table) of the lamp for each grid points

The intensity value are interpolated by using the bilinear interpolation method for all grid points of area of measurement for different lamp

5.5.1 I-Table for MH Lamp:

The interpolated intensity value of the lamp are shown in the table 5.5.1

	1	2	3	4	5	6	7	8	9	10	11
A	293.248	281.656	273	281.656	293.248	295.092	220.58	165.886	163.038	152.198	142.961
B	269.064	261.226	253.122	261.226	269.045	266.312	199.59	154.504	153.299	148.489	141.263
C	210.364	210.498	205.92	210.484	210.43	210.862	176.786	146.654	143.883	143.095	140.245
D	192.685	193.377	193.764	193.378	192.685	183.122	176.178	159.912	147.893	142.482	143.286
E	216.957	214.168	212.77	214.168	216.974	209.484	191.11	173.347	159.636	151.904	141.286
F	243.624	244.383	242.666	244.383	243.627	237.761	213.382	180.144	169.538	161.255	142.931

Table 5.5.1: Intensity value (cd) of the grid points (MH-150W)

5.5.2 I-Table for HVSP Lamp:

The interpolated intensity value of the lamp are shown in the table 5.5.2

	1	2	3	4	5	6	7	8	9	10	11
A	161.584	158.75	155	158.746	161.58	154.86	149.57	143.27	140.114	139.02	138.40
B	160.2	160.44	158.74	160.444	160.2	153.55	149.126	142.12	139.962	139.10	138.35
C	156.26	160.2	161.58	160.2	156.26	151.04	146.792	143.27	139.742	138.94	138.23
D	151.04	153.55	154.86	153.548	151.04	148.39	143.276	141.11	139.406	138.68	138.02
E	146.78	149.13	149.57	149.126	146.78	143.27	141.11	139.67	138.994	138.35	137.67
F	141.924	142.81	143.28	142.814	141.92	140.6	139.67	139.11	138.534	137.98	137.47

Table 5.5.2: Intensity value (cd) of the grid points (SON-150W)

5.5.3 I-Table for CWLED Lamp:

The interpolated intensity value of the lamp are shown in the table 5.5.3

	1	2	3	4	5	6	7	8	9	10	11
A	331.6	289.132	264	243.196	208.816	168.516	116.66	95.874	83.456	75.144	68.974
B	327.291	286.263	259.672	239.116	205.535	165.681	118.32	94.92	82.041	82.133	67.89
C	313.32	273.215	251.168	230.13	193.91	158.18	115.486	91.862	79.56	72.297	66.103
D	299.592	264.103	241.37	216.222	180.41	145.328	106.713	85.835	75.737	69.012	63.478
E	312.485	270.23	226.04	195.91	162.603	128.548	96.62	80.495	71.19	65.219	60.539
F	294.152	244.31	200.104	171.642	142.484	112.786	89.113	73.56	66.85	61.514	57.555

Table 5.5.3: Intensity value (cd) of the grid points (LED-101W)

5.6 Luminance co-efficient (q) value for all grid points

To get the theoretical photopic luminance (Lp) value illuminance (E) value multiplied with measured luminance coefficient (q) value as shown in Table 5.6 .

	1	2	3	4	5	6	7	8	9	10	11
A	0.031881	0.024912	0.02387	0.02237	0.023689	0.021556	0.028255	0.0285	0.021507	0.02522	0.031881
B	0.03657	0.03055	0.023655	0.02282	0.019538	0.02024	0.019912	0.023021	0.026141	0.031288	0.03657
C	0.043366	0.03295	0.03245	0.023448	0.021939	0.021214	0.018937	0.02264	0.025775	0.03221	0.043366
D	0.03137	0.028795	0.024324	0.022253	0.02412	0.0195	0.019203	0.024975	0.023389	0.032894	0.03137
E	0.026802	0.021933	0.026183	0.019869	0.020071	0.019808	0.022644	0.021461	0.024451	0.039205	0.026802
F	0.026	0.031966	0.02878	0.027669	0.023383	0.02386	0.028924	0.03047	0.034421	0.037794	0.026

Table 5.6 Measured Luminance co-efficient (q) value for all grid points

Chapter: 6 SIMULATION OF PHOTOPIC LUMINANCE (L_p)

In this chapter the simulation of photopic luminance (L_a) using MATLAB simulation software has been discussed. Photopic Luminance (L_p) values are calculated for all the grid points for 3 different types of main light sources:

6.1 Metal Halide (MH) Lamp:

Photopic luminance (L_p) values are simulated (in cd/m^2) for MH lamp using MATLAB software. The coding in M-file is shown below:

```
x=[1.5:-0.5:-1];
y=[-2.5:0.5:2.5];
[xx,yy]=meshgrid(x,y);
hm=3.6
a1=((xx-2.2).^2 + (yy+1).^2).^0.5
b1=(a1.^2 + hm.^2).^0.5
a2=((xx-2.2).^2 + (yy-1).^2).^0.5
b2=(a2.^2 + hm.^2).^0.5
c1=hm./b1
c2=hm./b2
gamma1=acosd(c1)
gamma2=acosd(c2)
d1=(cosd(gamma1)).^3.*hm.^-2
d2=(cosd(gamma2)).^3.*hm.^-2
filename = 'Mh1.xlsx';
I1 = xlsread(filename, 'A1:F11')
filename = 'Mh2.xlsx';
I2 = xlsread(filename, 'A1:F11')
E1=d1.*I1
E2=d2.*I2
Eh=E1+E2
filename = 'p.xlsx';
p = xlsread(filename, 'A1:F11')
Lp=p.*Eh
```

The illuminance (E_h) value for all grid points were calculated using MATLAB (the Inverse Square Law of illumination). The calculated illuminance values are shown in the table 6.1.1 and simulated Photopic luminance (L_p) values are shown in the table 6.1.2.

	1	2	3	4	5	6	7	8	9	10	11
A	20.9205	23.6104	26.094	28.7485	33.5838	38.6802	33.5838	28.7485	26.094	23.6104	20.9205
B	17.9537	20.2835	22.132	24.257	27.8491	31.728	27.8491	24.257	22.132	20.2835	17.9537
C	13.224	15.1145	16.4609	17.9779	19.9914	21.9498	19.9914	17.9779	16.4609	15.1145	13.224
D	10.8578	12.2373	13.6104	14.9259	16.1101	16.1747	16.1101	14.9259	13.6104	12.2373	10.8578
E	10.0579	11.3277	12.4652	13.6867	14.8618	15.3973	14.8618	13.6867	12.4652	11.3277	10.0579
F	9.2689	10.5672	11.512	12.4446	13.7066	14.3797	13.7066	12.4446	11.512	10.5672	9.2689

Table 6.1.3 the illuminance (E_h) value for all grid points

	1	2	3	4	5	6	7	8	9	10	11
A	0.7718	0.7527	0.6501	0.6862	0.7513	0.9163	0.7239	0.8123	0.7437	0.5078	0.5276
B	0.8169	0.7418	0.6761	0.5738	0.6355	0.6199	0.5637	0.483	0.5095	0.5302	0.5617
C	1.119	0.6555	0.5424	0.5834	0.4688	0.4816	0.4241	0.3404	0.3727	0.3896	0.4259
D	0.4495	0.3839	0.3919	0.3631	0.3585	0.3901	0.3141	0.2866	0.3399	0.2862	0.3572
E	0.3645	0.3036	0.2734	0.3584	0.2953	0.309	0.2944	0.3099	0.2675	0.277	0.3943
F	0.2446	0.2747	0.368	0.3582	0.3792	0.3362	0.327	0.3599	0.3508	0.3637	0.3503
Average L_p = 0.476365											

Table 6.1.4 simulated Photopic luminance (L_p) values

6.2 High Pressure Sodium Vapour (HPSV) lamp:

Photopic luminance (L_p) values are simulated (in cd/m^2) for HPSV lamp using MATLAB software. The coding in M-file is shown below:

```
x=[1.5:-0.5:-1];
y=[-2.5:0.5:2.5];
[xx,yy]=meshgrid(x,y);
hm=3.6
a1=((xx-2.2).^2 + (yy+1).^2).^0.5
b1=(a1.^2 + hm.^2).^0.5
a2=((xx-2.2).^2 + (yy-1).^2).^0.5
b2=(a2.^2 + hm.^2).^0.5
c1=hm./b1
c2=hm./b2
gamma1=acosd(c1)
gamma2=acosd(c2)
d1=(cosd(gamma1)).^3.*hm.^-2
d2=(cosd(gamma2)).^3.*hm.^-2
filename = 'Son1.xlsx';
I1 = xlsread(filename, 'A1:F11')
filename = 'Son2.xlsx';
I2 = xlsread(filename, 'A1:F11')
E1=d1.*I1
E2=d2.*I2
Eh=E1+E2
filename = 'p.xlsx';
p = xlsread(filename, 'A1:F11')
Lp=p.*Eh
```

The calculated illuminance values are shown in the table 6.2.1 and simulated Photopic luminance (L_p) values are shown in the table 6.2.2.

	1	2	3	4	5	6	7	8	9	10	11
A	13.175	15.109	16.773	18.662	20.127	20.298	20.127	18.662	16.773	15.109	13.175
B	12.109	13.981	15.561	17.053	18.187	18.294	18.187	17.053	15.561	13.982	12.109
C	10.646	12.376	13.847	14.972	15.571	15.723	15.570	14.972	13.847	12.376	10.646
D	9.073	10.380	11.525	12.351	12.836	13.107	12.836	12.351	11.525	10.38	9.073
E	7.626	8.629	9.469	10.102	10.453	10.531	10.453	10.102	9.470	8.629	7.626
F	6.324	7.037	7.663	8.131	8.416	8.503	8.416	8.131	7.663	7.037	6.324

Table 6.2.1 the illuminance (E_h) value for all grid points

	1	2	3	4	5	6	7	8	9	10	11
A	0.486	0.4817	0.4178	0.4455	0.4502	0.4808	0.4339	0.5273	0.478	0.3249	0.3323
B	0.551	0.5113	0.4754	0.4034	0.415	0.3574	0.3681	0.3396	0.3582	0.3655	0.3789
C	0.9008	0.5367	0.4562	0.4858	0.3651	0.3449	0.3303	0.2835	0.3135	0.319	0.3429
D	0.3756	0.3256	0.3319	0.3004	0.2856	0.3161	0.2503	0.2372	0.2878	0.2428	0.2984
E	0.2764	0.2313	0.2077	0.2645	0.2077	0.2114	0.207	0.2287	0.2032	0.211	0.299
F	0.1669	0.183	0.2449	0.234	0.2329	0.1988	0.2008	0.2352	0.2335	0.2422	0.239
Average L_p = 0.33745											

Table 6.2.2 simulated Photopic luminance (L_p) values

6.3 Cool White LED (CWLED):

Photopic luminance (L_p) values are simulated (in cd/m^2) for CWLED lamp using MATLAB software. The coding in M-file is shown below:

```
x=[1.5:-0.5:-1];
y=[-2.5:0.5:2.5];
[xx,yy]=meshgrid(x,y);
hm=3.6
a1=((xx-2.2).^2 + (yy+1).^2).^0.5
b1=(a1.^2 + hm.^2).^0.5
a2=((xx-2.2).^2 + (yy-1).^2).^0.5
b2=(a2.^2 + hm.^2).^0.5
c1=hm./b1
c2=hm./b2
gamma1=acosd(c1)
gamma2=acosd(c2)
d1=(cosd(gamma1)).^3.*hm.^-2
```

```
d2=(cosd(gamma2)).^3.*hm.^-2
filename = 'Led1.xlsx';
I1 = xlsread(filename, 'A1:F11')
filename = 'Led2.xlsx';
I2 = xlsread(filename, 'A1:F11')
E1=d1.*I1
E2=d2.*I2
Eh=E1+E2
filename = 'p.xlsx';
p = xlsread(filename, 'A1:F11')
Lp=p.*Eh
```

The calculated illuminance values are shown in the table 6.3.1 and simulated Photopic luminance (L_p) values are shown in the table 6.3.2.

	1	2	3	4	5	6	7	8	9	10	11
A	21.095	21.492	22.1785	22.484	21.5758	22.0888	21.576	22.484	22.178	21.493	21.096
B	19.119	19.664	19.8188	20.0826	19.4653	19.739	19.465	20.083	19.819	19.665	19.119
C	16.245	16.321	16.7536	16.8684	16.205	16.4659	16.205	16.868	16.754	16.321	16.245
D	13.399	13.454	13.6428	13.4009	12.7484	12.8365	12.748	13.401	13.643	13.454	13.399
E	11.717	11.415	10.6458	10.1663	9.5658	9.4484	9.566	10.166	10.646	11.415	11.717
F	9.229	8.599	7.8495	7.3964	7.0157	6.8213	7.016	7.396	7.849	8.599	9.229

7

Table 6.3.5 the illuminance (E_h) value for all grid points

	1	2	3	4	5	6	7	8	9	10	11
A	0.7782	0.6852	0.5525	0.5367	0.4827	0.5233	0.4651	0.6353	0.6321	0.4622	0.532
B	0.8699	0.7191	0.6055	0.4751	0.4442	0.3857	0.394	0.3999	0.4562	0.5141	0.5982
C	1.3746	0.7078	0.552	0.5474	0.38	0.3612	0.3438	0.3194	0.3793	0.4207	0.5233
D	0.5547	0.4221	0.3928	0.326	0.2837	0.3096	0.2486	0.2573	0.3407	0.3147	0.4408
E	0.4246	0.306	0.2335	0.2662	0.1901	0.1896	0.1895	0.2302	0.2285	0.2791	0.4594
F	0.2436	0.2236	0.2509	0.2129	0.1941	0.1595	0.1674	0.2139	0.2392	0.296	0.3488
Average L_p = 0.41658											

Table 6.3.2 simulated Photopic luminance (L_p) values

6.4 Simulated Photopic luminance (L_p) values for all different Lamps

Simulated Photopic luminance (L_p) values for all different Lamps are shown in Table 6.4.

Average Photopic Luminance(cd/m^2)	
MH	0.476365
HPSV	0.33745
CWLED	0.41658

Table 6.4 Simulated Photopic luminance (L_p) values for all different Lamps

Chapter: 7 SIMULATION OF ADAPTATION LUMINANCE (L_a)

In the previous chapter, we measured photopic luminance (L_p). In the current chapter, in this chapter the simulation of adaptation luminance (L_a) using MATLAB simulation software has been discussed. One of the key steps in this process is the calculation of visual angles between the source and task points, which, in this case, are represented by grid points, and these angles are determined in degrees using MATLAB.

To arrive at the adaptation luminance (L_a) for each grid point, we perform the following calculation: we add the photopic luminance (L_p) and the veiling luminance (L_v) associated with that specific grid point. This combined value gives us the adaptation luminance (L_a).

$$L_a = L_p + L_v$$

Prior to the simulation of adaptation luminance (La), we conducted simulations for veiling luminance values. As previously outlined in the 'Experimental Procedure' chapter, this study considered three distinct veiling luminance models to calculate the 'Surrounding Luminance Effect.' These models include the Fry model, the CIE general disability glare equation model, and the Uchida and Ohno model. For this specific experiment, we employed the Uchida and Ohno model.

$$\mathbf{L_v} = \frac{\mathbf{260}}{\boldsymbol{\theta^3}} \boldsymbol{E_v}$$

7.1 Vertical Illuminance Values for SLE

Vertical illuminance (E_v) due to the SLE sources is measured under three different conditions.

- When only SLE of position 1 is on.
- SLE of position 2 is on.
- SLE of position 3 is on.

- **When only SLE of position 1 is on.**

Vertical Illuminance (E_{v1}) for all the grid points is measured using Luxmeter (in Lux) and listed below in Table 7.1.1:

	1	2	3	4	5	6	7	8	9	10	11
A	0.3	0.5	0.7	1	1.4	1.9	2.4	3.9	5.4	7.1	9.9
B	0.2	0.3	0.6	0.8	1	1.8	2.6	4.1	5.9	7.9	11.9
C	0.1	0.2	0.2	0.4	0.6	1	1.7	3	5.6	8.6	14.1
D	0.1	0.1	0.1	0.2	0.3	1.4	1.5	2.9	5.2	9.2	15.3
E	0.1	0.2	0.2	0.1	0.1	0.1	0.8	1.7	2.4	6.3	11.2
F	0.1	0.1	0.1	0.1	0.1	0.1	0.1	0.1	0.1	0.1	0.4

Table 7.1.1: Vertical illuminance (E_{v1}) for SLE 1

- **When only SLE of position 2 is on.**

  Vertical Illuminance (E_{v2}) for all the grid points is measured using Luxmeter (in Lux) and listed below in Table 7.1.2:

	1	2	3	4	5	6	7	8	9	10	11
A	2.3	2.7	4.8	6.5	8.2	10	11.2	10.5	9.7	7.2	6.2
B	2.3	3.1	4.1	6.8	9.7	13	14.6	14.4	12.4	9.4	7
C	1.9	2.8	4.5	7	12.6	17.6	20.1	18.1	15.4	11.4	6.1
D	6.5	10.9	18.3	26.1	26	20.4	13	6.1	3	2.3	1.2
E	0.5	0.6	2.1	4.9	12.5	24	34.5	32.4	20	8.6	3.6
F	0.2	0.2	0.4	1	4	6	11	10	5	0.7	0.6

Table 7.1.2: Vertical illuminance (E_{v2}) for SLE 2

- **When only SLE of position 3 is on.**

  Vertical Illuminance (E_{v3}) for all the grid points is measured using Luxmeter (in Lux) and listed below in Table 7.1.3:

	1	2	3	4	5	6	7	8	9	10	11
A	12.8	12.1	10.3	9.5	7.8	5.6	3.8	2.8	2.2	1.4	1
B	20.5	19	15.5	110.9	8.3	5.1	3.5	2.5	1.9	1.1	0.7
C	26.7	24.6	17.8	12.7	8.9	5	3.4	2	1.1	0.8	0.6
D	37.3	33.2	22.3	14.2	7.6	4.3	2.5	1.3	0.9	0.6	0.3
E	43.7	39.2	23.1	8.7	4.8	2.3	1.2	0.6	0.4	0.3	0
F	26.2	23.9	12	4.4	1	0.7	0.4	0.1	0.2	0.2	0.2

Table 7.1.3: Vertical illuminance (E_{v3}) for SLE 3

7.2 Veiling Luminance (L_v) Values for SLE

Under the framework of the Uchida and Ohno model, we evaluate veiling luminance (L_v) arising from the Surrounding Luminance Effect (SLE) sources in MATLAB simulation.

$$\mathbf{L_v} = \frac{260}{\theta^3} E_v$$

The coding in M-file is shown below:

```
x=[1.5:-0.5:-1];
y=[-2.5:0.5:2.5];
[xx,yy]=meshgrid(x,y);
a3=(1.4^2+(yy+6).^2).^0.5
b3=(((xx+1.7).^2)+((yy+2.5).^2)+(2.15^2)).^0.5
c3=(15.7025)^0.5
d3=((a3.^2)-(b3.^2)+(c3^2))./(2*c3)
e3=d3./a3
theta3=acosd(e3)
h3=theta3.^(-3)
i3=260*h3
filename = 'Ev3.xlsx';
Ev3 = xlsread(filename, 'A1:F11')
Lv3= i3.*Ev3
a1=(1.4^2+(yy+6).^2).^0.5
b1=(((xx+1.7).^2)+((3.9-yy).^2)+(2.15^2)).^0.5
c1=((0.75^2)+9.9^2+1.7^2)^0.5
d1=((a1.^2)-(b1.^2)+(c1^2))./(2*c1)
e1=d1./a1
theta1=acosd(e1)
h1=theta1.^(-3)
```

```
i1=260*h1

filename = 'Ev1.xlsx';

Ev1 = xlsread(filename, 'A1:F11')

Lv1= i1.*Ev1

a2=(1.4^2+(yy+6).^2).^0.5

b2=(((xx+1.7).^2)+((1-yy).^2)+(2.15^2)).^0.5

c2=((0.75^2)+7^2+1.7^2)^0.5

d2=((a2.^2)-(b2.^2)+(c2^2))./(2*c2)

e2=d2./a2

theta2=acosd(e2)

h2=theta2.^(-3)

i2=260*h2

filename = 'Ev2.xlsx';

Ev2 = xlsread(filename, 'A1:F11')

Lv2= i2.*Ev2

Lv=Lv1+Lv2+Lv3
```

Here, we have L_{v1}, L_{v2}, and L_{v3} representing the veiling luminance values when only the Surrounding Luminance Effect (SLE) of position 1, position 2, and position 3 is active, respectively. When we consider all SLE positions being active simultaneously, the total veiling luminance, L_v (Table 7.2.4) is calculated as the sum of L_{v1} (Table 7.2.1), L_{v2} (Table 7.2.2), and L_{v3} (Table 7.2.3). The data for these luminance values are provided below in Table.

	1	2	3	4	5	6	7	8	9	10	11
A	0.0014	0.003	0.0051	0.0086	0.0141	0.0219	0.0314	0.057	0.0875	0.1264	0.1922
B	0.0013	0.0025	0.0061	0.0096	0.0141	0.0292	0.0478	0.0844	0.1346	0.1979	0.3247
C	0.0009	0.0023	0.0028	0.0068	0.012	0.0231	0.0446	0.0882	0.1825	0.3075	0.5484
D	0.0012	0.0016	0.002	0.0048	0.0085	0.0461	0.0562	0.122	0.2425	0.4703	0.8495
E	0.0016	0.0042	0.0054	0.0033	0.0039	0.0046	0.0418	0.0999	0.1563	0.4496	0.8667
F	0.002	0.0027	0.0034	0.0042	0.0051	0.0059	0.0068	0.0077	0.0085	0.0093	0.0403

Table 7.2.1: Veiling luminance (L_{v1}) for SLE 1

	1	2	3	4	5	6	7	8	9	10	11
A	0.0072	0.0104	0.0222	0.0351	0.0508	0.0701	0.0877	0.0909	0.0919	0.0741	0.0689
B	0.0102	0.0169	0.0268	0.052	0.085	0.1287	0.161	0.175	0.1645	0.135	0.1081
C	0.0119	0.0218	0.0421	0.0767	0.1583	0.2493	0.3163	0.3127	0.2893	0.2308	0.1322
D	0.0578	0.1213	0.2456	0.4107	0.4688	0.4137	0.2919	0.1498	0.0797	0.0655	0.0364
E	0.0061	0.0093	0.0394	0.108	0.3155	0.6797	1.0781	1.1019	0.7319	0.3354	0.1485
F	0.0032	0.004	0.0098	0.0288	0.132	0.2218	0.4471	0.4404	0.2357	0.035	0.0315

Table 7.2.2: Veiling luminance (L_{v2}) for SLE 2

	1	2	3	4	5	6	7	8	9	10	11
A	0.0156	0.0175	0.0172	0.018	0.0164	0.013	0.0096	0.0077	0.0064	0.0044	0.0033
B	0.0359	0.0391	0.0365	0.2931	0.0242	0.0163	0.0121	0.0092	0.0075	0.0046	0.0031
C	0.0677	0.0725	0.0595	0.0471	0.0361	0.0219	0.0159	0.0099	0.0058	0.0044	0.0034
D	0.1364	0.1396	0.105	0.0734	0.0424	0.0256	0.0158	0.0086	0.0062	0.0043	0.0022
E	0.2238	0.2282	0.1487	0.0606	0.0357	0.018	0.0098	0.0051	0.0035	0.0027	0
F	0.175	0.1796	0.0986	0.0387	0.0093	0.0068	0.004	0.001	0.0021	0.0021	0.0022

Table 7.2.3: Veiling luminance (L_{v3}) for SLE 3

	1	2	3	4	5	6	7	8	9	10	11
A	0.0242	0.0309	0.0444	0.0617	0.0814	0.1051	0.1287	0.1556	0.1859	0.2049	0.2644
B	0.0474	0.0584	0.0693	0.3547	0.1234	0.1742	0.2209	0.2687	0.3066	0.3374	0.4358
C	0.0805	0.0966	0.1044	0.1307	0.2065	0.2943	0.3769	0.4109	0.4775	0.5427	0.684
D	0.1954	0.2624	0.3526	0.4889	0.5198	0.4854	0.3639	0.2804	0.3284	0.5401	0.8881
E	0.2315	0.2417	0.1934	0.1719	0.3551	0.7023	1.1298	1.2069	0.8917	0.7877	1.0152
F	0.1802	0.1863	0.1118	0.0717	0.1464	0.2345	0.458	0.4491	0.2463	0.0464	0.074

Table 7.2.4: Veiling luminance (L_v) all SLE positions being active

7.3 Adaptation Luminance (L_a)

Point specific adaptation luminance (L_a) values are calculated using MATLAB for all the grid points for different types of main light sources.

7.3.1 Metal Halide (MH) Lamp:

For MH lamp adaptation luminances are simulated in 4 different conditions as shown below:

i. Measurement of La when MH & SLE1are on.

Adaptation luminance values are simulated (in cd/m2) for MH lamp along with the effect of SLE1 using MATLAB software. The coding in M-file is shown below:

```
x=[1.5:-0.5:-1];
y=[-2.5:0.5:2.5];
[xx,yy]=meshgrid(x,y);
a1=(1.4^2+(yy+6).^2).^0.5
b1=(((xx+1.7).^2)+((3.9-yy).^2)+(2.15^2)).^0.5
c1=((0.75^2)+9.9^2+1.7^2)^0.5
d1=((a1.^2)-(b1.^2)+(c1^2))./(2*c1)
e1=d1./a1
theta1=acosd(e1)
h1=theta1.^(-3)
i1=260*h1
filename = 'Ev1.xlsx';
Ev1 = xlsread(filename, 'A1:F11')
Lv1= i1.*Ev1
hm=3.6
r1=((xx-2.2).^2 + (yy+1).^2).^0.5
s1=(r1.^2 + hm.^2).^0.5
r2=((xx-2.2).^2 + (yy-1).^2).^0.5
s2=(r2.^2 + hm.^2).^0.5
t1=hm./s1
t2=hm./s2
gamma1=acosd(t1)
gamma2=acosd(t2)
u1=(cosd(gamma1)).^3.*hm.^-2
u2=(cosd(gamma2)).^3.*hm.^-2
filename = 'Mh1.xlsx';
I1 = xlsread(filename, 'A1:F11')
filename = 'Mh2.xlsx';
I2 = xlsread(filename, 'A1:F11')
E1=u1.*I1
E2=u2.*I2
Eh=E1+E2
filename = 'p.xlsx';
p = xlsread(filename, 'A1:F11')
Lp=p.*Eh
La=Lp+Lv1
```

	1	2	3	4	5	6	7	8	9	10	11
A	0.7732	0.7557	0.6551	0.6949	0.7654	0.9382	0.7553	0.8693	0.8312	0.6342	0.7198
B	0.8182	0.7442	0.6822	0.5834	0.6496	0.6491	0.6115	0.5674	0.6441	0.7281	0.8864
C	1.1198	0.6577	0.5452	0.5902	0.4808	0.5047	0.4687	0.4287	0.5552	0.6971	0.9743
D	0.4507	0.3855	0.3939	0.3679	0.367	0.4362	0.3704	0.4086	0.5824	0.7565	1.2067
E	0.3661	0.3078	0.2788	0.3617	0.2992	0.3136	0.3362	0.4098	0.4239	0.7266	1.261
F	0.2466	0.2774	0.3714	0.3624	0.3843	0.3422	0.3339	0.3676	0.3593	0.373	0.3907
Average L_a = 0.56967											

Table 7.3.1.1 L_a when MH& SLE1 are on

ii. Measurement of L_a when MH & SLE2 are on.

Adaptation luminance values are simulated (in cd/m2) for MH lamp along with the effect of SLE2 using MATLAB software. The coding in M-file is shown below:

```
x=[1.5:-0.5:-1];
y=[-2.5:0.5:2.5];
[xx,yy]=meshgrid(x,y);
a2=(1.4^2+(yy+6).^2).^0.5
b2=(((xx+1.7).^2)+((1-yy).^2)+(2.15^2)).^0.5
c2=((0.75^2)+7^2+1.7^2)^0.5
d2=((a2.^2)-(b2.^2)+(c2^2))./(2*c2)
e2=d2./a2
theta2=acosd(e2)
h2=theta2.^(-3)
i2=260*h2
filename = 'Ev2.xlsx';
Ev2 = xlsread(filename, 'A1:F11')
Lv2= i2.*Ev2
hm=3.6
r1=((xx-2.2).^2 + (yy+1).^2).^0.5
s1=(r1.^2 + hm.^2).^0.5
r2=((xx-2.2).^2 + (yy-1).^2).^0.5
s2=(r2.^2 + hm.^2).^0.5
t1=hm./s1
t2=hm./s2
gamma1=acosd(t1)
gamma2=acosd(t2)
u1=(cosd(gamma1)).^3.*hm.^-2
u2=(cosd(gamma2)).^3.*hm.^-2
filename = 'Mh1.xlsx';
I1 = xlsread(filename, 'A1:F11')
filename = 'Mh2.xlsx';
I2 = xlsread(filename, 'A1:F11')
E1=u1.*I1
E2=u2.*I2
```

```
Eh=E1+E2
filename = 'p.xlsx';
p = xlsread(filename, 'A1:F11')
Lp=p.*Eh
La=Lp+Lv2
```

	1	2	3	4	5	6	7	8	9	10	11
A	0.779	0.7631	0.6722	0.7213	0.8021	0.9864	0.8116	0.9031	0.8356	0.5819	0.5965
B	0.8271	0.7587	0.7029	0.6258	0.7206	0.7486	0.7247	0.658	0.674	0.6652	0.6698
C	1.1309	0.6773	0.5845	0.6601	0.6271	0.7308	0.7404	0.6532	0.6619	0.6204	0.5581
D	0.5073	0.5051	0.6375	0.7738	0.8273	0.8038	0.6061	0.4364	0.4196	0.3517	0.3935
E	0.3707	0.3129	0.3128	0.4663	0.6108	0.9888	1.3725	1.4119	0.9994	0.6124	0.5428
F	0.2478	0.2788	0.3778	0.387	0.5113	0.558	0.7742	0.8004	0.5865	0.3987	0.3818
Average L_a = 0.658161											

Table 7.3.1.2 L_a when MH& SLE2 are on

iii. Measurement of La when MH & SLE 3 are on.

Adaptation luminance values are simulated (in cd/m^2) for MH lamp along with the effect of SLE3 using MATLAB software. The coding in M-file is shown below:

```
x=[1.5:-0.5:-1];
y=[-2.5:0.5:2.5];
[xx,yy]=meshgrid(x,y);
a3=(1.4^2+(yy+6).^2).^0.5
b3=(((xx+1.7).^2)+((yy+2.5).^2)+(2.15^2)).^0.5
c3=(15.7025)^0.5
d3=((a3.^2)-(b3.^2)+(c3^2))./(2*c3)
e3=d3./a3
theta3=acosd(e3)
h3=theta3.^(-3)
i3=260*h3
filename = 'Ev3.xlsx';
Ev3 = xlsread(filename, 'A1:F11')
Lv3= i3.*Ev3
hm=3.6
r1=((xx-2.2).^2 + (yy+1).^2).^0.5
s1=(r1.^2 + hm.^2).^0.5
r2=((xx-2.2).^2 + (yy-1).^2).^0.5
s2=(r2.^2 + hm.^2).^0.5
```

```
t1=hm./s1
t2=hm./s2
gamma1=acosd(t1)
gamma2=acosd(t2)
u1=(cosd(gamma1)).^3.*hm.^-2
u2=(cosd(gamma2)).^3.*hm.^-2
filename = 'Mh1.xlsx';
I1 = xlsread(filename, 'A1:F11')
filename = 'Mh2.xlsx';
I2 = xlsread(filename, 'A1:F11')
E1=u1.*I1
E2=u2.*I2
Eh=E1+E2
filename = 'p.xlsx';
p = xlsread(filename, 'A1:F11')
Lp=p.*Eh
La=Lp+Lv3
```

	1	2	3	4	5	6	7	8	9	10	11
A	0.7874	0.7702	0.6672	0.7042	0.7677	0.9293	0.7336	0.8199	0.7501	0.5122	0.5309
B	0.8528	0.7808	0.7126	0.8669	0.6598	0.6362	0.5757	0.4922	0.517	0.5348	0.5648
C	1.1867	0.728	0.6018	0.6305	0.5049	0.5035	0.44	0.3504	0.3784	0.394	0.4294
D	0.5859	0.5235	0.4969	0.4364	0.4009	0.4158	0.3299	0.2952	0.3461	0.2905	0.3594
E	0.5883	0.5318	0.4221	0.419	0.331	0.3271	0.3042	0.315	0.271	0.2797	0.3943
F	0.4196	0.4544	0.4665	0.3968	0.3885	0.343	0.331	0.361	0.3529	0.3659	0.3525
Average L_a = 0.518333											

Table 7.3.1.3 L_a when MH& SLE3 are on

iv. Measurement of L_a when MH & all SLEs are on.

Adaptation luminance values are simulated (in cd/m^2) for MH lamp along with the effect of all SLEs using MATLAB software. The coding in M-file is shown below:

```
x=[1.5:-0.5:-1];
y=[-2.5:0.5:2.5];
[xx,yy]=meshgrid(x,y);
a3=(1.4^2+(yy+6).^2).^0.5
b3=(((xx+1.7).^2)+((yy+2.5).^2)+(2.15^2)).^0.5
c3=(15.7025)^0.5
d3=((a3.^2)-(b3.^2)+(c3^2))./(2*c3)
```

```
e3=d3./a3
theta3=acosd(e3)
h3=theta3.^(-3)
i3=260*h3
filename = 'Ev3.xlsx';
Ev3 = xlsread(filename, 'A1:F11')
Lv3= i3.*Ev3
a1=(1.4^2+(yy+6).^2).^0.5
b1=(((xx+1.7).^2)+((3.9-yy).^2)+(2.15^2)).^0.5
c1=((0.75^2)+9.9^2+1.7^2)^0.5
d1=((a1.^2)-(b1.^2)+(c1^2))./(2*c1)
e1=d1./a1
theta1=acosd(e1)
h1=theta1.^(-3)
i1=260*h1
filename = 'Ev1.xlsx';
Ev1 = xlsread(filename, 'A1:F11')
Lv1= i1.*Ev1
a2=(1.4^2+(yy+6).^2).^0.5
b2=(((xx+1.7).^2)+((1-yy).^2)+(2.15^2)).^0.5
c2=((0.75^2)+7^2+1.7^2)^0.5
d2=((a2.^2)-(b2.^2)+(c2^2))./(2*c2)
e2=d2./a2
theta2=acosd(e2)
h2=theta2.^(-3)
i2=260*h2
filename = 'Ev2.xlsx';
Ev2 = xlsread(filename, 'A1:F11')
Lv2= i2.*Ev2
Lv=Lv1+Lv2+Lv3
hm=3.6
r1=((xx-2.2).^2 + (yy+1).^2).^0.5
s1=(r1.^2 + hm.^2).^0.5
r2=((xx-2.2).^2 + (yy-1).^2).^0.5
s2=(r2.^2 + hm.^2).^0.5
t1=hm./s1
t2=hm./s2
gamma1=acosd(t1)
gamma2=acosd(t2)
u1=(cosd(gamma1)).^3.*hm.^-2
u2=(cosd(gamma2)).^3.*hm.^-2
filename = 'Mh1.xlsx';
I1 = xlsread(filename, 'A1:F11')
```

```
filename = 'Mh2.xlsx';
I2 = xlsread(filename, 'A1:F11')
E1=u1.*I1
E2=u2.*I2
Eh=E1+E2
filename = 'p.xlsx';
p = xlsread(filename, 'A1:F11')
Lp=p.*Eh
La=Lp+Lv
```

	1	2	3	4	5	6	7	8	9	10	11
A	0.796	0.7836	0.6945	0.7479	0.8326	1.0214	0.8526	0.9678	0.9295	0.7127	0.792
B	0.8643	0.8002	0.7455	0.9285	0.7589	0.7941	0.7846	0.7517	0.8161	0.8677	0.9975
C	1.1995	0.7521	0.6468	0.7141	0.6752	0.7758	0.8009	0.7514	0.8502	0.9323	1.1099
D	0.645	0.6463	0.7445	0.8519	0.8783	0.8755	0.6781	0.567	0.6683	0.8263	1.2453
E	0.596	0.5453	0.4668	0.5303	0.6504	1.0114	1.4242	1.5169	1.1593	1.0647	1.4095
F	0.4248	0.461	0.4797	0.4299	0.5256	0.5707	0.785	0.8091	0.5971	0.4102	0.4243
Average L_a = 0.793433											

Table 7.3.1.4 L_a when MH& all SLEs are on

7.3.2 High Pressure Sodium Vapour (HPSV) lamp:

For HPSV lamp adaptation luminances are simulated in 4 different conditions as shown below:

i. Measurement of L_a when HPSV & SLE1are on.

Adaptation luminance values are simulated (in cd/m^2) for HPSV lamp along with the effect of SLE1 using MATLAB software. The coding in M-file is shown below:

```
x=[1.5:-0.5:-1];
y=[-2.5:0.5:2.5];
[xx,yy]=meshgrid(x,y);
a1=(1.4^2+(yy+6).^2).^0.5
b1=(((xx+1.7).^2)+((3.9-yy).^2)+(2.15^2)).^0.5
c1=((0.75^2)+9.9^2+1.7^2)^0.5
d1=((a1.^2)-(b1.^2)+(c1^2))./(2*c1)
e1=d1./a1
theta1=acosd(e1)
```

```
h1=theta1.^(-3)
i1=260*h1
filename = 'Ev1.xlsx';
Ev1 = xlsread(filename, 'A1:F11')
Lv1= i1.*Ev1
hm=3.6
r1=((xx-2.2).^2 + (yy+1).^2).^0.5
s1=(r1.^2 + hm.^2).^0.5
r2=((xx-2.2).^2 + (yy-1).^2).^0.5
s2=(r2.^2 + hm.^2).^0.5
t1=hm./s1
t2=hm./s2
gamma1=acosd(t1)
gamma2=acosd(t2)
u1=(cosd(gamma1)).^3.*hm.^-2
u2=(cosd(gamma2)).^3.*hm.^-2
filename = 'Son1.xlsx';
I1 = xlsread(filename, 'A1:F11')
filename = 'Son2.xlsx';
I2 = xlsread(filename, 'A1:F11')
E1=u1.*I1
E2=u2.*I2
Eh=E1+E2
filename = 'p.xlsx';
p = xlsread(filename, 'A1:F11')
Lp=p.*Eh
La=Lp+Lv1
```

	1	2	3	4	5	6	7	8	9	10	11
A	0.4874	0.4847	0.4229	0.4541	0.4643	0.5028	0.4652	0.5843	0.5655	0.4513	0.5244
B	0.5523	0.5138	0.4814	0.413	0.4291	0.3866	0.4159	0.424	0.4929	0.5634	0.7036
C	0.9017	0.539	0.4591	0.4926	0.3771	0.368	0.3749	0.3718	0.496	0.6265	0.8913
D	0.3768	0.3272	0.3338	0.3052	0.2942	0.3622	0.3065	0.3592	0.5303	0.7131	1.148
E	0.278	0.2355	0.2131	0.2678	0.2116	0.2159	0.2489	0.3287	0.3596	0.6606	1.1657
F	0.1689	0.1856	0.2484	0.2382	0.2379	0.2048	0.2076	0.2429	0.242	0.2515	0.2794
Average L_a =0.430758											

Table 7.3.2.1 L_a when HPSV & SLE1 are on

ii. Measurement of L_a when HPSV & SLE2 are on.

Adaptation luminance values are simulated (in cd/m^2) for HPSV lamp along with the effect of SLE2 using MATLAB software. The coding in M-file is shown below:

```
x=[1.5:-0.5:-1];
y=[-2.5:0.5:2.5];
[xx,yy]=meshgrid(x,y);
a2=(1.4^2+(yy+6).^2).^0.5
b2=(((xx+1.7).^2)+((1-yy).^2)+(2.15^2)).^0.5
c2=((0.75^2)+7^2+1.7^2)^0.5
d2=((a2.^2)-(b2.^2)+(c2^2))./(2*c2)
e2=d2./a2
theta2=acosd(e2)
h2=theta2.^(-3)
i2=260*h2
filename = 'Ev2.xlsx';
Ev2 = xlsread(filename, 'A1:F11')
Lv2= i2.*Ev2
hm=3.6
r1=((xx-2.2).^2 + (yy+1).^2).^0.5
s1=(r1.^2 + hm.^2).^0.5
r2=((xx-2.2).^2 + (yy-1).^2).^0.5
s2=(r2.^2 + hm.^2).^0.5
t1=hm./s1
t2=hm./s2
gamma1=acosd(t1)
gamma2=acosd(t2)
u1=(cosd(gamma1)).^3.*hm.^-2
u2=(cosd(gamma2)).^3.*hm.^-2
filename = 'Son1.xlsx';
I1 = xlsread(filename, 'A1:F11')
filename = 'Son2.xlsx';
I2 = xlsread(filename, 'A1:F11')
E1=u1.*I1
E2=u2.*I2
Eh=E1+E2
filename = 'p.xlsx';
p = xlsread(filename, 'A1:F11')
Lp=p.*Eh
La=Lp+Lv2
```

	1	**2**	**3**	**4**	**5**	**6**	**7**	**8**	**9**	**10**	**11**
A	0.4932	0.4921	0.44	0.4805	0.5011	0.551	0.5216	0.6181	0.5699	0.3991	0.4011
B	0.5611	0.5282	0.5022	0.4554	0.5001	0.4861	0.5291	0.5146	0.5227	0.5005	0.4869
C	0.9127	0.5585	0.4984	0.5626	0.5234	0.5942	0.6466	0.5962	0.6027	0.5498	0.4751
D	0.4334	0.4469	0.5775	0.7111	0.7544	0.7298	0.5422	0.387	0.3675	0.3083	0.3348
E	0.2825	0.2405	0.2471	0.3725	0.5232	0.8911	1.2852	1.3307	0.9351	0.5464	0.4474
F	0.1701	0.187	0.2547	0.2628	0.3649	0.4206	0.6479	0.6756	0.4692	0.2772	0.2705
Average L_a = 0.519241											

Table 7.3.2.2 L_a when HPSV & SLE2 are on

iii. Measurement of La when HPSV & SLE 3 are on.

Adaptation luminance values are simulated (in cd/m^2) for HPSV lamp along with the effect of SLE3 using MATLAB software. The coding in M-file is shown below:

```
x=[1.5:-0.5:-1];
y=[-2.5:0.5:2.5];
[xx,yy]=meshgrid(x,y);
a3=(1.4^2+(yy+6).^2).^0.5
b3=(((xx+1.7).^2)+((yy+2.5).^2)+(2.15^2)).^0.5
c3=(15.7025)^0.5
d3=((a3.^2)-(b3.^2)+(c3^2))./(2*c3)
e3=d3./a3
theta3=acosd(e3)
h3=theta3.^(-3)
i3=260*h3
filename = 'Ev3.xlsx';
Ev3 = xlsread(filename, 'A1:F11')
Lv3= i3.*Ev3
hm=3.6
r1=((xx-2.2).^2 + (yy+1).^2).^0.5
s1=(r1.^2 + hm.^2).^0.5
r2=((xx-2.2).^2 + (yy-1).^2).^0.5
s2=(r2.^2 + hm.^2).^0.5
t1=hm./s1
t2=hm./s2
gamma1=acosd(t1)
gamma2=acosd(t2)
u1=(cosd(gamma1)).^3.*hm.^-2
u2=(cosd(gamma2)).^3.*hm.^-2
filename = 'Son1.xlsx';
I1 = xlsread(filename, 'A1:F11')
filename = 'Son2.xlsx';
I2 = xlsread(filename, 'A1:F11')
E1=u1.*I1
E2=u2.*I2
Eh=E1+E2
filename = 'p.xlsx';
p = xlsread(filename, 'A1:F11')
Lp=p.*Eh
La=Lp+Lv3
```

	1	2	3	4	5	6	7	8	9	10	11
A	0.5016	0.4992	0.435	0.4634	0.4667	0.4939	0.4435	0.5349	0.4845	0.3293	0.3356
B	0.5869	0.5504	0.5119	0.6964	0.4393	0.3737	0.3802	0.3488	0.3657	0.3701	0.3819
C	0.9685	0.6092	0.5157	0.533	0.4012	0.3669	0.3463	0.2935	0.3193	0.3234	0.3463
D	0.512	0.4652	0.4369	0.3738	0.3281	0.3418	0.2661	0.2458	0.294	0.2471	0.3007
E	0.5002	0.4595	0.3564	0.3251	0.2434	0.2294	0.2169	0.2338	0.2067	0.2137	0.299
F	50.3419	0.3626	0.3435	0.2727	0.2421	0.2056	0.2048	0.2362	0.2356	0.2444	0.2412
Average L_a = 0.37943											

Table 7.3.2.3 L_a when HPSV & SLE3 are on

iv. Measurement of L_a when HPSV & all SLEs are on.

Adaptation luminance values are simulated (in cd/m^2) for HPSV lamp along with the effect of all SLEs using MATLAB software. The coding in M-file is shown below:

```
x=[1.5:-0.5:-1];
y=[-2.5:0.5:2.5];
[xx,yy]=meshgrid(x,y);
a3=(1.4^2+(yy+6).^2).^0.5
b3=(((xx+1.7).^2)+((yy+2.5).^2)+(2.15^2)).^0.5
c3=(15.7025)^0.5
d3=((a3.^2)-(b3.^2)+(c3^2))./(2*c3)
e3=d3./a3
theta3=acosd(e3)
h3=theta3.^(-3)
i3=260*h3
filename = 'Ev3.xlsx';
Ev3 = xlsread(filename, 'A1:F11')
Lv3= i3.*Ev3
a1=(1.4^2+(yy+6).^2).^0.5
b1=(((xx+1.7).^2)+((3.9-yy).^2)+(2.15^2)).^0.5
c1=((0.75^2)+9.9^2+1.7^2)^0.5
d1=((a1.^2)-(b1.^2)+(c1^2))./(2*c1)
e1=d1./a1
theta1=acosd(e1)
h1=theta1.^(-3)
i1=260*h1
filename = 'Ev1.xlsx';
Ev1 = xlsread(filename, 'A1:F11')
Lv1= i1.*Ev1
a2=(1.4^2+(yy+6).^2).^0.5
b2=(((xx+1.7).^2)+((1-yy).^2)+(2.15^2)).^0.5
c2=((0.75^2)+7^2+1.7^2)^0.5
d2=((a2.^2)-(b2.^2)+(c2^2))./(2*c2)
e2=d2./a2
theta2=acosd(e2)
h2=theta2.^(-3)
```

```
i2=260*h2
filename = 'Ev2.xlsx';
Ev2 = xlsread(filename, 'A1:F11')
Lv2= i2.*Ev2
Lv=Lv1+Lv2+Lv3
hm=3.6
r1=((xx-2.2).^2 + (yy+1).^2).^0.5
s1=(r1.^2 + hm.^2).^0.5
r2=((xx-2.2).^2 + (yy-1).^2).^0.5
s2=(r2.^2 + hm.^2).^0.5
t1=hm./s1
t2=hm./s2
gamma1=acosd(t1)
gamma2=acosd(t2)
u1=(cosd(gamma1)).^3.*hm.^-2
u2=(cosd(gamma2)).^3.*hm.^-2
filename = 'Son1.xlsx';
I1 = xlsread(filename, 'A1:F11')
filename = 'Son2.xlsx';
I2 = xlsread(filename, 'A1:F11')
E1=u1.*I1
E2=u2.*I2
Eh=E1+E2
filename = 'p.xlsx';
p = xlsread(filename, 'A1:F11')
Lp=p.*Eh
La=Lp+Lv
```

	1	**2**	**3**	**4**	**5**	**6**	**7**	**8**	**9**	**10**	**11**
A	0.5103	0.5126	0.4623	0.5071	0.5316	0.5859	0.5626	0.6828	0.6639	0.5298	0.5966
B	0.5983	0.5697	0.5447	0.7581	0.5384	0.5316	0.589	0.6082	0.6648	0.7029	0.8147
C	0.9813	0.6333	0.5607	0.6165	0.5716	0.6392	0.7072	0.6944	0.791	0.8617	1.0269
D	0.5711	0.588	0.6844	0.7893	0.8054	0.8015	0.6142	0.5176	0.6162	0.7829	1.1866
E	0.5079	0.473	0.4011	0.4364	0.5628	0.9137	1.3368	1.4357	1.095	0.9987	1.3142
F	0.3471	0.3693	0.3567	0.3057	0.3792	0.4333	0.6587	0.6843	0.4798	0.2887	0.313
Average L_a = 0.654515											

Table 7.3.2.4 L_a when HPSV & all SLEs are on

7.3.3 Cool White LED (CWLED)

For CWLED lamp adaptation luminances are simulated in 4 different conditions as shown below:

i. Measurement of L_a when CWLED & SLE1 are on.

Adaptation luminance values are simulated (in cd/m^2) for CWLED lamp along with the effect of SLE1 using MATLAB software. The coding in M-file is shown below:

```
x=[1.5:-0.5:-1];
y=[-2.5:0.5:2.5];
[xx,yy]=meshgrid(x,y);
a1=(1.4^2+(yy+6).^2).^0.5
b1=(((xx+1.7).^2)+((3.9-yy).^2)+(2.15^2)).^0.5
c1=((0.75^2)+9.9^2+1.7^2)^0.5
d1=((a1.^2)-(b1.^2)+(c1^2))./(2*c1)
e1=d1./a1
theta1=acosd(e1)
h1=theta1.^(-3)
i1=260*h1
filename = 'Ev1.xlsx';
Ev1 = xlsread(filename, 'A1:F11')
Lv1= i1.*Ev1
hm=3.6
r1=((xx-2.2).^2 + (yy+1).^2).^0.5
s1=(r1.^2 + hm.^2).^0.5
r2=((xx-2.2).^2 + (yy-1).^2).^0.5
s2=(r2.^2 + hm.^2).^0.5
t1=hm./s1
t2=hm./s2
gamma1=acosd(t1)
gamma2=acosd(t2)
u1=(cosd(gamma1)).^3.*hm.^-2
u2=(cosd(gamma2)).^3.*hm.^-2
filename = 'Led1.xlsx';
I1 = xlsread(filename, 'A1:F11')
filename = 'Led2.xlsx';
I2 = xlsread(filename, 'A1:F11')
E1=u1.*I1
E2=u2.*I2
Eh=E1+E2
filename = 'p.xlsx';
p = xlsread(filename, 'A1:F11')
Lp=p.*Eh
La=Lp+Lv1
```

	1	**2**	**3**	**4**	**5**	**6**	**7**	**8**	**9**	**10**	**11**
A	0.7796	0.6882	0.5576	0.5453	0.4967	0.5452	0.4965	0.6923	0.7196	0.5886	0.7242
B	0.8712	0.7216	0.6115	0.4847	0.4583	0.4149	0.4418	0.4843	0.5909	0.7119	0.9229
C	1.3755	0.7101	0.5549	0.5542	0.392	0.3844	0.3884	0.4077	0.5618	0.7282	1.0717
D	0.5559	0.4236	0.3948	0.3308	0.2922	0.3557	0.3048	0.3794	0.5832	0.785	1.2903
E	0.4263	0.3102	0.2389	0.2695	0.194	0.1942	0.2313	0.3301	0.3848	0.7287	1.3261
F	0.2456	0.2263	0.2543	0.2171	0.1992	0.1654	0.1742	0.2216	0.2477	0.3053	0.3892
Average L_a = 0.509885											

Table 7.3.3.1 L_a when CWLED & SLE1 are on

ii. Measurement of L_a when CWLED & SLE2 are on.

Adaptation luminance values are simulated (in cd/m^2) for CWLED lamp along with the effect of SLE2 using MATLAB software. The coding in M-file is shown below:

```
x=[1.5:-0.5:-1];
y=[-2.5:0.5:2.5];
[xx,yy]=meshgrid(x,y);
a2=(1.4^2+(yy+6).^2).^0.5
b2=(((xx+1.7).^2)+((1-yy).^2)+(2.15^2)).^0.5
c2=((0.75^2)+7^2+1.7^2)^0.5
d2=((a2.^2)-(b2.^2)+(c2^2))./(2*c2)
e2=d2./a2
theta2=acosd(e2)
h2=theta2.^(-3)
i2=260*h2
filename = 'Ev2.xlsx';
Ev2 = xlsread(filename, 'A1:F11')
Lv2= i2.*Ev2
hm=3.6
r1=((xx-2.2).^2 + (yy+1).^2).^0.5
s1=(r1.^2 + hm.^2).^0.5
r2=((xx-2.2).^2 + (yy-1).^2).^0.5
s2=(r2.^2 + hm.^2).^0.5
t1=hm./s1
t2=hm./s2
gamma1=acosd(t1)
gamma2=acosd(t2)
u1=(cosd(gamma1)).^3.*hm.^-2
u2=(cosd(gamma2)).^3.*hm.^-2
filename = 'Led1.xlsx';
I1 = xlsread(filename, 'A1:F11')
filename = 'Led2.xlsx';
I2 = xlsread(filename, 'A1:F11')
E1=u1.*I1
E2=u2.*I2
Eh=E1+E2
filename = 'p.xlsx';
p = xlsread(filename, 'A1:F11')
Lp=p.*Eh
La=Lp+Lv2
```

	1	2	3	4	5	6	7	8	9	10	11
A	0.7854	0.6956	0.5747	0.5718	0.5335	0.5934	0.5528	0.7261	0.724	0.5364	0.6009
B	0.8801	0.736	0.6323	0.527	0.5292	0.5143	0.555	0.5749	0.6207	0.649	0.7063
C	1.3865	0.7296	0.5942	0.6241	0.5383	0.6105	0.6601	0.6322	0.6686	0.6515	0.6554
D	0.6126	0.5433	0.6384	0.7367	0.7525	0.7233	0.5405	0.4071	0.4204	0.3802	0.4771
E	0.4308	0.3152	0.2729	0.3741	0.5056	0.8694	1.2676	1.3321	0.9604	0.6145	0.6078
F	0.2467	0.2276	0.2607	0.2417	0.3262	0.3813	0.6145	0.6544	0.4749	0.331	0.3803
Average L_a = 0.598367											

Table 7.3.3.2 L_a when CWLED & SLE2 are on

iii. Measurement of L_a when CWLED & SLE 3 are on.

Adaptation luminance values are simulated (in cd/m^2) for CWLED lamp along with the effect of SLE3 using MATLAB software. The coding in M-file is shown below:

```
x=[1.5:-0.5:-1];
y=[-2.5:0.5:2.5];
[xx,yy]=meshgrid(x,y);
a3=(1.4^2+(yy+6).^2).^0.5
b3=(((xx+1.7).^2)+((yy+2.5).^2)+(2.15^2)).^0.5
c3=(15.7025)^0.5
d3=((a3.^2)-(b3.^2)+(c3^2))./(2*c3)
e3=d3./a3
theta3=acosd(e3)
h3=theta3.^(-3)
i3=260*h3
filename = 'Ev3.xlsx';
Ev3 = xlsread(filename, 'A1:F11')
Lv3= i3.*Ev3
hm=3.6
r1=((xx-2.2).^2 + (yy+1).^2).^0.5
s1=(r1.^2 + hm.^2).^0.5
r2=((xx-2.2).^2 + (yy-1).^2).^0.5
s2=(r2.^2 + hm.^2).^0.5
t1=hm./s1
t2=hm./s2
gamma1=acosd(t1)
gamma2=acosd(t2)
u1=(cosd(gamma1)).^3.*hm.^-2
u2=(cosd(gamma2)).^3.*hm.^-2
```

```
filename = 'Led1.xlsx';
I1 = xlsread(filename, 'A1:F11')
filename = 'Led2.xlsx';
I2 = xlsread(filename, 'A1:F11')
E1=u1.*I1
E2=u2.*I2
Eh=E1+E2
filename = 'p.xlsx';
p = xlsread(filename, 'A1:F11')
Lp=p.*Eh
La=Lp+Lv3
```

	1	2	3	4	5	6	7	8	9	10	11
A	0.7938	0.7027	0.5697	0.5547	0.4991	0.5363	0.4747	0.6429	0.6385	0.4666	0.5353
B	0.9058	0.7582	0.6419	0.7681	0.4684	0.4019	0.406	0.4091	0.4637	0.5186	0.6012
C	1.4423	0.7803	0.6115	0.5945	0.4161	0.3832	0.3597	0.3294	0.3851	0.4251	0.5267
D	0.6911	0.5617	0.4978	0.3993	0.3261	0.3352	0.2643	0.2659	0.3469	0.319	0.443
E	0.6484	0.5341	0.3822	0.3268	0.2258	0.2077	0.1993	0.2353	0.232	0.2818	0.4594
F	0.4186	0.4032	0.3495	0.2515	0.2034	0.1663	0.1714	0.215	0.2413	0.2981	0.351
Average L_a = 0.458538											

Table 7.3.3.3 L_a when CWLED & SLE3 are on

iv. Measurement of L_a when CWLED & all SLEs are on.

Adaptation luminance values are simulated (in cd/m^2) for CWLED lamp along with the effect of all SLEs using MATLAB software. The coding in M-file is shown below:

```
x=[1.5:-0.5:-1];
y=[-2.5:0.5:2.5];
[xx,yy]=meshgrid(x,y);
a3=(1.4^2+(yy+6).^2).^0.5
b3=(((xx+1.7).^2)+((yy+2.5).^2)+(2.15^2)).^0.5
c3=(15.7025)^0.5
d3=((a3.^2)-(b3.^2)+(c3^2))./(2*c3)
e3=d3./a3
theta3=acosd(e3)
h3=theta3.^(-3)
i3=260*h3
filename = 'Ev3.xlsx';
Ev3 = xlsread(filename, 'A1:F11')
Lv3= i3.*Ev3
```

```
a1=(1.4^2+(yy+6).^2).^0.5
b1=(((xx+1.7).^2)+((3.9-yy).^2)+(2.15^2)).^0.5
c1=((0.75^2)+9.9^2+1.7^2)^0.5
d1=((a1.^2)-(b1.^2)+(c1^2))./(2*c1)
e1=d1./a1
theta1=acosd(e1)
h1=theta1.^(-3)
i1=260*h1
filename = 'Ev1.xlsx';
Ev1 = xlsread(filename, 'A1:F11')
Lv1= i1.*Ev1
a2=(1.4^2+(yy+6).^2).^0.5
b2=(((xx+1.7).^2)+((1-yy).^2)+(2.15^2)).^0.5
c2=((0.75^2)+7^2+1.7^2)^0.5
d2=((a2.^2)-(b2.^2)+(c2^2))./(2*c2)
e2=d2./a2
theta2=acosd(e2)
h2=theta2.^(-3)
i2=260*h2
filename = 'Ev2.xlsx';
Ev2 = xlsread(filename, 'A1:F11')
Lv2= i2.*Ev2
Lv=Lv1+Lv2+Lv3
hm=3.6
r1=((xx-2.2).^2 + (yy+1).^2).^0.5
s1=(r1.^2 + hm.^2).^0.5
r2=((xx-2.2).^2 + (yy-1).^2).^0.5
s2=(r2.^2 + hm.^2).^0.5
t1=hm./s1
t2=hm./s2
gamma1=acosd(t1)
gamma2=acosd(t2)
u1=(cosd(gamma1)).^3.*hm.^-2
u2=(cosd(gamma2)).^3.*hm.^-2
filename = 'Led1.xlsx';
I1 = xlsread(filename, 'A1:F11')
filename = 'Led2.xlsx';
I2 = xlsread(filename, 'A1:F11')
E1=u1.*I1
E2=u2.*I2
Eh=E1+E2
filename = 'p.xlsx';
p = xlsread(filename, 'A1:F11')
Lp=p.*Eh
La=Lp+Lv
```

	1	2	3	4	5	6	7	8	9	10	11
A	0.8025	0.7161	0.5969	0.5984	0.564	0.6283	0.5938	0.7908	0.818	0.6671	0.7964
B	0.9173	0.7776	0.6748	0.8297	0.5676	0.5598	0.6149	0.6686	0.7628	0.8515	1.034
C	1.4551	0.8044	0.6565	0.6781	0.5865	0.6555	0.7206	0.7304	0.8568	0.9634	1.2073
D	0.7502	0.6845	0.7454	0.8148	0.8034	0.795	0.6125	0.5377	0.6691	0.8548	1.3289
E	0.6561	0.5476	0.4269	0.4381	0.5452	0.892	1.3193	1.4371	1.1202	1.0668	1.4745
F	0.4237	0.4099	0.3627	0.2846	0.3405	0.394	0.6253	0.6631	0.4855	0.3424	0.4228
Average L_a = 0.733638											

Table 7.3.3.4 L_a when CWLED & all SLEs are on

7.4 Simulated Adaptation Luminance (L_a) values for all different Lamps

Simulated adaptation Luminance (L_a) values for all different Lamps when all SLEs are on are shown in Table 7.4.

Average Adaptation Luminance(cd/m^2)	
MH	0.793433
HPSV	0.654515
CWLED	0.731638

Table 7.4 Simulated Adaptation luminance (L_a) values for all different Lamps & all SLEs are on

CHAPTER 8: RESULT ANALYSIS

In this research, photopic luminance (L_p) measurements were conducted across the entire measurement area. Subsequently, the adaptation luminance (L_a) was calculated for this specific measurement area using the method outlined in the previous chapter. These luminance values are then subjected to a comparative analysis, shedding light on the characteristics of the adaptation field within the mesopic photometry system. Additionally, we investigate the performance of various lamps under these diverse conditions.

8.1 Comparison of Average Photopic Luminance (L_p)

Photopic luminance (L_p) measurements across the entire measurement area for MH, HPSV and CWLED are below in Table 8.1:

Average Photopic Luminance(cd/m^2)	
MH	0.476365
HPSV	0.33745
CWLED	0.41658

Table 8.1 Comparison of Average Photopic Luminance (L_p)

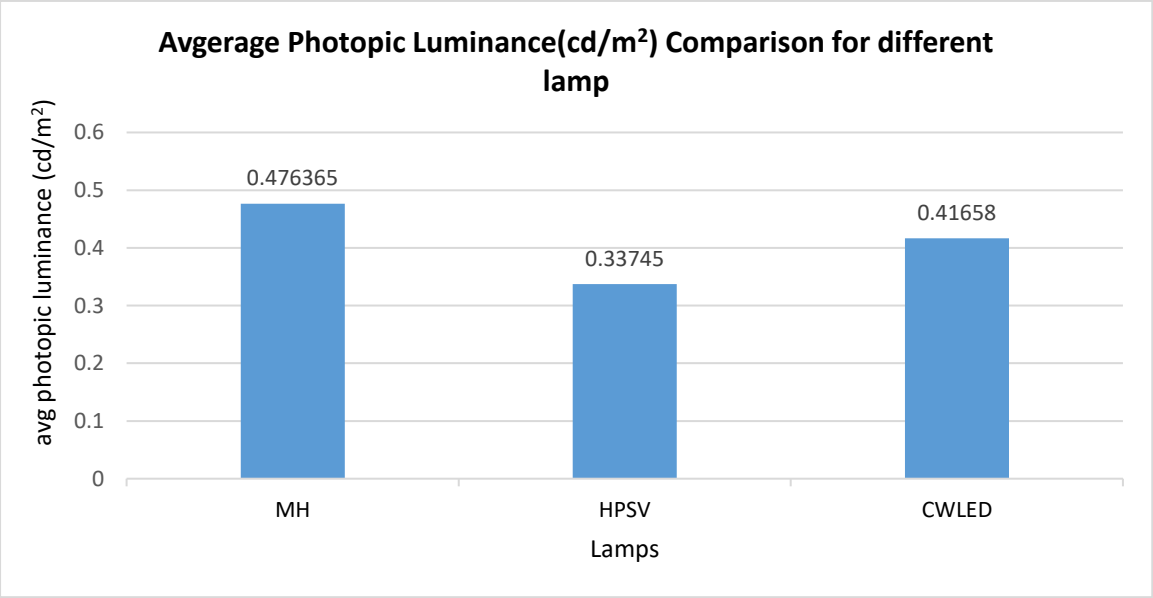

Indeed, the comparison of Photopic luminance (L_p) values shows that Metal Halide (MH) lighting, despite its higher power consumption (150 watts), has the highest Lp value, indicating a high perceived brightness. On the other hand, High-Pressure Sodium Vapour (HPSV) lighting, with the same power rating has the lowest L_p value, suggesting lower perceived brightness. Cool White LED (CWLED) lighting, despite its lower power rating (101 watts), falls in between in terms of L_p value, indicating a moderate level of perceived brightness.

Considering the energy perspective, Cool White LED (CWLED) lighting offers a more energy-efficient solution compared to Metal Halide (MH) lighting. It consumes less power (101 watts) while still providing a reasonable level of perceived brightness. This efficiency can translate into cost savings and reduced energy consumption, making CWLED lighting a preferred choice for outdoor lighting applications where energy efficiency is a key consideration. Therefore, from an energy-efficiency standpoint, CWLED lighting is a more attractive option for outdoor lighting when compared to MH lighting, despite the relatively close L_p values between the two.

8.2 Comparison of average adaptation (L_a) for different SLE positions

The positioning of surrounding light sources plays a pivotal role in influencing veiling luminance, consequently leading to variations in adaptation luminance. In this study, we examine the impact of the placement of three distinct surrounding light sources, each at a different position. We present a comparison of the average adaptation luminances across these differing surrounding light source positions, as shown below:

Average Adaptation Luminance(cd/m^2)			
	SLE of Position 1	**SLE of Position 2**	**SLE of Position 3**
MH	0.56967	0.658161	0.518333
HPSV	0.430758	0.519241	0.37943
CWLED	0.509885	0.598367	0.458538

Table 8.4: Effect of surrounding source position

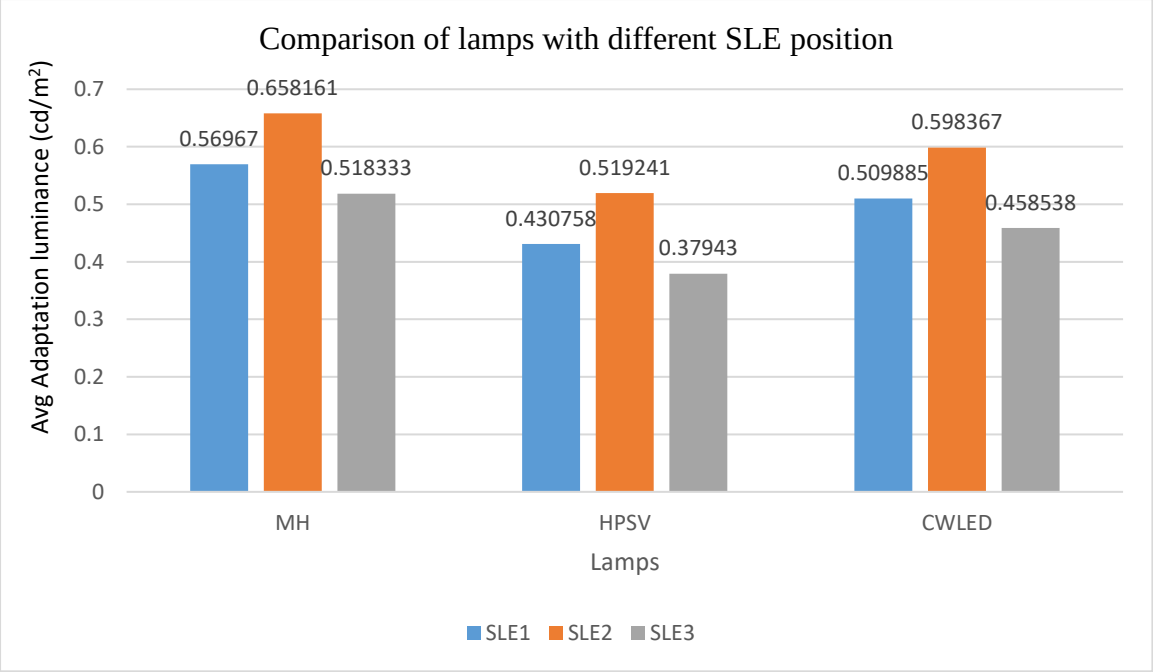

In the observations, it becomes evident that, across all types of light sources, the average adaptation luminance follows a specific pattern: Surrounding light source at position 2 yields the highest average adaptation luminance, followed by Surrounding light source at position 1, and lastly, Surrounding light source at position 3. This pattern suggests that the average adaptation luminance is maximized when the surrounding light source is closest to the main light source, and it diminishes as the distance from the main light source increases. Therefore, we can deduce that adaptation luminance doesn't depend on the observer's position.

8.3 Simulated Adaptation Luminance (L_a) values when all SLEs are on

Simulated adaptation Luminance (L_a) measurements across the entire measurement area for MH, HPSV and CWLED (when all SLEs are on) are below in Table 8.3:

Average Adaptation Luminance(cd/m^2)	
MH	0.793433
HPSV	0.654515
CWLED	0.731638

Table 8.3 Simulated Adaptation luminance (L_a) values for all different Lamps & all SLEs are on

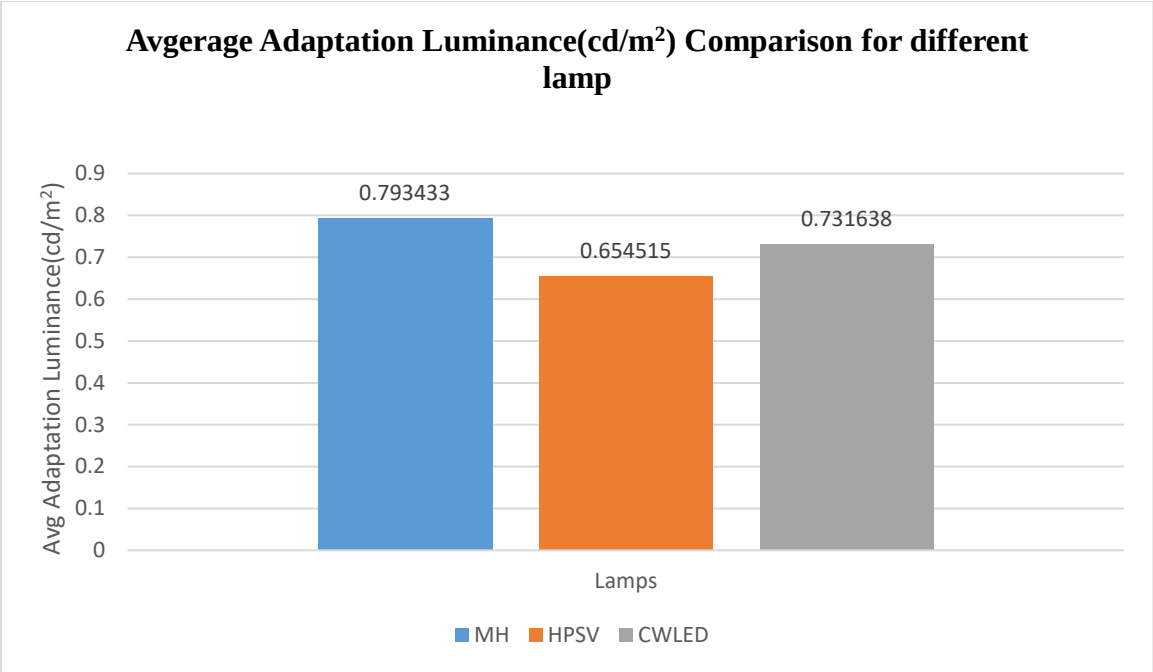

In the observations, it is clear that Metal Halide (MH) lighting has a higher average adaptation luminance than other types of light sources. However, from an energy efficiency standpoint, Cool White LED (CWLED) lighting emerges as the more efficient option compared to Metal Halide (MH) lighting. CWLED consumes less power than Metal Halide (MH) lighting while still delivering nearly equivalent adaptation luminance.

8.4 Comparison of Adaptation Luminance (L_a) and Photopic Luminance (L_p)

Comparison between average Adaptation Luminance (L_a) and average Photopic Luminance (L_p) are shown in table 8.4

Lamps	Average L_p(cd/m^2)	Average L_a(cd/m^2)
MH	0.476365	0.793433
HPSV	0.33745	0.654515
CWLED	0.41658	0.731638

Table 8.4 Comparison between average Adaptation Luminance (L_a) and average Photopic Luminance (L_p)

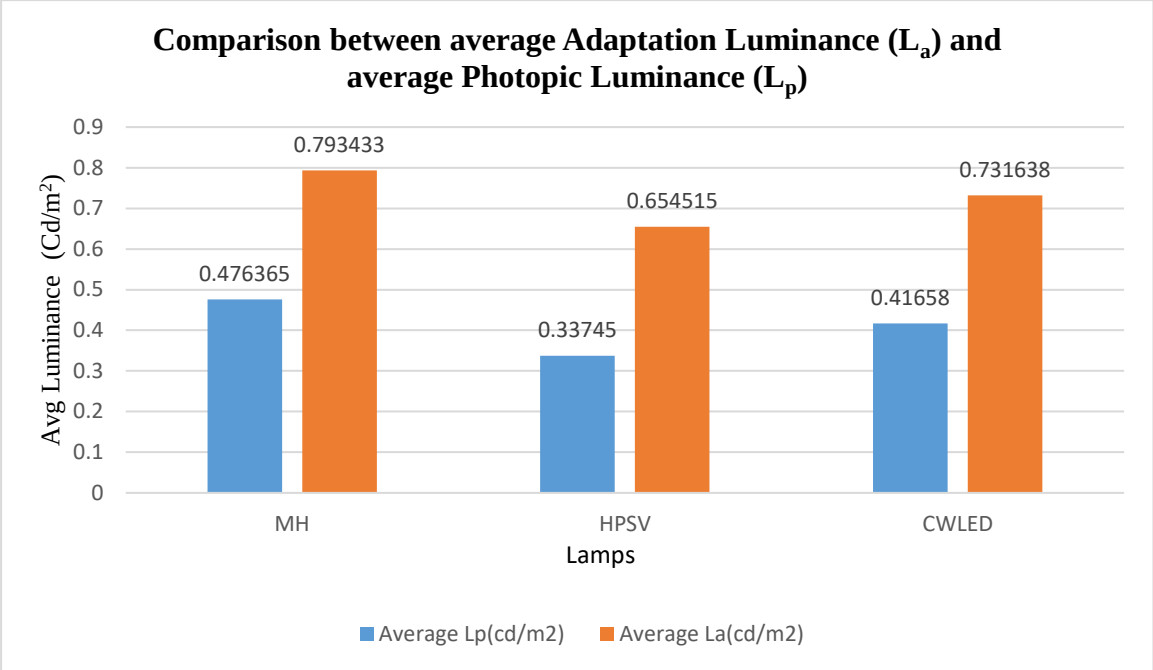

CHAPTER 9: CONCLUSIONS & FUTURE SCOPE

The comprehensive studies conducted on adaptation luminance and lamp performance in the mesopic photometry system have yielded significant insights and findings. This experiment have demonstrated that adaptation luminance plays a crucial role in mesopic vision. It is found that the visual system's sensitivity and performance are highly dependent on the initial adaptation level, suggesting the need for adaptive lighting systems that adjust to changing luminance conditions. The evaluation of different lamp types and their performance in mesopic conditions has revealed valuable information for lighting designers and engineers. CWLED lamps, in particular, have shown promise in providing efficient and effective illumination within the mesopic range. Therefore, from an energy-efficiency standpoint, CWLED lighting is a more attractive option for outdoor lighting when compared to MH lighting.

While this thesis has provided valuable insights into adaptation luminance and lamp performance in mesopic photometry systems, several avenues for future research and development can be explored. The future scope of research in this field holds significant promise for advancing our understanding of lighting technologies and their impact on human visual performance in various environmental conditions. Beyond the effects of dust, rain, and ambient temperature variations, which undoubtedly influence lamp performance and visual perception, particular attention should be directed towards assessing the performance of LEDs under foggy weather conditions, as fog presents a unique challenge for visibility. Furthermore, to enhance the accuracy of experimental data, future studies should prioritize the elimination of obstructions and mitigating the effects of reflected light, whether by refining laboratory setups or by conducting experiments in more controlled and real-world outdoor environments. These advancements will contribute to more comprehensive and applicable insights into optimizing lighting solutions for diverse scenarios and environmental challenges.

Investigating the potential impacts of mesopic lighting on human health, including its effects on circadian rhythms and sleep patterns, is a burgeoning area of interest. Such research can provide valuable insights into the long-term consequences of mesopic lighting solutions.

The integration of adaptive and intelligent lighting systems stands as a promising future frontier in the study of adaptation luminance and lamp performance in mesopic photometry systems. The development of systems that can dynamically adjust lighting levels and spectral characteristics in response to mesopic conditions, leveraging sensor data and advanced algorithms, represents a fertile area for exploration. Such research could not only enhance visual comfort and performance but also usher in significant energy savings and sustainability benefits, ultimately reshaping the landscape of lighting technology and design in the mesopic realm.

References

1. Commission Internationale de l'Eclairage. Recommended System for Mesopic Photometry Based on Visual Performance. CIE Publication 191-2010, Vienna: CIE, 2010.
2. https://en.wikipedia.org/wiki/Mesopic_vision.
3. S Fotios, C Cheal, S Fox and J Uttley. The transition between lit and unlit sections of road and detection of driving hazards after dark. Lighting Res. Technol. 2019; 51: 243–261.
4. Commission Internationale de l'Eclairage. CIE 115:2010. Lighting of Roads for Motor and Pedestrian Traffic. Vienna: CIE, 2010.
5. AASHTO, Roadway Lighting Design Guide, American Association of State Highway and Transportation Officials, Washington DC, 2005.
6. Judd DB. Report of US Secretariat Committee on colorimetry and artificial daylight. CIE Compte Rendu, 12th Session, Stockholm, vol. I, part 7. CIE Central Bureau, New York, 1951: 1–49.
7. Zwinkels JC, Ikonen E, Fox NP, Ulm G, Rastello ML. Photometry, radiometry and 'the candela': evolution in the classical and quantum world. Metrologia 2010; 47: R15–R32.
8. Bureau International des Poids et Mesures. Principles Governing Photometry Monographie 83/1. Paris: BIPM, 1983.
9. Berman SM. Energy efficiency consequences of scotopic sensitivity. Journal of the Illuminating Engineering Society 1992; 21: 3–14.
10. Commission Internationale de l'Eclairage. The Basis of Physical Photometry. CIE Technical Report 18.2. Vienna: CIE, 1983.
11. M Shpak, P Kärhä and E Ikonen Mathematical limitations of the CIE mesopic photometry system. Lighting Res. Technol. 2017; Vol. 49: 111–121.
12. Narisada K. Visual perception in non-uniform fields. Journal of Light and Visual Environment 1992; 16: 81–88.
13. Narisada K. Perception under road lighting conditions with complex surroundings. Journal of Light and Visual Environment 1995; 19: 5–14.
14. Commission Internationale de l'Eclairage. CIE Equations for Disability Glare. CIE Publication 146. Vienna: CIE, 2002.
15. Stiles WS, Crawford BH. The effect of a glaring light source on extra foveal vision. Proceedings of the Royal Society London B 1937; 122: 255–280.
16. Uchida T, Ohno Y. Angular Characteristics of the Surrounding Luminance Effect on Peripheral Adaptation State in the Mesopic Range. Proceedings of CIE 2014 Lighting Quality and Energy Efficiency, Kuala Lumpur, Malaysia, April 23–26. Vienna: Commission Internationale de l'Eclairage, 2014:, pp. 273–280
17. N. Suttisinthong, B. Seewirote, A. Ngaopitakkul, C. Jettanasen, "Feasibility Study and Impact of Energy Consumption Reduction Using T5 Fluorescent lamp in Building". Published in: 2014 International Conference on Intelligent Green Building and Smart Grid (IGBSG)
18. Flesch, Peter (2006). Light and light sources: high-intensity discharge lamps. Springer. pp. 45–46. ISBN 978-3-540-32684-7.
19. US patent 4171498, Dietrich Fromm et al., "High pressure electric discharge lamp containing metal halides", issued 1979-10-16.

20. US patent 3234421, Gilbert H. Reiling, "Metallic halide electric discharge lamps", issued 1966-02-08.
21. Kulshreshtha, Alok K. (2009). Basic Electrical Engineering: Principles and Applications. India: Tata McGraw-Hill Education. p. 801. ISBN 978-0-07-014100-1. Archived from the original on 2023-04-20. Retrieved 2020-10-17.
22. General Electric, Fluorescent Lamps Technical Bulletin TP 111R, December 1978
23. Department of Public Works (1980). San Jose: Study and report on low-pressure sodium lighting. San Jose: City of San Jose. p. 8. Archived from the original on 2016-03-04. Retrieved 2013-12-06.
24. Luginbuhl, Christian B. "Low-Pressure Sodium Issues and FAQ". Flagstaff, Arizona: U.S. Naval Observatory. Archived from the original on 2015-09-10. Retrieved 2013-12-05.
25. Edwards, Kimberly D. "Light Emitting Diodes" (PDF). University of California, Irvine. p. 2. Archived from the original (PDF) on February 14, 2019. Retrieved January 12, 2019.
26. "Solid-State Lighting: Comparing LEDs to Traditional Light Sources". Eere.energy.gov. Archived from the original on May 5, 2009.
27. Tanabe, S.; Fujita, S.; Yoshihara, S.; Sakamoto, A.; Yamamoto, S. (2005). Ferguson, Ian T; Carrano, John C; Taguchi, Tsunemasa; Ashdown, Ian E (eds.). "YAG glass-ceramic phosphor for white LED (II): luminescence characteristics" (PDF). Proceedings of SPIE. Fifth International Conference on Solid State Lighting. 5941: 594112. Bibcode:2005SPIE.5941..193T. doi:10.1117/12.614681. S2CID 38290951. Archived from the original (PDF) on May 11, 2011.
28. "Blue LEDs: A health hazard?". texyt.com. January 15, 2007. Retrieved September 3, 2007.
29. Holladay LL. The fundamentals of glare and visibility. Journal of the Optical Society of America 1926; 12: 271–319.
30. H Davson. Physiology of the eye. 5th ed. London: Macmillan Academic and Professional Ltd.; 1990.
31. Aguilar M, Stiles WS. Saturation of the rod mechanism of the retina at high levels of stimulation. Opt Acta (Lond) 1954;1:59–65.
32. Barlow, H. B. (1958). "Temporal and spatial summation in human vision at different background intensities". The Journal of Physiology. 141 (2): 337–350. doi:10.1113/jphysiol.1958.sp005978. PMC 1358805. PMID 13539843.
33. H Davson. Physiology of the eye. 5th ed. London: Macmillan Academic and Professional Ltd.; 1990.
34. Uchida T, Ohno Y. Defining the visual adaptation field for mesopic photometry: Does a high-luminance source affect peripheral adaptation? Lighting Research and Technology 2014; 46: 533.
35. Uchida T, Ohno Y. Angular Characteristics of the Surrounding Luminance Effect on Peripheral Adaptation State in the Mesopic Range. Proceedings of CIE 2014 Lighting Quality and Energy Efficiency, Kuala Lumpur, Malaysia, April 23–26. Vienna: Commission Internationale de l'Eclairage, 2014:, pp.273–280.
36. T Uchida, M Ayama, Y Akashi , N Hara , T Kitano ,Y Kodaira and K Sakai. Adaptation luminance simulation for CIE mesopic photometry system implementation. Lighting Res. Technol. 2016; Vol. 48: 14–25.

37. Fry GA. A re-evaluation of the scatter theory of glare. Journal of the Illuminating Engineering Society 1954; 49: 98–102.
38. Bowmaker, J K; Dartnall, H J (1 January 1980). "Visual pigments of rods and cones in a human retina". The Journal of Physiology. 298 (1): 501–511. doi:10.1113/jphysiol.1980.sp013097. PMC 1279132. PMID 7359434.
39. Do MT, Yau KW (October 2010). "Intrinsically photosensitive retinal ganglion cells". Physiological Reviews. 90 (4): 1547–81. doi:10.1152/physrev.00013.2010. PMC 4374737. PMID 20959623.
40. Ecker JL, Dumitrescu ON, Wong KY, Alam NM, Chen SK, LeGates T, et al. (July 2010). "Melanopsin-expressing retinal ganglion-cell photoreceptors: cellular diversity and role in pattern vision". Neuron. 67 (1): 49–60. doi:10.1016/j.neuron.2010.05.023. PMC 2904318. PMID 20624591.